MICRORNA EXPRESSION AND PROTEIN ACETYLATION PATTERN IN RESPIRATORY AND LIMB MUSCLES OF PARP-1$^{-/-}$ AND PARP-2$^{-/-}$ MICE WITH LUNG CANCER CACHEXIA

Alba Chacon-Cabrera[1,2], Clara Fermoselle[1], Ida Salmela[3], Jose Yelamos[4,5], and Esther Barreiro[1,2]

[1]Pulmonology Department-Lung Cancer Research Group, IMIM-*Hospital del Mar*, *Parc de Salut Mar*, Health and Experimental Sciences Department (CEXS), *Universitat Pompeu Fabra* (UPF), Barcelona Biomedical Research Park (PRBB),C/ Dr. Aiguader, 88, Barcelona, E-08003 Spain.

[2]*Centro de Investigación en Red de Enfermedades Respiratorias* (CIBERES), *Instituto de Salud Carlos* III (ISCIII), Barcelona, Spain.

[3]Department of Biosciences, Division of Genetics, University of Helsinki, Helsinki, Finland.

[4]Cancer Research Program, Hospital del Mar Medical Research Institute (IMIM), Barcelona, Spain

[5]*Centro de Investigación en Red de Enfermedades Hepáticas y Digestivas* (CIBERehd), *Instituto de Salud Carlos* III (ISCIII), C/ Monforte de Lemos 5, Madrid, E-28029 Spain.

Corresponding author: Dr. Esther Barreiro, Pulmonology Department, IMIM-Hospital del Mar, PRBB, C/ Dr. Aiguader, 88, Barcelona, E-08003 Spain, Telephone: (+34) 93 316 0385, Fax: (+34) 93 316 0410, e-mail: ebarreiro@imim.es.

Running title: Muscle-enriched microRNAs and hyperacetylation in cachexia

Word count: 6,184

ABSTRACT

Background: Current treatment options for cachexia, which impairs disease prognosis, are limited. Muscle-enriched microRNAs and protein acetylation are involved in muscle wasting including lung cancer (LC) cachexia. Poly(ADP-ribose) polymerases (PARP) are involved in muscle metabolism. We hypothesized that muscle-enriched microRNA, protein hyperacetylation, and expression levels of myogenic transcription factors (MTFs) and downstream targets, muscle loss and function improve in LC cachectic Parp-$1^{-/-}$ and Parp-$2^{-/-}$ mice. **Methods:**Body and muscle weights, grip strength, muscle phenotype, muscle-enriched microRNAs (miR-1, -133, -206, and -486), protein acetylation, acetylated levels of FoxO1, FoxO3, and PGC-1α, histone deacetylases (HDACs) including SIRT1, MTFs, and downstream targets(α-actin, PGC-1α, and creatine kinase) were evaluated in diaphragm and gastrocnemius of LC (LP07 adenocarcinoma) wild type (WT), Parp-$1^{-/-}$ and Parp-$2^{-/-}$ mice. **Results:**Compared to WT cachectic animals, in both respiratory and limb muscles of Parp-$1^{-/-}$ and Parp-$2^{-/-}$ cachectic mice: downregulation of muscle-specific microRNAs was counterbalanced especially in gastrocnemius of Parp-$1^{-/-}$ mice; increased protein acetylation was attenuated (improvement in HDAC3, SIRT-1, and acetylated FoxO3 levels in both muscles,acetylated FoxO1 levels in the diaphragm); reduced MTFs and creatine kinaselevels were mitigated; body and muscle weights, strength, and muscle fiber sizes improved, while tumor weight and growth decreased. **Conclusions:**These molecular findings may explain the improvements seen in body and muscle weights, limb muscle force and fiber sizes in both Parp-$1^{-/-}$ and Parp-$2^{-/-}$ cachectic mice. **General significance:**PARP-1 and -2 play a role in cancer-induced cachexia, thus selective pharmacological inhibition of PARP-1 and -2 may be of interest in clinical settings. **Word count**: 250. **KEY WORDS**: cancer-induced cachexia; muscle-enriched microRNAs; protein hyperacetylation; myogenic transcription factors; muscle structure and function; Parp-$1^{-/-}$ and Parp-$2^{-/-}$ mice.

1. Introduction

Systemic manifestations of chronic conditions such as muscle mass loss and dysfunction further impair the patients' prognosis and their quality of life [7,19,20]. In advanced malignancies, the prevalence of cachexia characterized by muscle loss and body composition alterations ranges from 60-80% especially in patients bearing tumors from the gastrointestinal and respiratory tracts[19,20,25,38,47,48,50]. Despite that progress in the etiology of cachexia has been recently achieved several mechanisms that could help design novel therapeutic strategies remain to be explored in more detail.

Recent evidence has demonstrated that muscle-enriched microRNAs (miR-1, -133, -206, and -486) are involved in myogenesis and muscle plasticity to environmental stimuli. For instance, miR-1 and -133 regulated hypertrophy in response to muscle overload [30] and atrophy in spaceflight and hindlimb suspension experimental models [31]. Moreover, in respiratory [41] and limb muscles of patients with chronic obstructive pulmonary disease (COPD) with a wide range of airway obstruction and body composition [26,42,43] and severe atrophy of fast-twitch fibers and quadriceps weakness, the expression of muscle-enriched microRNAs and other epigenetic events such as lysine-hyperacetylation of histones and other proteins [43], were shown to be differentially regulated compared to the controls.

Recently, poly(ADP-ribosyl)ation, a post-translational modification of proteins in which ADP-ribose moiety of NAD^+ molecules is transferred to acceptor residues of target proteins by members of the poly(ADP-ribose) polymerase (PARP) family, has emerged as a new regulator of epigenetic events in cells [45]. Among the seventeen members of the PARP family, PARP-1 and PARP-2 play a fundamental role in epigenetic processes through the orchestration of several chromatin-based biological activities [59]. For instance, PARP-1 inhibition using pharmacological agents or knockout mice was shown to increase the levels of type III histone deacetylase SIRT1 activity and to improve oxidative metabolism in the

animals[5]. Moreover, inhibition of PARP-2 also induced an increase in mitochondrial content and SIRT1 protein levels in limb muscles of the knockout mice [4]. Collectively, these findings suggest that PARP seems to play a relevant role in muscle metabolism through specific epigenetic events. Nonetheless, identification of whether PARP-1 and -2 may influence body weight loss, limb strength and other epigenetic features in *in vivo* models of cancer-induced cachexia remains to be elucidated. In this regard, it would be of scientific and clinical interest to identify the extent to which PARP inhibition may improve muscle mass and force loss in cancer cachexia, for which current therapies are extremely limited[19,20,25,38,47,48,50]. Those findings would facilitate the design of selective PARP inhibitors that may promote the restoration of muscle mass and force in cachexia. Moreover, investigations focused on the study of whether respiratory muscles may also be affected in cachectic rodents are scarce [12,46]. We believe that given the relevance of these muscles in the body, the analysis of the diaphragm deserves further attention in models of cancer-induced cachexia.

On this basis and in view of the findings reported so far on the potential role of PARP-1 and -2 in muscle metabolism, in the current investigation, we hypothesized that Parp-$1^{-/-}$ and Parp-$2^{-/-}$ mice may develop less severe muscle wasting when transplanted with a tumor that induces severe cachexia. Additionally, we also hypothesized that muscle-specificmicroRNA and protein acetylation profile would be differentially expressed in both respiratory and limb muscles of Parp-$1^{-/-}$ and Parp-$2^{-/-}$ mice with cancer cachexia. Accordingly, the study objectives were to assess after a one-month study period, in diaphragm and in a limb muscle of similar fiber type composition (gastrocnemius) of Parp-$1^{-/-}$ and Parp-$2^{-/-}$ mice transplanted with a lung tumor (adenocarcinoma)-inducing cachexia: 1) the effects of PARP -1 and -2 selective deletions on body and muscle weights, grip strength, muscle phenotype, and tumor size, 2) levels of expression of muscle-enriched microRNAs, 3) total protein

hyperacetylationlevels and those of transcription factors involved in muscle wasting, 4) levels of myogenic transcription factors(MTFs) and their downstream targets, and 5) potential correlations between physiological and molecular variables in cachectic wild type, Parp-$1^{-/-}$ and Parp-$2^{-/-}$ mice.

2. Methods

2.1. Animal model

Tumor. LP07 is a cell line derived from the transplantable P07 lung tumor that appeared spontaneously in the lung of a BALB/c mouse [12,17,18,53]. The rates of tumor growth and tumor kinetics have been well characterized in previous investigations aimed to specifically explore the effects of several drugs on identical transplanted tumors [18,37].

*Mice***.** BALB/c mice were obtained from Harlan *Interfauna Ibérica SL* (Barcelona, Spain). Parp-$1^{-/-}$ and Parp-$2^{-/-}$ mice (strain 129/Sv x C57BL/6), kindly provided by Dr. de Murcia [15,16,32] (Strasbourg, France), were backcrossed on BALB/c background for twelve generations. Genotyping was performed by PCR analysis using tail DNA as previously described. All experiments were performed on two-month old littermate female mice (body weight ~20 g), on a BALB/c background. Mice were kept under pathogen-free conditions in the animal house facility at the Barcelona Biomedical Research Park (PRBB), with a 12:12 h light:dark cycle.

Experimental design and Ethics. In all experimental groups (except for control rodents), LP07 viable cells ($4x10^5$) resuspended in 0.2 mL minimal essential media (MEM) were subcutaneously inoculated in the left flank of female BALB/c mice on day 1, and were studied for a period of one month. Fifty-nine mice were used in the study, which were subdivided into the following experimental groups: 1) control wild type (N=14), inoculation of 0.2 mL MEM in the left flank; 2) LC cachexia wild type group (N=13), inoculation of LP07 cells; 3) control Parp-$1^{-/-}$ (N=8), inoculation of 0.2 mL MEM in the left flank; 4) LC

cachectic Parp-$1^{-/-}$ mice (N=12), inoculation of LP07 cells; 5) control Parp-$2^{-/-}$ (N=6), inoculation of 0.2 mL MEM in the left flank; and 6) LC cachectic Parp-$2^{-/-}$ mice (N=6), inoculation of LP07 cells.

A fraction of the diaphragm and gastrocnemius muscle specimens of the transgenic mice were also used in another investigation aimed to assess protein catabolism and anabolism and structural alterations in those muscles (data submitted).

All animal experiments were conducted in the animal facilities at PRBB. This controlled study was designed in accordance with the ethical standards on animal experimentation (EU 2010/63 CEE, *Real Decreto* 53/2013 BOE 34, Spain) at PRBB and the Helsinki convention for the use and care of animals. Ethical approval was obtained by the Animal Research Committee (Animal welfare department, Catalonia, EBP-09-1228).

2.2. *In vivo* measurements in the mice

Body weight and grip strength gains were calculated as the percentage of the measurements performed at the end of the study period (30 days) with respect to the same measurements obtained at baseline. Body weight and food intake were measured every day during the entire duration of the study, whereas limb force (grip strength) was determined on days 0 and 30 in all animals as previously shown[10,12,33,51,54,57]. Moreover, the ratio of tumor weight to total body weight on the day of sacrifice (day 30) was also calculated.

2.3. Sacrifice and sample collection

Mice from all the experimental groups were sacrificed on day 30 post-inoculation of LP07 cells or MEM (control animals). Prior to sacrifice, each mouse was inoculated intraperitoneally with 0.1 mL sodium pentobarbital (60 mg/Kg). In all cases, the pedal and blink reflexes were evaluated in order to verify total anesthetic depth. At this time, the following samples were obtained from all animals: diaphragm and gastrocnemius muscles and the subcutaneous tumor. LC cachectic mice were macroscopically of smaller size than healthy

control rodents [12]. Frozen tissues were used for immunoblotting and real-time polymerase chain reaction assay (qRT-PCR) techniques.

2.4. Biological analyses

Muscle RNA isolation. Total RNA was first isolated from snap-frozen skeletal muscles using Trizol reagent following the manufacturer's protocol (Life technologies, Carlsbad, CA, USA). Total RNA concentrations were determined photometrically using the NanoDrop 1000 (Thermo Scientific, Waltham, MA, USA).

MicroRNA reverse transcription (RT). MicroRNA RT was performed using TaqMan® microRNA assays (Life Technologies) following the manufacturer's instructions.

*Real time-PCR amplification (qRT-PCR).*TaqMan based qPCR reactions were performed using the ABI PRISM 7900HT Sequence Detector System (Applied BioSystems, Foster City, CA, USA) together with a commercially available predesigned microRNA assay, and probes as shown in Table 1 [27].

Immunoblotting of 1D electrophoresis in muscle and tumor samples. Protein levels of the different molecular markers analyzed in the study were explored by means of immunoblotting procedures as previously described[8,12]. Protein levels of total acetylated proteins, HDACs, myogenic transcription factors, signaling pathways, and downstream targets were identified using specific primary antibodies as thoroughly described in the online supplementary material. In order to validate equal protein loading among various lanes, SDS-PAGE gels were stained with Coomassie Blue, and the glycolytic enzyme glyceraldehyde-3-phosphate dehydrogenase (GAPDH) was used as the protein loading controls in all the immunoblots (Figure E1, and GAPDH immunoblots accompanying each study antigen).

Tumor specimens. Following identical procedures as described above, in the subcutaneous tumors from all the animals, the following markers were also analyzed with the objective to assess whether Parp deletion may have had an effect on tumor growth or degradation: B-cell

lymphoma (bcl)-2, bax, light chain (LC)3B,NAD-dependent protein deacetylase sirtuin-1 (SIRT1), and GAPDH. Furthermore, in order to confirm that tumors express PARP-1 and PARP-2 proteins in each group of knockout mice (cachectic animals), those proteins were also detected in the actual tumors of all groups of tumor-bearing mice using selective antibodies: anti-PARP-1 antibody (Clon A6.4.12) and anti-PARP-2 antibody (rabbit polyclonal antibody raised against full length mouse PARP-2)[3]. Antigens from all samples were detected as described above.

Immunohistochemistry. On 3-micrometer muscle paraffin-embedded sections from diaphragms and gastrocnemius muscles of all study groups, MyHC-I and –II isoforms were identified using specific antibodies[12,43,44].

Furthermore, in the subcutaneous tumor of the target mice (both wild type and knockout rodents), cell proliferation was measured using ki-67 as a marker (anti-ki67 antibody, Millipore Iberica, CA, USA) on the three micrometer tumor paraffin-embedded sections using immunohistochemical procedures as previously described [12,43,44].

2.5. Statistical Analysis

Normality of the study variables were checked using the Shapiro-Wilk test. Physiologic, structural, and molecular results are expressed as mean (standard deviation). For the purpose of the study, results obtained in the diaphragm and gastrocnemius muscles were subsequently analyzed as follows: 1) LC cachectic wild type mice versus their respective non-tumor controls, 2) LC cachectic Parp-$1^{-/-}$ animals versus their respective knockout non-tumor controls, 3) LC cachectic Parp-$2^{-/-}$ mice versus their respective knockout non-tumor controls, and 4) any of the non-tumor knockout mice versus non-tumor wild type animals. Comparisons described in points 1, 2, and 3 above were analyzed using the Student's *T- test*, while comparisons described in point 4 were assessed using one-way analysis of variance (ANOVA), in which *Dunnett's post hoc* analysis was used to adjust for multiple comparisons

among the three study groups. Moreover, values of the markers quantified in the tumors were compared among the three different groups of cancer cachectic rodents using ANOVA, in which *Dunnett's post hoc* analysis was also employed to adjust for multiple comparisons among the groups. The existence of potential correlations between different variables was only tested in the LC cachectic groups of mice (both wild type and knockout mice). Specifically, correlations between physiological and biological variables were explored using the Pearson's correlation coefficient. A level of significance of $P \leq 0.05$ was established. The sample size chosen was based on previous studies[4,5,12,21,22,28], where very similar approaches were employed and on assumptions of 80% power to detect an improvement of more than 20% in measured outcomes at a level of significance of $P \leq 0.05$.

3. Results

3.1. Physiological characteristics

LC-induced cachexia. As shown in Table 2 and Figure 1, at the end of the study period (day 30), cachectic wild type mice exhibited a reduction in body weight gain compared to their respective controls. Actual body weights of animals in all study are depicted in Figure 1. Food intake did not differ between any of the cachectic mice and their respective control animals (Table 2). Diaphragm and gastrocnemius muscle weights and limb strength gain were significantly reduced in cachectic wild type mice. Importantly, in Parp-$1^{-/-}$ mice, a statistically significant reduction in these parameters was also observed, but to a much lesser extent than in the wild type animals. In cachectic Parp-$2^{-/-}$ mice, no significant differences were observed in muscle weights and body or limb strength gains between cachectic and non-cachectic mice. No significant correlations were found between muscle weight changes and fiber type sizes in any study muscle of the LC cachectic mice (Parp-$1^{-/-}$and Parp-$2^{-/-}$).

Effects of PARP deletion on non-cachectic control animals. As illustrated in Table 2, non-cachectic knockout animals (Parp-$1^{-/-}$ and Parp-$2^{-/-}$) exhibited a reduction in the weights of their muscles (diaphragm and gastrocnemius) compared to wild type non-tumor animals. However, body weight at baseline and both body weight and limb strength gains did not significantly differ among any of the non-cachectic groups of mice.

3.2. Tumor characteristics

Effects of PARP deletion on cachectic animals. The expression of PARP-1 and PARP-2 was confirmed in the subcutaneous tumors of the wild type and both groups of knockout mice. (Figure E2A). Compared to cachectic wild type animals, subcutaneous tumor weight and theratio of tumor to total body weight were significantly reduced in both knockout cachectic mice (Parp-$1^{-/-}$ and Parp-$2^{-/-}$, Table 3). Moreover, ki-67 (cell proliferation marker) was decreased in both knockout cachectic mice (Parp-$1^{-/-}$ and Parp-$2^{-/-}$) compared to cachectic wild type rodents (Table 3). Compared to cachectic wild type mice, subcutaneous tumors of both cachectic Parp-$1^{-/-}$ and Parp-$2^{-/-}$ animals exhibited a decrease in Bcl-2 protein levels, while Bax protein content was increased (Table 3 and Figures E2B and E2C). LC3 II/LC3 I levels were significantly increased in the subcutaneous tumor of both knockout cachectic mice (Parp-$1^{-/-}$ and Parp-$2^{-/-}$) compared to cachectic wild type animals, whereasSIRT1 levels did not differ between wild type and either Parp-$1^{-/-}$ or Parp-$2^{-/-}$ cachectic animals (Table 3 and Figure E2D and E2E).

3.3. Muscle structure

LC-induced cachexia. The proportions of type I and II fibers did not differ between cachectic and non-cachectic conditions in any experimental group of mice. The size of both slow- and fast-twitch fibers was significantly reduced in diaphragm and gastrocnemius of cachectic wild type mice compared to non-cachectic control wild type animals (Table 4). In Parp-$2^{-/-}$mice, the size of type I and type II fibers in both muscles did not show any significant difference

between cachectic and non-cachectic animals (Table 4). Compared to Parp-$1^{-/-}$ mice, in LC-cachectic Parp-$1^{-/-}$ animals, no significant differences were seen in the size of either slow- or fast-twitch fibers in the diaphragm, while in the gastrocnemius a tendency to improve the size of type I (p=0.089) and type II (p=0.067, Table 4) was observed. A significant correlation was found between type II fiber size and miR-133 expression in the gastrocnemius of the cachectic wild type mice (r=0.938, p=0.000), but not in the tumor-bearing knockout mice (r=-0.603, p=0.114 and r=-0.101, p=0.849, Parp-$1^{-/-}$ and Parp-$2^{-/-}$ mice, respectively) (Figure 3E). No significant relationships were observed between type I fiber size and miR-133 expression in the gastrocnemius of any of the three groups of cachectic animals (wild type mice r=0.256, p=0.474; Parp-$1^{-/-}$ mice r=-0.114, p=0.789; and Parp-$2^{-/-}$ r=-0.142, p=0.788).

Effects of PARP deletion on non-cachectic control animals. Proportions or sizes of type I and type II fibers did not differ between wild type and either Parp-$1^{-/-}$ or Parp-$2^{-/-}$ non-cachectic control mice in any study muscle (Table 4).

3.4. Expression microRNA in respiratory and limb muscles

LC-induced cachexia. Expression levels of miR-1 were decreased in both diaphragm and gastrocnemius of LC cachectic wild type, and cachectic Parp-$1^{-/-}$ and Parp-$2^{-/-}$ mice compared to their respective non-cachectic control animals (Figures 2A and 2B). Both diaphragm and gastrocnemius of cachectic wild type and Parp-$2^{-/-}$ mice exhibited a decrease in miR-133 expression compared to their respective non-tumor control mice (Figures 2C and 2D), while miR-133 expression was down-regulated only in the diaphragm of cachectic Parp-$1^{-/-}$ animals (Figures 2C and 2D). Compared to their respective non-cachectic controls, levels of miR-206 were downregulated in both respiratory and limb muscles of cachectic wild type rodents, while the expression of this myomiR was decreased only in the diaphragm of both groups of cachectic knockout mice (Figures 3A and 3B). Expression levels of miR-486 were down-regulated in both muscles of cachectic wild type and Parp-$2^{-/-}$ mice compared to their

respective non-tumor control animals (Figures 3C and 3D). However, miR-486 levels did not differ between cachectic and non-cachectic Parp-$1^{-/-}$ mice in any muscle (Figures 3C and 3D).

Effects of PARP deletion on non-cachectic control animals. Levels of miR-1 did not differ between non-cachectic Parp-$1^{-/-}$ and non-cachectic wild type mice in any study muscle (Figures 2A and 2B). However, levels of miR-1 were greater in the diaphragm of non-cachectic Parp-$2^{-/-}$ animals compared to non-cachectic wild type controls (Figures 2A and 2B). Expression levels of miR-133 were upregulated in the diaphragm of both groups of non-cachectic knockout mice compared to non-cachectic wild type control animals. Nevertheless, in the gastrocnemius of non-cachectic Parp-$1^{-/-}$ and Parp-$2^{-/-}$ controls, levels of miR-133 were down-regulated compared to non-cachectic wild type control animals (Figures 2C and 2D). Compared to wild type control animals, diaphragm and gastrocnemius of both groups of non-cachectic knockout mice showed an increase in miR-206 expression (Figures 3A and 3B). Levels of miR-486 were down-regulated in the diaphragm and gastrocnemius of non-cachectic control Parp-$1^{-/-}$ animals compared to non-cachectic control wild type rodents (Figures 3C and 3D). However, in the diaphragm of non-cachectic Parp-$2^{-/-}$ animals, expression levels of miR-486 were increased compared to wild type mice, while in the gastrocnemius were decreased (Figures 3C and 3D).

3.5. Protein acetylation levels in respiratory and limb muscles

LC-induced cachexia. Compared to non-cachectic wild type controls, total protein acetylation levels were increased in both respiratory and limb muscles of cachectic wild type rodents (Figures 4A, 4B, and E3). Total protein acetylation levels in both muscles did not show any significant difference between cachectic and non-cachectic animals in any of the knockout groups of mice (Figures 4A, 4B, and E3). Acetylated FoxO1 content was increased in the diaphragm but not in the limb muscle of wild type cachectic mice compared to their non-cachectic controls (Figures 4C, 4D, and E4). Acetylated FoxO1 levels did not differ between

cachectic and non-cachectic conditions in any muscle of the knockout groups of mice (Figures 4C, 4D, and E4).Compared to cachectic wild type controls, acetylated FoxO3 content was increased in both diaphragm and gastrocnemius muscles of cachectic wild type animals (Figures 4E, 4F, and E5). In Parp-$1^{-/-}$ mice, acetylated FoxO3 levels did not differ in any muscle between cachectic and non-cachectic conditions (Figures 4E, 4F, and E5). Compared to non-cachectic Parp-$2^{-/-}$ mice, acetylated levels of FoxO3 were decreased in the diaphragm of cachectic Parp-$2^{-/-}$ animals, while no differences between these two groups were seen in the gastrocnemius (Figure 4E, 4F, and E5). Acetylated levels of PGC-1α did not significantly differ between cachectic and non-cachectic conditions in either wild type or any of the two groups of knockout mice in any study muscle (Figures 4G, 4H, and E6).

Effects of PARP deletion on non-cachectic control animals. Total protein acetylation levels, and acetylated levels of FoxO1, FoxO3, and PGC-1αdid not significantly differ between non-cachectic wild type and either Parp-$1^{-/-}$ or Parp-$2^{-/-}$ non-cachectic control mice in any muscle (Figures 4A-4H, and E3-E6).

3.6. Histone deacetylase levels in respiratory and limb muscles

LC-induced cachexia. Compared to their respective non-cachectic controls, HDAC3 and HDAC6 levels were decreased in both respiratory and limb muscles of cachectic wild type rodents, whereas no differences were seen in any of the study muscles of the knockout cachectic animals (Figures 5A-5D, E7, and E8). SIRT1 levels were reduced in both muscles of cachectic wild type animals compared to their non-cachectic controls, while no differences were observed in any of the study muscles of the knockout cachectic animals (Parp-$1^{-/-}$ or Parp-$2^{-/-}$) compared to their respective non-cachectic rodents (Figures 5E, 5F, and E9). A significant positive correlation was found between HDAC3 and SIRT1 levels in the gastrocnemius of the cachectic wild type mice ($r=0.724$, $p=0.042$), but not in the knockout mice ($r=0.495$, $p=0.259$ and $r=-0.036$, $p=0.955$, Parp-$1^{-/-}$ and Parp-$2^{-/-}$ mice, respectively).

Effects of PARP deletion on non-cachectic control animals. HDAC3, HDAC6, and SIRT1 levels did not significantly differ between non-cachectic wild type and either Parp-$1^{-/-}$ or Parp-$2^{-/-}$ non-cachectic control mice in any study muscle (Figures 5A-5F, and E7-E9).

3.7. Myogenic transcription factors and downstream markers

LC-induced cachexia. In the diaphragm and gastrocnemius of cachectic wild type mice, protein levels of MEF2C and MEF2D were reduced compared to non-cachectic wild type controls (Figures 6A-6D, E10, and E11). MEF2C and MEF2D levels did not significantly differ between cachectic knockout animals and their respective non-tumor controls in any muscle (Figures 6A-6D, E10, and E11). YY1 levels were decreased in both muscles of the cachectic rodents compared to their respective non-cachectic controls (Figures 6E, 6F, and E12). Protein levels of α-actin and total PGC-1α did not significantly differ between cachectic and non-cachectic conditions in either wild type or any of the two groups of knockout mice in any study muscle (Figures 7A-7D, E13 and E14). Creatine kinase protein content was diminished in both muscles of cachectic wild type animals compared to their non-cachectic controls (Figures 7E-7F, and E15). Creatine kinase levels were decreased in the diaphragm but not in the gastrocnemius of both knockout cachectic mice (Parp-$1^{-/-}$ and Parp-$2^{-/-}$) compared to their respective non-cachectic controls (Figures 7E-7F, and E15).

Effects of PARP deletion on non-cachectic control animals. Protein levels of MEF2C and MEF2D did not differ between either non-cachectic Parp-$1^{-/-}$ or Parp-$2^{-/-}$ and non-cachectic wild type controls in any study muscle (Figures 6A-6D, E10 and E11). Compared to non-cachectic wild type animals, YY1 levels were reduced in the diaphragm of both groups of knockout mice, whereas no significant differences were observed in the gastrocnemius (Figures 6E, 6F and E12). Protein levels of α-actin and total PGC-1α did not significantly differ between non-cachectic wild type and either Parp-$1^{-/-}$ or Parp-$2^{-/-}$ non-cachectic control mice in any muscle (Figures 7A-7D, E13 and E14). Compared to non-cachectic wild type

rodents, creatine kinase protein content was reduced in the diaphragm of both non-cachectic knockout mice (Parp-$1^{-/-}$ and Parp-$2^{-/-}$), while no significant differences were observed in the gastrocnemius (Figures 7E-7F, and E15).

4. Discussion

Expression levels of the muscle-enriched miR-1, -133, -206, and -486 were significantly downregulated in both diaphragm and gastrocnemius muscles of wild type LC cachectic mice compared to the non-cachectic wild type rodents. These findings are in agreement with those reported in previous investigations conducted on patients with severe COPD [26], in whom miR-1 levels were reduced in the vastus lateralis, and those of miR-1, -133, and -206 that were decreased in the diaphragm of patients with moderate COPD [41]. Interestingly, muscle-enriched microRNAs target different cellular pathways that are involved in myogenesis in different models[9,11,41-43].

In the current investigation, compared to the non-tumor bearing animals, the diaphragm of LC cachectic Parp-$1^{-/-}$ mice showed a decreased expression of miR1, -133, or -206 while miR-486 expression did not differ between these two groups of rodents. In the gastrocnemius muscle, cachectic Parp-$1^{-/-}$ mice only exhibited a significant downregulation of miR-1, but not of the other muscle-enriched microRNAs, compared to their respective non-cachectic controls. Moreover, a significant correlation between the size of type II fibersand miR-133 levels, which is predominantly expressed in fast-twitch fibers together with miR-1[62], was also found in the gastrocnemius of LC cachectic wild type mice, and such a correlation was lost in the cachectic knockout animals. In the diaphragm of LC cachectic Parp-$2^{-/-}$ mice, muscle-enriched miR-1, -133, -206, or -486 were also downregulated compared to their respective non-cachectic Parp-$2^{-/-}$ rodents. In the limb muscle, expression of the same

microRNAs was also downregulated in Parp-2$^{-/-}$ cachectic mice, except for miR-206 whose levels did not differ between cachectic and non-cachectic animals in the limb muscle.

Expression of miR-133 induces myoblast proliferation by inhibiting myotube formation, miR-486 is involved in hypertrophy, and miR-1 and -206 promote cell differentiation and innervation[11,14,26,34,39]through several downstream mechanisms that favor protein synthesis and muscle growth [43]. The mechanisms accounting for the regulation of PARP-1 and -2 on the expression of muscle-enriched microRNAs have not been so far demonstrated. Indeed, the current study is the first to report a potential association between PARP-1 and -2 expressions and muscle-specific microRNAs in a model of cancer cachexia. Nonetheless, in view of the present findings, it could be hypothesized that particularly in the gastrocnemius of LC cachectic mice, PARP-1 inhibition most likely favorsmuscle proliferation and differentiation (miR-133, miR-206, and miR-486) processes, while PARP-2 may rather promote muscle differentiation (miR-206). In the diaphragm, PARP-1 deletion favored the expression of miR-486, whereas no significant effects on microRNA expression were seen in LC cachectic Parp-2 $^{-/-}$ animals.

Taken together, these findings suggest that PARP-1 rather than PARP-2 inhibition seems to exert more beneficial effects on muscle-enriched microRNA expression of cachectic limb muscles in this specific animal model of LC cachexia. In fact, PARP-1 has been demonstrated to interact with nuclear factor (NF)-κB [23,36], and the transcriptional activity of NF-κB was recently shown to increase in the gastrocnemius muscle inthe animals of the same model of cancer cachexia[12]. On this basis, it is likely that inhibition of PARP activity, especially of PARP-1, may have prevented a further decrease in the expression of muscle-specific microRNAs by blocking NF-κB activity, particularly in the limb muscle of the cachectic animals. Differences in the activity between respiratory and limb muscles, despite their similar fiber type composition, and in the contribution to total body and muscle mass loss of

each type of muscle may account for the differential pattern of muscle-specific microRNA expression observed in muscles of Parp-$1^{-/-}$ mice. Conclusively, the prevention of a further downregulation of the expression of these muscle-specific microRNAs may partly account for the improvement in body weight and limb muscle force lose observed in both groups of knockout mice with cancer cachexia compared to tumor-bearing wild type mice.

Interestingly, in order to assess the potential effects of either PARP-1 or -2 deficiencies on both types of muscles under normal conditions, levels of the different markers were also statistically analyzed in non-cachectic control muscles of all the study groups. In this regard, in the diaphragm, non-cachectic Parp-$1^{-/-}$ mice exhibited a significant rise in miR-133 and -206 expressions, while miR-486 levels were downregulated compared to non-cachectic wild type animals. In the same muscle, the expression of miR-1, -133, -206, and -486 was upregulated in non-cachectic control Parp-$2^{-/-}$ mice compared to wild type mice, implying that both proliferation and differentiation processes were favored by PARP-2 inhibition in healthy diaphragms. In the gastrocnemius, PARP-1 deficiency induced a significant downregulation of miR-133 and -486 expressions, whereas PARP-2 deficiency led to an upregulation of miR-206 and to a concomitant downregulation of miR-486 in non-cachectic animals compared to control wild type mice. PARP-2 deficiency rather than PARP-1 seemed to exert more beneficial effects in terms of muscle-enriched microRNA upregulation in non-cachectic muscles, particularly in the diaphragm. The elucidation of the mechanisms whereby either PARP-1 or -2 deletions may differentially regulate the expression of muscle-enriched microRNAs in respiratory and limb muscles under normal conditions (no underlying disease) is beyond the scope of the current study and should be the subject of future research.

Hyperacetylation of proteins, which relies to a great extent on histone deacetylase (HDAC) activity, may lead to muscle mass loss by rendering proteins more prone to degradation by the action of histone acetyl transferases that may have ubiquitin-ligase activity

and by dissociation of proteins from cellular chaperones [1]. In the current study, in the respiratory and limb muscles of wild type LC cachectic animals compared to their respective non-cachectic controls, total protein acetylation levels were increased, while those of HDAC3, HDAC6, and SIRT1 were reduced. These findings are in agreement with previous investigations, in which levels of HDAC3 and HDAC6 and SIRT1 were also reduced in models of muscle wasting[2,43,49]. Collectively, these findings imply that reduced HDAC activity drives protein hyperacetylation in skeletal muscles in models of muscle wasting[2,43,49]. Importantly, in Parp-$1^{-/-}$ and Parp-$2^{-/-}$ mice, protein acetylation levels did not significantly differ between cancer cachexia and non-cachetic control conditions in respiratory or limb muscles, thus suggesting that PARP-1 and -2 deficiencies have prevented these muscles from undergoing further protein acetylation. Importantly, the content of HDAC3, HDAC6, and SIRT1 showed no statistically significant difference in either diaphragm or gastrocnemius muscles between cancer cachectic and non-cachectic controls in Parp-$1^{-/-}$ and Parp-$2^{-/-}$ mice. Clearly, these results point towards a beneficial effect of PARP-1 and -2 deficiencies on HDAC content in skeletal muscles in LC cachexia. The absence of HDAC3, HDAC6, and SIRT1 downregulation together with the absence of a rise in protein hyperacetylation levels in Parp-$1^{-/-}$ and Parp-$2^{-/-}$ cancer cachectic mice may greatly account for the improvements seen in these animals in terms of body and muscle weights, limb muscle strength, and fiber sizes compared to differences observed in the wild type cachectic rodents.

Furthermore, the levels of acetylation of specific transcription factors were also measured in the current study. Interestingly, compared to non-cachectic animals, in wild type LC cachectic mice, acetylation levels of FoxO3 were significantly increased in the diaphragm and gastrocnemius, while a rise in acetylated FoxO1 levels was only seen in the respiratory muscle of the same rodents. Acetylated levels of PGC-1alpha did not vary between cachectic and non-cachectic mice in any of the experimental groups. Importantly, in Parp-$1^{-/-}$ and Parp-

$2^{-/-}$ mice, no significant differences were seen in FoxO1 and FoxO3 acetylation levels. These findings suggest that acetylation of these atrophy signaling pathways, particularly of the latter, favors muscle protein loss as shown in other models [52], which may have been partly prevented by PARP1/2 inhibition in this study.

Myogenic regulatory factors control myogenesis and muscle remodeling in response to injury in adult muscles. Furthermore, they may also orchestrate muscle phenotype by determining the fiber type of a given muscle. For instance, MEF2 family of transcription factors plays a relevant role in muscle phenotype determination of fast- and slow-twitch muscle fibers in mice [40]. Importantly, MEF2 is regulated by acetylation and deacetylation mediated by class II HDACs that can directly bind and inhibit MEF2-regulated transcription of genes [61]. In the present study, protein levels of MEF2C and MEF2D were significantly decreased in the wild type cachectic mice compared to the non-cachectic control rodents. Nonetheless, in Parp-$1^{-/-}$ and Parp-$2^{-/-}$ cancer cachectic mice, MEF2C and MEF2D levels did not significantly differ in either respiratory or limb muscles from those detected in the non-cachectic control knockout mice. Interestingly, these findings are also in line with the lack of statistically significant differences in HDAC3 and HDAC6 levels observed between tumor-bearing and control animals deficient in PARP-1 and -2 proteins. Taken together, these results indicate that muscle fiber type composition was not modified in any of the study groups or experimental conditions, and the size of slow- and fast-twitch muscle fibers improved in Parp-$1^{-/-}$ and Parp-$2^{-/-}$ cancer cachectic mice compared to the tumor-bearing wild type rodents.

YY1 is a transcription factor involved in histone modification and in the inhibition of muscle regeneration through the transcriptional silencing of myofibrillar genes [56]. Moreover, in a previous study [35], protein levels of YY1 inversely correlated with the reduced size of slow- and fast-twitch muscle fibers in the vastus lateralis of patients with COPD. In the current investigation, YY1 levels were significantly reduced in the cachectic

animals compared to non-cachectic controls in the three experimental groups. Besides, as deficiency of PARP-1 and -2 induced an increase in the size of slow- and fast-twitch fibers in both muscles in cachectic animals (no significant differences were observed between cancer cachectic and non-cachectic control mice), it is likely that reduced levels of YY1 may have partly contributed to the improvement in the fiber sizes of those muscles.

Interestingly, levels of muscle creatine kinase protein, which is regulated by YY1 [55] and MEF2 [60], but not those of actin or PGC-1α,were significantly reduced in the diaphragm and gastrocnemius of wild type cachectic animals compared to the controls as previously shown to occur in diaphragm [29]and quadriceps of cachectic patients with COPD and LC [44]. Inhibition of PARP-1 and -2 induced similar effects in both muscles of the tumor bearing mice: while creatine kinase protein content remained significantly lower than in the controls, such a decrease was attenuated in the gastrocnemius of the knockout cachectic mice. Furthermore, creatine kinase levels also significantly decreased in the non-tumor knockout animals compared to the healthy wild type controls. Collectively, these findings suggest that the regulation of creatine kinase in the diaphragm is likely to be mediated by YY1 (similar pattern of expression) in both non-tumor and tumor-bearing mice of wild type and knockout groups, while PARP-1 and -2 predominantly restored creatine kinase levels in the limb muscle as shown to occur in other models [13].

4.2. Study critique

It is likely that the 30-40% reduction in tumor burdenobserved in both groups of knockout mice may have partly contributed to favoring body and muscle mass gain in the rodents, albeit tumors did express PARP-1 and -2 proteins. In fact, inhibition of both PARP-1 and -2 induced a reduction in tumor weights in the animals. Moreover, tumor growth as measured by ki-67 (cell proliferation marker) significantly decreased in the cachectic knockout mice, while levels of the proapoptotic bax and autophagy marker rose in the tumors of the same rodents

compared to wild type mice.Tumor levels of SIRT1 protein, however, did not significantly differ among the study groups. It is likely that other pathways may signal autophagy in this study as shown in other models[24]. The mechanisms whereby PARP-1 and -2 inhibition in the host may contribute to reducing tumor burden of adenocarcinoma cells that express both molecules remain to be elucidated in future studies, as they are beyond the scope of the current investigation. However, recent data from our group (submitted) point towards a paramount role of depletion of major antioxidants and increased oxidative stress levels, which may have further promoted apoptosis and autophagy of the cancer cells in the Parp-$1^{-/-}$ and Parp-$2^{-/-}$ mice. On the other hand, reduction of tumor burden after cancer resection was also shown to improve muscle atrophy and protein catabolism in actual cancer patients [58], suggesting that this factor also plays a relevant role in the improvement of muscle wasting.

Another limitation is related to the lack of measurements on the progression of tumor size throughout the study protocol in the tumor-bearing animals. In the study, tumor weights were only available at the time of sacrifice in all experimental groups. Nonetheless, the tumors induced by the lung adenocarcinoma cells (LP07) used in the current investigation, have been thoroughly characterized, especially tumor growth and kineticsin previous studies [17,18,37,53].

The study of other limb muscles would have also been of interest. However, our specific goal was to analyze a limb muscle of similar fiber type composition as that of the main respiratory muscle, the diaphragm.In the gastrocnemius of LC cachectic Parp-$1^{-/-}$ mice, the large variability of the muscle fiber sizes especially of the fast-twitch fibers, which did not statistically differ from those in their respective non-cachectic controls, may account for the absence of a correspondence between these parameters and the significantly smaller size of the muscle.Despite that lipid or water content within the myofibers could have also been contributing factors, no actual water vacuoles or lipid accumulation was found within the

muscle fibers of the animals in the study groups (data not shown). As in previous investigations [4-6], the analysis of other markers involved in muscle metabolism such as mitochondrial respiratory chain function in response to PARP-1 and -2 inhibition will be of interest in future research. Indeed, a previous study from our group showed alterations of oxygen uptake and respiratory chain complexes in both diaphragm and gastrocnemius of wild type cancer cachectic mice that were partially restored in response to several pharmacological agents[21].

Future research should focus on the assessment of whether selective pharmacological inhibitors of PARP-1 and -2 exert similar beneficial effects on muscles in models of cancer cachexia and eventually in patients with cancer cachexia for whom currently available therapies are scarce[38,47,48].

4.3. Conclusions

PARP-1 rather than PARP-2 inhibition seems to exert more beneficial effects on muscle-enriched microRNA expressionparticularly in the gastrocnemius in this specific animal model of LC cachexia. Furthermore, in both groups of knockout animals, the rise in protein acetylation levels and that of transcription factors in diaphragm and gastrocnemius of the tumor-bearing rodents was attenuated probably through improvements in HDAC3 and SIRT1 levels. Also, in both groups of Parp-$1^{-/-}$ and Parp-$2^{-/-}$ LC cachectic mice, the decrease in myogenic regulatory factors seen in the wild type cancer cachectic animals was mitigated in their respiratory and limb muscles. These molecular features may partly account for the improvements seen in the mouse phenotype as defined by body and muscle weights, limb muscle force and fiber sizes in both Parp-$1^{-/-}$ and Parp-$2^{-/-}$ cancer cachectic mice, which imply a potential clinical applicability of selective inhibition of PARP-1 and -2 to be tested in future studies. Indeed, currently available drugs, e.g. olaparib, inhibit PARP-1/2 activities. Evidence

from the present investigation should prompt research on the potential beneficial effects and safety concerns of pharmacological PARP-1/2 inhibitors on muscle mass loss and wasting.

ACKNOWLEDGEMENTS

The authors are thankful to Mr. Francisco Sanchez for his technical assistance with the animal experiments and to Ms. Coral Ampurdanes for her contribution to mouse genotyping.

Authors' conflicts of interest in relation to the study: None to declare.

Editorial support: None to declare.

This study has been supported by CIBERES, FIS 11/02029, FIS 14/00713; SEPAR 2013; FUCAP 2011; FUCAP 2012, and *Fundació La Marató de TV3* (2013-4130).

Reference List

1. N. Alamdari, Z. Aversa, E. Castillero, and P.O. Hasselgren, Acetylation and deacetylation--novel factors in muscle wasting, Metabolism 62 (2013) pp. 1-11.

2. N. Alamdari, I.J. Smith, Z. Aversa, and P.O. Hasselgren, Sepsis and glucocorticoids upregulate p300 and downregulate HDAC6 expression and activity in skeletal muscle, Am. J. Physiol Regul. Integr. Comp Physiol 299 (2010) p. R509-R520.

3. S. Aoufouchi, Monoclonal Antibodies A4.3; A6.4.12; B5.3.9; B15.4.13 Anti-Poly(ADP-Ribose) Polymerase., 1997, p. 583.

4. P. Bai, C. Canto, A. Brunyanszki, A. Huber, M. Szanto, Y. Cen, H. Yamamoto, S.M. Houten, B. Kiss, H. Oudart, P. Gergely, M.J. Menissier-de, V. Schreiber, A.A. Sauve, and J. Auwerx, PARP-2 regulates SIRT1 expression and whole-body energy expenditure, Cell Metab 13 (2011) pp. 450-460.

5. P. Bai, C. Canto, H. Oudart, A. Brunyanszki, Y. Cen, C. Thomas, H. Yamamoto, A. Huber, B. Kiss, R.H. Houtkooper, K. Schoonjans, V. Schreiber, A.A. Sauve, M.J. Menissier-de, and J. Auwerx, PARP-1 inhibition increases mitochondrial metabolism through SIRT1 activation, Cell Metab 13 (2011) pp. 461-468.

6. P. Bai, L. Nagy, T. Fodor, L. Liaudet, and P. Pacher, Poly(ADP-ribose) polymerases as modulators of mitochondrial activity, Trends Endocrinol. Metab 26 (2015) pp. 75-83.

7. E. Barreiro, V. Bustamante, P. Cejudo, J.B. Galdiz, J. Gea, L.P. de, J. Martinez-Llorens, F. Ortega, L. Puente-Maestu, J. Roca, and J.M. Rodriguez-Gonzalez Moro, Guidelines for the Evaluation and Treatment of Muscle Dysfunction in Patients With Chronic Obstructive Pulmonary Disease, Arch. Bronconeumol. 51 (2015) pp. 384-395.

8. E. Barreiro, L. del Puerto-Nevado, E. Puig-Vilanova, S. Perez-Rial, F. Sanchez, L. Martinez-Galan, S. Rivera, J. Gea, N. Gonzalez-Mangado, and G. Peces-Barba, Cigarette smoke-induced oxidative stress in skeletal muscles of mice, Respir. Physiol Neurobiol. 182 (2012) pp. 9-17.

9. E. Barreiro and J. Gea, Epigenetics and muscle dysfunction in chronic obstructive pulmonary disease, Transl. Res. 165 (2015) pp. 61-73.

10. E. Barreiro, J. Marin-Corral, F. Sanchez, V. Mielgo, F.J. Alvarez, J.B. Galdiz, and J. Gea, Reference values of respiratory and peripheral muscle function in rats, J. Anim Physiol Anim Nutr. (Berl) 94 (2010) p. e393-e401.

11. E. Barreiro and J.I. Sznajder, Epigenetic regulation of muscle phenotype and adaptation: a potential role in COPD muscle dysfunction, J. Appl. Physiol (1985.) 114 (2013) pp. 1263-1272.

12. A. Chacon-Cabrera, C. Fermoselle, A.J. Urtreger, M. Mateu-Jimenez, M.J. Diament, E.D. De Kier Joffe, M. Sandri, and E. Barreiro, Pharmacological strategies in lung cancer-induced cachexia: effects on muscle proteolysis, autophagy, structure, and weakness, J. Cell Physiol 229 (2014) pp. 1660-1672.

13. J. Chen, Y. Sun, X. Mao, Q. Liu, H. Wu, and Y. Chen, RANKL up-regulates brain-type creatine kinase via poly(ADP-ribose) polymerase-1 during osteoclastogenesis, J. Biol. Chem. 285 (2010) pp. 36315-36321.

14. J.F. Chen, E.M. Mandel, J.M. Thomson, Q. Wu, T.E. Callis, S.M. Hammond, F.L. Conlon, and D.Z. Wang, The role of microRNA-1 and microRNA-133 in skeletal muscle proliferation and differentiation, Nat. Genet. 38 (2006) pp. 228-233.

15. J.M. de Murcia, C. Niedergang, C. Trucco, M. Ricoul, B. Dutrillaux, M. Mark, F.J. Oliver, M. Masson, A. Dierich, M. LeMeur, C. Walztinger, P. Chambon, and M.G. de, Requirement of poly(ADP-ribose) polymerase in recovery from DNA damage in mice and in cells, Proc. Natl. Acad. Sci. U. S. A 94 (1997) pp. 7303-7307.

16. M.G. de, V. Schreiber, M. Molinete, B. Saulier, O. Poch, M. Masson, C. Niedergang, and M.J. Menissier de, Structure and function of poly(ADP-ribose) polymerase, Mol. Cell Biochem. 138 (1994) pp. 15-24.

17. M.J. Diament, C. Garcia, I. Stillitani, V.M. Saavedra, T. Manzur, L. Vauthay, and S. Klein, Spontaneous murine lung adenocarcinoma (P07): A new experimental model to study paraneoplastic syndromes of lung cancer, Int. J. Mol. Med. 2 (1998) pp. 45-50.

18. M.J. Diament, G.D. Peluffo, I. Stillitani, L.C. Cerchietti, A. Navigante, S.M. Ranuncolo, and S.M. Klein, Inhibition of tumor progression and paraneoplastic syndrome development in a murine lung adenocarcinoma by medroxyprogesterone acetate and indomethacin, Cancer Invest 24 (2006) pp. 126-131.

19. W.J. Evans, J.E. Morley, J. Argiles, C. Bales, V. Baracos, D. Guttridge, A. Jatoi, K. Kalantar-Zadeh, H. Lochs, G. Mantovani, D. Marks, W.E. Mitch, M. Muscaritoli, A. Najand, P. Ponikowski, F.F. Rossi, M. Schambelan, A. Schols, M. Schuster, D. Thomas, R. Wolfe, and S.D. Anker, Cachexia: a new definition, Clin. Nutr. 27 (2008) pp. 793-799.

20. K. Fearon, F. Strasser, S.D. Anker, I. Bosaeus, E. Bruera, R.L. Fainsinger, A. Jatoi, C. Loprinzi, N. MacDonald, G. Mantovani, M. Davis, M. Muscaritoli, F. Ottery, L. Radbruch, P. Ravasco, D. Walsh, A. Wilcock, S. Kaasa, and V.E. Baracos, Definition and classification of cancer cachexia: an international consensus, Lancet Oncol. 12 (2011) pp. 489-495.

21. C. Fermoselle, E. Garcia-Arumi, E. Puig-Vilanova, A.L. Andreu, A.J. Urtreger, E.D. De Kier Joffe, A. Tejedor, L. Puente-Maestu, and E. Barreiro, Mitochondrial dysfunction and therapeutic approaches in respiratory and limb muscles of cancer cachectic mice, Exp. Physiol 98 (2013) pp. 1349-1365.

22. C. Fermoselle, F. Sanchez, and E. Barreiro, [Reduction of muscle mass mediated by myostatin in an experimental model of pulmonary emphysema], Arch. Bronconeumol. 47 (2011) pp. 590-598.

23. P.O. Hassa and M.O. Hottiger, A role of poly (ADP-ribose) polymerase in NF-kappaB transcriptional activation, Biol. Chem. 380 (1999) pp. 953-959.

24. J. Kim, M. Kundu, B. Viollet, and K.L. Guan, AMPK and mTOR regulate autophagy through direct phosphorylation of Ulk1, Nat. Cell Biol. 13 (2011) pp. 132-141.

25. V. Leiro-Fernandez, C. Mouronte-Roibas, C. Ramos-Hernandez, M. Botana-Rial, A. Gonzalez-Pineiro, E. Garcia-Rodriguez, C. Represas-Represas, and A. Fernandez-Villar, Changes in clinical presentation and staging of lung cancer over two decades, Arch. Bronconeumol. 50 (2014) pp. 417-421.

26. A. Lewis, J. Riddoch-Contreras, S.A. Natanek, A. Donaldson, W.D. Man, J. Moxham, N.S. Hopkinson, M.I. Polkey, and P.R. Kemp, Downregulation of the serum response factor/miR-1 axis in the quadriceps of patients with COPD, Thorax 67 (2012) pp. 26-34.

27. K.J. Livak and T.D. Schmittgen, Analysis of relative gene expression data using real-time quantitative PCR and the 2(-Delta Delta C(T)) Method, Methods 25 (2001) pp. 402-408.

28. J. Marin-Corral, C.C. Fontes, S. Pascual-Guardia, F. Sanchez, M. Olivan, J.M. Argiles, S. Busquets, F.J. Lopez-Soriano, and E. Barreiro, Redox balance and carbonylated proteins in limb and heart muscles of cachectic rats, Antioxid. Redox. Signal. 12 (2010) pp. 365-380.

29. J. Marin-Corral, J. Minguella, A.L. Ramirez-Sarmiento, S.N. Hussain, J. Gea, and E. Barreiro, Oxidised proteins and superoxide anion production in the diaphragm of severe COPD patients, Eur. Respir. J. 33 (2009) pp. 1309-1319.

30. J.J. McCarthy and K.A. Esser, MicroRNA-1 and microRNA-133a expression are decreased during skeletal muscle hypertrophy, J. Appl. Physiol 102 (2007) pp. 306-313.

31. J.J. McCarthy, K.A. Esser, C.A. Peterson, and E.E. Dupont-Versteegden, Evidence of MyomiR network regulation of beta-myosin heavy chain gene expression during skeletal muscle atrophy, Physiol Genomics 39 (2009) pp. 219-226.

32. M.J. Menissier de, M. Ricoul, L. Tartier, C. Niedergang, A. Huber, F. Dantzer, V. Schreiber, J.C. Ame, A. Dierich, M. LeMeur, L. Sabatier, P. Chambon, and M.G. de, Functional interaction between PARP-1 and PARP-2 in chromosome stability and embryonic development in mouse, EMBO J. 22 (2003) pp. 2255-2263.

33. K.T. Murphy, A. Chee, J. Trieu, T. Naim, and G.S. Lynch, Importance of functional and metabolic impairments in the characterization of the C-26 murine model of cancer cachexia, Dis. Model. Mech. 5 (2012) pp. 533-545.

34. N. Nakajima, T. Takahashi, R. Kitamura, K. Isodono, S. Asada, T. Ueyama, H. Matsubara, and H. Oh, MicroRNA-1 facilitates skeletal myogenic differentiation without affecting osteoblastic and adipogenic differentiation, Biochem. Biophys. Res. Commun. 350 (2006) pp. 1006-1012.

35. S.A. Natanek, J. Riddoch-Contreras, G.S. Marsh, N.S. Hopkinson, W.D. Man, J. Moxham, M.I. Polkey, and P.R. Kemp, Yin Yang 1 expression and localisation in quadriceps muscle in COPD, Arch. Bronconeumol. 47 (2011) pp. 296-302.

36. F.J. Oliver, M.J. Menissier-de, C. Nacci, P. Decker, R. Andriantsitohaina, S. Muller, G. de la Rubia, J.C. Stoclet, and M.G. de, Resistance to endotoxic shock as a consequence of defective NF-kappaB activation in poly (ADP-ribose) polymerase-1 deficient mice, EMBO J. 18 (1999) pp. 4446-4454.

37. G.D. Peluffo, I. Stillitani, V.A. Rodriguez, M.J. Diament, and S.M. Klein, Reduction of tumor progression and paraneoplastic syndrome development in murine lung adenocarcinoma by nonsteroidal antiinflammatory drugs, Int. J. Cancer 110 (2004) pp. 825-830.

38. J.C. Penalver Cuesta, A.C. Jorda, F.N. Mancheno, J.A. Ceron Navarro, Q.K. de Aguiar, M.M. Arraras, F.J. Vera Sempere, and J.D. Padilla Alarcon, Prognostic Factors in Non-Small Cell Lung Cancer Less than 3 Centimeters: Actuarial Analysis, Accumulative Incidence and Risk Groups, Arch. Bronconeumol. (2015).

39. E. Perdiguero, P. Sousa-Victor, E. Ballestar, and P. Munoz-Canoves, Epigenetic regulation of myogenesis, Epigenetics. 4 (2009) pp. 541-550.

40. M.J. Potthoff, H. Wu, M.A. Arnold, J.M. Shelton, J. Backs, J. McAnally, J.A. Richardson, R. Bassel-Duby, and E.N. Olson, Histone deacetylase degradation and MEF2 activation promote the formation of slow-twitch myofibers, J. Clin. Invest 117 (2007) pp. 2459-2467.

41. E. Puig-Vilanova, R. Aguilo, A. Rodriguez-Fuster, J. Martinez-Llorens, J. Gea, and E. Barreiro, Epigenetic mechanisms in respiratory muscle dysfunction of patients with chronic obstructive pulmonary disease, PLoS. One. 9 (2014) p. e111514.

42. E. Puig-Vilanova, P. Ausin, J. Martinez-Llorens, J. Gea, and E. Barreiro, Do epigenetic events take place in the vastus lateralis of patients with mild chronic obstructive pulmonary disease?, PLoS. One. 9 (2014) p. e102296.

43. E. Puig-Vilanova, J. Martinez-Llorens, P. Ausin, J. Roca, J. Gea, and E. Barreiro, Quadriceps muscle weakness and atrophy are associated with a differential epigenetic profile in advanced COPD, Clin. Sci. (Lond) 128 (2015) pp. 905-921.

44. E. Puig-Vilanova, D.A. Rodriguez, J. Lloreta, P. Ausin, S. Pascual-Guardia, J. Broquetas, J. Roca, J. Gea, and E. Barreiro, Oxidative stress, redox signaling pathways, and autophagy in cachectic muscles of male patients with advanced COPD and lung cancer, Free Radic. Biol. Med. 79C (2014) pp. 91-108.

45. D. Quenet, R.R. El, V. Schreiber, and F. Dantzer, The role of poly(ADP-ribosyl)ation in epigenetic events, Int. J. Biochem. Cell Biol. 41 (2009) pp. 60-65.

46. B.M. Roberts, B. Ahn, A.J. Smuder, M. Al-Rajhi, L.C. Gill, A.W. Beharry, S.K. Powers, D.D. Fuller, L.F. Ferreira, and A.R. Judge, Diaphragm and ventilatory dysfunction during cancer cachexia, FASEB J. 27 (2013) pp. 2600-2610.

47. M. Rodriguez, M.T. Gomez Hernandez, N.M. Novoa, J.L. Aranda, M.F. Jimenez, and G. Varela, Morbidity and mortality in octogenarians with lung cancer undergoing pneumonectomy, Arch. Bronconeumol. 51 (2015) pp. 219-222.

48. M. Rodriguez, M.T. Gomez Hernandez, N.M. Novoa, J.L. Aranda, M.F. Jimenez, and G. Varela, Poorer Survival in Stage IB Lung Cancer Patients After Pneumonectomy, Arch. Bronconeumol. 51 (2015) pp. 223-226.

49. K. Sadoul, C. Boyault, M. Pabion, and S. Khochbin, Regulation of protein turnover by acetyltransferases and deacetylases, Biochimie 90 (2008) pp. 306-312.

50. P. Sanchez-Salcedo, J. Berto, J.P. de-Torres, A. Campo, A.B. Alcaide, G. Bastarrika, J.C. Pueyo, A. Villanueva, J.I. Echeveste, M.D. Lozano, M.J. Garcia-Velloso, L.M. Seijo, J. Garcia, W. Torre, M.J. Pajares, R. Pio, L.M. Montuenga, and J.J. Zulueta, Lung cancer screening: fourteen year experience of the Pamplona early detection program (P-IELCAP), Arch. Bronconeumol. 51 (2015) pp. 169-176.

51. M. Toledo, S. Busquets, S. Sirisi, R. Serpe, M. Orpi, J. Coutinho, R. Martinez, F.J. Lopez-Soriano, and J.M. Argiles, Cancer cachexia: physical activity and muscle force in tumour-bearing rats, Oncol. Rep. 25 (2011) pp. 189-193.

52. A.H. Tseng, L.H. Wu, S.S. Shieh, and D.L. Wang, SIRT3 interactions with FOXO3 acetylation, phosphorylation and ubiquitinylation mediate endothelial cell responses to hypoxia, Biochem. J. 464 (2014) pp. 157-168.

53. A.J. Urtreger, M.J. Diament, S.M. Ranuncolo, C. Del, V, L.I. Puricelli, S.M. Klein, and E.D. De Kier Joffe, New murine cell line derived from a spontaneous lung tumor induces paraneoplastic syndromes, Int. J. Oncol. 18 (2001) pp. 639-647.

54. A. Vignaud, A. Ferry, A. Huguet, M. Baraibar, C. Trollet, J. Hyzewicz, G. Butler-Browne, J. Puymirat, G. Gourdon, and D. Furling, Progressive skeletal muscle weakness in transgenic mice expressing CTG expansions is associated with the activation of the ubiquitin-proteasome pathway, Neuromuscul. Disord. 20 (2010) pp. 319-325.

55. C.K. Vincent, A. Gualberto, C.V. Patel, and K. Walsh, Different regulatory sequences control creatine kinase-M gene expression in directly injected skeletal and cardiac muscle, Mol. Cell Biol. 13 (1993) pp. 1264-1272.

56. H. Wang, E. Hertlein, N. Bakkar, H. Sun, S. Acharyya, J. Wang, M. Carathers, R. Davuluri, and D.C. Guttridge, NF-kappaB regulation of YY1 inhibits skeletal myogenesis through transcriptional silencing of myofibrillar genes, Mol. Cell Biol. 27 (2007) pp. 4374-4387.

57. L.A. Whittemore, K. Song, X. Li, J. Aghajanian, M. Davies, S. Girgenrath, J.J. Hill, M. Jalenak, P. Kelley, A. Knight, R. Maylor, D. O'Hara, A. Pearson, A. Quazi, S. Ryerson, X.Y. Tan, K.N. Tomkinson, G.M. Veldman, A. Widom, J.F. Wright, S. Wudyka, L. Zhao, and N.M. Wolfman, Inhibition of myostatin in adult mice increases skeletal muscle mass and strength, Biochem. Biophys. Res. Commun. 300 (2003) pp. 965-971.

58. J.P. Williams, B.E. Phillips, K. Smith, P.J. Atherton, D. Rankin, A.L. Selby, S. Liptrot, J. Lund, M. Larvin, and M.J. Rennie, Effect of tumor burden and subsequent surgical resection on skeletal muscle mass and protein turnover in colorectal cancer patients, Am. J. Clin. Nutr. 96 (2012) pp. 1064-1070.

59. J. Yelamos, J. Farres, L. Llacuna, C. Ampurdanes, and J. Martin-Caballero, PARP-1 and PARP-2: New players in tumour development, Am. J. Cancer Res. 1 (2011) pp. 328-346.

60. A. Zetser, E. Gredinger, and E. Bengal, p38 mitogen-activated protein kinase pathway promotes skeletal muscle differentiation. Participation of the Mef2c transcription factor, J. Biol. Chem. 274 (1999) pp. 5193-5200.

61. C.L. Zhang, T.A. McKinsey, and E.N. Olson, Association of class II histone deacetylases with heterochromatin protein 1: potential role for histone methylation in control of muscle differentiation, Mol. Cell Biol. 22 (2002) pp. 7302-7312.

62. D. Zhang, X. Wang, Y. Li, L. Zhao, M. Lu, X. Yao, H. Xia, Y.C. Wang, M.F. Liu, J. Jiang, X. Li, and H. Ying, Thyroid hormone regulates muscle fiber type conversion via miR-133a1, J. Cell Biol. 207 (2014) pp. 753-766.

FIGURE LEGENDS

Figure 1: Graphical representation of the progression of body weight in mice from all experimental groups. The following signs have been used in each group: non-cachectic control wild type animals (blue diamonds, N=10), LC cachectic wild type mice (squares, N=10), non-cachectic control Parp-$1^{-/-}$ rodents (triangles, N=8), LC cachectic Parp-$1^{-/-}$ mice (purple squares, N=12), non-cachectic control Parp-$2^{-/-}$ rodents (green squares, N=6), and LC cachectic Parp-$2^{-/-}$ animals (circles, N=6) over the study period (1 month).

Figure 2: Mean values and standard deviation of miR-1 (top panels, A and B) and miR-133a (bottom panels, C and D) expression in the diaphragm (left panels) and gastrocnemius (right panels) muscles. Statistical significance is represented as follows: *, $p \leq 0.05$, **, $p \leq 0.01$, ***, and $p \leq 0.001$ between either wild type, Parp-$1^{-/-}$, or Parp-$2^{-/-}$ LC cachectic mice and their respective non-cachectic control rodents; †, $p \leq 0.05$, and †††, $p \leq 0.001$ between any of the non-cachectic control knockout animals and non-cachectic wild type mice.

Figure 3: Mean values and standard deviation of miR-206 (top panels, A and B) and miR-486 (bottom panels, C and D) expression in the diaphragm (left panels) and gastrocnemius (right panels). Statistical significance is represented as follows: *, $p \leq 0.05$, **, $p \leq 0.01$, ***, $p \leq 0.001$, and n.s., non-significant differences between either wild type, Parp-$1^{-/-}$, or Parp-$2^{-/-}$ LC cachectic mice and their respective non-cachectic control rodents; †, $p \leq 0.05$, ††, $p \leq 0.01$, and †††, $p \leq 0.001$ between any of the non-cachectic control knockout animals and non-cachectic wild type mice. A significant correlation was found between type II fiber size and miR-133 expression in the gastrocnemius of the cachectic wild type mice. No significant correlations were observed between type II fiber size and miR-133 expression in the gastrocnemius of any of the cachectic knockout animals (panel E).

Figure 4: Mean values and standard deviation of total acetylated proteins (panels A and B), acetylated FoxO1 (panels C and D),acetylated FoxO3 (panels E and F), and acetylated PGC-

1α (panelsG and H) in the diaphragm (left panels) and gastrocnemius (right panels) muscles, as measured by optical densities in arbitrary units (OD, a.u.). Statistical significance is represented as follows: *, p≤0.05, **, p≤0.01, ***, p≤0.001, and n.s., non-significant differences between either wild type, Parp-$1^{-/-}$, or Parp-$2^{-/-}$ LC cachectic mice and their respective non-cachectic control animals.

Figure 5: Mean values and standard deviation of HDAC3 (top panels, A and B), HDAC6 (medium panels, C and D), and SIRT1 (bottom panels, E and F) in the diaphragm (left panels) and gastrocnemius (right panels) muscles, as measured by optical densities in arbitrary units (OD, a.u.). Statistical significance is represented as follows: *, p≤0.05, **, p≤0.01, and n.s., non-significant differences between either wild type, Parp-$1^{-/-}$, or Parp-$2^{-/-}$ LC cachectic mice and their respective non-cachectic control animals.

Figure 6: Mean values and standard deviation of the transcription factors MEF2C (top panels, A and B), MEF2D (medium panels, C and D), and YY1 (bottom panels, E and F) protein content in the diaphragm (left panels) and gastrocnemius (right panels) muscles, as measured by optical densities in arbitrary units (OD, a.u.). Statistical significance is represented as follows: *, p≤0.05, **, p≤0.01, ***, p≤0.001, and n.s., non-significant differences between either wild type, Parp-$1^{-/-}$, or Parp-$2^{-/-}$ LC cachectic mice and their respective non-cachectic control animals; ††, p≤0.01 between any of the non-cachectic control knockout animals and non-cachectic wild type mice.

Figure 7: Mean values and standard deviation of α-actin skeletal muscle (top panels, A and B), total PGC-1α (medium panels, C and D), and creatine kinase (bottom panels, E and F) protein content in the diaphragm (left panels) and gastrocnemius (right panels) muscles, as measured by optical densities in arbitrary units (OD, a.u.). Statistical significance is represented as follows: *, p≤0.05, ***, p≤0.001, and n.s., non-significant differences between either wild type, Parp-$1^{-/-}$, or Parp-$2^{-/-}$ LC cachectic mice and their respective non-cachectic

control animals; ††, $p \leq 0.01$ between any of the non-cachectic control knockout animals and non-cachectic wild type mice.

Table 1. MicroRNA assays and probes used for the quantitative analyses of the target genes using real-time PCR.

Assay Name	**Assay ID**	**miRBase accession number**
Muscle-specific, myomiRs		
hsa-miR-1	002222	MIMAT0000416
hsa-miR-133a	002246	MIMAT0000427
hsa-miR-206	000510	MIMAT0000462
Other miRNAs (highly expressed in muscles)		
hsa-miR-486	001278	MIMAT0002177
		NCBI Accession number
U6 snRNA, housekeeping gene	001973	NR_004394

Abbreviations: ID, identification; hsa, homo sapiens; miR, microRNA; MIMAT, mature microRNA; snRNA, small nuclear RNA; NR, non-coding RNA RefSeq database category.

Table 2. Physiological characteristics of wild type, Parp-1$^{-/-}$, and Parp-2$^{-/-}$ mice at the end of the studyperiod.

	Wild type mice		Parp-1$^{-/-}$ mice		Parp-2$^{-/-}$ mice	
	Control	LC cachexia	Control	LC cachexia	Control	LC cachexia
Age at baseline (weeks)	10	10, n.s.	10	10, n.s.	10	10, n.s.
Body weight at baseline (g)	20.30 (1.03)	19.60 (1.13), n.s.	19.28 (0.78)	18.61 (0.93), n.s.	19.25 (1.06)	19.89 (0.92), n.s.
Body weight gain (%)	+8.35 (2.35)	-6.55 (6.80), ***	+6.96 (2.23)	+1.55 (3.69), **	+4.34 (2.87)	+3.06 (6.81), n.s.
Food intake (g/24h)	3.2 (0.5)	3.1 (0.4), n.s.	3.3 (0.6)	3.1 (0.4), n.s.	3.2 (0.4)	3.2 (0.3), n.s.
Diaphragm weight (g)	0.089 (0.01)	0.069 (0.008), ***	0.073 (0.01), ††	0.062 (0.007), *	0.076 (0.012), †	0.086 (0.013), n.s.
Gastrocnemius weight (g)	0.116 (0.005)	0.082 (0.008), ***	0.105 (0.003), ††	0.096 (0.007), ***	0.096 (0.012), †††	0.098 (0.012), n.s.
Limb strength gain (%)	+10.03 (8.96)	-12.85 (7.14), ***	+12.86 (8.13)	-0.45 (6.08), **	+3.33 (1.99)	+2.10 (5.40), n.s.

Variables are presented as mean (standard deviation).In all animals, body weight and limb strength gains were calculated as the percentage of the measurements performed at the end of the study period (30 days) with respect to the same measurements obtained at baseline.

Definition of abbreviations: Parp-1$^{-/-}$ and Parp-2$^{-/-}$, poly-ADP ribose polymerase-1, and -2 knockout mice;LC, lung cancer.

Statistical significance: *, $p \leq 0.05$, **, $p \leq 0.01$, ***, $p \leq 0.001$, and n.s., non-significant differences between either wild type, Parp-1$^{-/-}$, or Parp-2$^{-/-}$ LC cachectic mice and their respective control (non-tumor) rodents; †, $p \leq 0.05$, †† $p \leq 0.01$, and †††, $p \leq 0.001$ between any of the control knockout animals and control (non-tumor) wild type mice.

Table 3. Subcutaneous tumor characteristics of wild type, Parp-1$^{-/-}$, and Parp-2$^{-/-}$ mice at the end of the studyperiod.

	Wild type mice	Parp-1$^{-/-}$ mice	Parp-2$^{-/-}$ mice
	LC cachexia	LC cachexia	LC cachexia
Subcutaneous tumor weight (g)	1.88 (0.54)	1.15 (0.33), **	1.26 (0.34), **
Ratio of tumor to total final body weight	10.2 (2.8)	6.1 (1.8), ***	6.2 (2.0), ***
Percentage of reduction in tumor weight		39	33
Cellular proliferation			
Ki-67 (%)	83.25 (2.8)	73.03 (7.9), **	75.14 (3.5), *
Apoptosis			
Bcl-2, OD (a.u.) (antiapopototic)	0.06 (0.03)	0.04 (0.01), *	0.03 (0.004), **
Bax, OD (a.u.) (proapoptotic)	0.010 (0.004)	0.016 (0.005),*	0.016 (0.002), *
Autophagy			
SIRT1, OD (a.u.)	0.07 (0.02)	0.09 (0.02), n.s.	0.09 (0.02), n.s.
LC3 II/LC3 I, OD (a.u.)	1.78 (0.6)	5.03 (2.2), *	8.30 (3.9), ***

Variables are presented as mean (standard deviation).

Definition of abbreviations: Parp-1$^{-/-}$ and Parp-2$^{-/-}$, poly-ADP ribose polymerase-1, and -2 knockout mice;LC, lung cancer;Bcl-2, B-cell lymphoma 2; Bax, Bcl-associated X protein; LC3, Light chain 3.

Statistical significance: *, $p \leq 0.05$, **, $p \leq 0.01$, ***, $p \leq 0.001$, and n.s., non-significant differences between any of the LC cachectic knockout groups of rodents and LC cachectic wild type mice.

Table 4. Muscle structural characteristics of wild type, Parp-1$^{-/-}$, and Parp-2$^{-/-}$ mice at the end of the study period.

		Wild type mice		Parp-1$^{-/-}$ mice		Parp-2$^{-/-}$ mice	
	Muscle	Control	LC cachexia	Control	LC cachexia	Control	LC cachexia
Fiber type composition							
Type I fibers (%)	Diaphragm	9 (2)	8 (3), n.s.	9 (1)	9 (2), n.s.	7 (2)	9 (2), n.s.
	Gastrocnemius	13 (3)	13 (3), n.s.	13 (2)	13 (2), n.s.	17 (4)	15 (2), n.s.
Type II fibers (%)	Diaphragm	91 (2)	92 (3), n.s.	91 (1)	91 (2), n.s.	92 (3)	90 (2), n.s.
	Gastrocnemius	87 (3)	87 (3), n.s.	87 (2)	87 (2), n.s.	83 (4)	85 (2), n.s.
Type I fibers area (μm^2)	Diaphragm	328 (66)	233 (34), ***	325 (77)	289 (58), n.s.	292 (49)	311 (67), n.s.
	Gastrocnemius	953 (114)	644 (120), ***	864 (109)	730 (190), p=0.089	775 (128)	707 (82), n.s.
Type II fibers area (μm^2)	Diaphragm	396 (81)	303 (69), *	384 (80)	371 (76), n.s.	344 (98)	395 (114), n.s.
	Gastrocnemius	939 (118)	728 (140), **	885 (99)	743 (182), p=0.067	801 (69)	714 (61), n.s.

Values are expressed as mean (standard deviation).

Definition of abbreviations: Parp-1$^{-/-}$ and Parp-2$^{-/-}$, poly-ADP ribose polymerase-1, and -2 knockout mice; LC, lung cancer; µm, micrometer; n.s., non-significant.

Statistical significance: *, p≤0.05, **, p≤0.01, ***, p≤0.001, and n.s., non-significant differences between either wild type, Parp-1$^{-/-}$, or Parp-2$^{-/-}$ LC cachectic mice and their respective control (non-tumor) rodents.

MICRORNA EXPRESSION AND PROTEIN ACETYLATION PATTERN IN RESPIRATORY AND LIMB MUSCLES OF PARP-1$^{-/-}$ AND PARP-2$^{-/-}$ MICE WITH LUNG CANCER CACHEXIA

Alba Chacon-Cabrera[1,2], Clara Fermoselle[1], Ida Salmela[3], Jose Yelamos[4,5], and Esther Barreiro[1,2]

[1]Pulmonology Department-Lung Cancer Research Group, IMIM-*Hospital del Mar*, *Parc de Salut Mar*, Health and Experimental Sciences Department (CEXS), *UniversitatPompeuFabra* (UPF), Barcelona Biomedical Research Park (PRBB),C/ Dr. Aiguader, 88, Barcelona, E-08003 Spain.

[2]*Centro de Investigación en Red de Enfermedades Respiratorias* (CIBERES), *Instituto de Salud Carlos* III (ISCIII), Barcelona, Spain.

[3]Department of Biosciences, Division of Genetics, University of Helsinki, Helsinki, Finland.

[4]Cancer Research Program, Hospital del Mar Medical Research Institute (IMIM), Barcelona, Spain

[5]*Centro de Investigación en Red de Enfermedades Hepáticas y Digestivas* (CIBERehd), *Instituto de Salud Carlos* III (ISCIII), C/ Monforte de Lemos 5, Madrid, E-28029 Spain.

Correspondingauthor: Dr. Esther Barreiro, PulmonologyDepartment, IMIM-Hospital del Mar, PRBB, C/ Dr. Aiguader, 88, Barcelona, E-08003 Spain, Telephone: (+34) 93 316 0385, Fax: (+34) 93 316 0410, e-mail: ebarreiro@imim.es.

Running title: Muscle-enriched microRNAs and hyperacetylation in cachexia

Word count: 6,184

ABSTRACT

Background: Current treatment options for cachexia, which impairs disease prognosis, are limited. Muscle-enriched microRNAs and protein acetylation are involved in muscle wasting including lung cancer (LC) cachexia. Poly(ADP-ribose) polymerases (PARP) are involved in muscle metabolism. We hypothesized that muscle-enriched microRNA, protein hyperacetylation, and expression levels of myogenic transcription factors (MTFs) and downstream targets, muscle loss and function improve in LC cachectic Parp-$1^{-/-}$ and Parp-$2^{-/-}$ mice. **Methods:**Body and muscle weights, grip strength, muscle phenotype, muscle-enriched microRNAs (miR-1, -133, -206, and -486), protein acetylation, acetylated levels of FoxO1, FoxO3, and PGC-1α, histone deacetylases (HDACs) including SIRT1, MTFs, and downstream targets(α-actin, PGC-1α, and creatine kinase) were evaluated in diaphragm and gastrocnemius of LC (LP07 adenocarcinoma) wild type (WT), Parp-$1^{-/-}$ and Parp-$2^{-/-}$ mice. **Results:**Compared to WT cachectic animals, in both respiratory and limb muscles of Parp-$1^{-/-}$ and Parp-$2^{-/-}$ cachectic mice: downregulation of muscle-specific microRNAs was counterbalanced especially in gastrocnemius of Parp-$1^{-/-}$ mice; increased protein acetylation was attenuated (improvement in HDAC3, SIRT-1, and acetylated FoxO3 levels in both muscles,acetylated FoxO1 levels in the diaphragm); reduced MTFs and creatine kinaselevels were mitigated; body and muscle weights, strength, and muscle fiber sizes improved, while tumor weight and growth decreased. **Conclusions:**These molecular findings may explain the improvements seen in body and muscle weights, limb muscle force and fiber sizes in both Parp-$1^{-/-}$ and Parp-$2^{-/-}$ cachectic mice. **General significance:**PARP-1 and -2 play a role in cancer-induced cachexia, thus selective pharmacological inhibition of PARP-1 and -2 may be of interest in clinical settings. **Word count**: 250. **KEY WORDS**: cancer-induced cachexia; muscle-enriched microRNAs; protein hyperacetylation; myogenic transcription factors; muscle structure and function; Parp-$1^{-/-}$ and Parp-$2^{-/-}$ mice.

1. Introduction

Systemic manifestations of chronic conditions such as muscle mass loss and dysfunction further impair the patients' prognosis and their quality of life [7,19,20]. In advanced malignancies, the prevalence of cachexia characterized by muscle loss and body composition alterations ranges from 60-80% especially in patients bearing tumors from the gastrointestinal and respiratory tracts[19,20,25,38,47,48,50]. Despite that progress in the etiology of cachexia has been recently achieved several mechanisms that could help design novel therapeutic strategies remain to be explored in more detail.

Recent evidence has demonstrated that muscle-enriched microRNAs (miR-1, -133, -206, and -486) are involved in myogenesis and muscle plasticity to environmental stimuli. For instance, miR-1 and -133 regulated hypertrophy in response to muscle overload [30] and atrophy in spaceflight and hindlimb suspension experimental models [31]. Moreover, in respiratory [41] and limb muscles of patients with chronic obstructive pulmonary disease (COPD) with a wide range of airway obstruction and body composition [26,42,43] and severe atrophy of fast-twitch fibers and quadriceps weakness, the expression of muscle-enriched microRNAs and other epigenetic events such as lysine-hyperacetylation of histones and other proteins [43], were shown to be differentially regulated compared to the controls.

Recently, poly(ADP-ribosyl)ation, a post-translational modification of proteins in which ADP-ribose moiety of NAD^+ molecules is transferred to acceptor residues of target proteins by members of the poly(ADP-ribose) polymerase (PARP) family, has emerged as a new regulator of epigenetic events in cells [45]. Among the seventeen members of the PARP family, PARP-1 and PARP-2 play a fundamental role in epigenetic processes through the orchestration of several chromatin-based biological activities [59]. For instance, PARP-1 inhibition using pharmacological agents or knockout mice was shown to increase the levels of type III histone deacetylase SIRT1 activity and to improve oxidative metabolism in the

animals[5]. Moreover, inhibition of PARP-2 also induced an increase in mitochondrial content and SIRT1 protein levels in limb muscles of the knockout mice [4]. Collectively, these findings suggest that PARP seems to play a relevant role in muscle metabolism through specific epigenetic events. Nonetheless, identification of whether PARP-1 and -2 may influence body weight loss, limb strength and other epigenetic features in *in vivo* models of cancer-induced cachexia remains to be elucidated. In this regard, it would be of scientific and clinical interest to identify the extent to which PARP inhibition may improve muscle mass and force loss in cancer cachexia, for which current therapies are extremely limited[19,20,25,38,47,48,50]. Those findings would facilitate the design of selective PARP inhibitors that may promote the restoration of muscle mass and force in cachexia. Moreover, investigations focused on the study of whether respiratory muscles may also be affected in cachectic rodents are scarce [12,46]. We believe that given the relevance of these muscles in the body, the analysis of the diaphragm deserves further attention in models of cancer-induced cachexia.

On this basis and in view of the findings reported so far on the potential role of PARP-1 and -2 in muscle metabolism, in the current investigation, we hypothesized that Parp-$1^{-/-}$ and Parp-$2^{-/-}$ mice may develop less severe muscle wasting when transplanted with a tumor that induces severe cachexia. Additionally, we also hypothesized that muscle-specificmicroRNA and protein acetylation profile would be differentially expressed in both respiratory and limb muscles of Parp-$1^{-/-}$ and Parp-$2^{-/-}$ mice with cancer cachexia. Accordingly, the study objectives were to assess after a one-month study period, in diaphragm and in a limb muscle of similar fiber type composition (gastrocnemius) of Parp-$1^{-/-}$ and Parp-$2^{-/-}$ mice transplanted with a lung tumor (adenocarcinoma)-inducing cachexia: 1) the effects of PARP -1 and -2 selective deletions on body and muscle weights, grip strength, muscle phenotype, and tumor size, 2) levels of expression of muscle-enriched microRNAs, 3) total protein

hyperacetylationlevels and those of transcription factors involved in muscle wasting, 4) levels of myogenic transcription factors(MTFs) and their downstream targets, and 5) potential correlations between physiological and molecular variables in cachectic wild type, Parp-$1^{-/-}$ and Parp-$2^{-/-}$ mice.

2. Methods

2.1. Animal model

Tumor. LP07 is a cell line derived from the transplantable P07 lung tumor that appeared spontaneously in the lung of a BALB/c mouse [12,17,18,53]. The rates of tumor growth and tumor kinetics have been well characterized in previous investigations aimed to specifically explore the effects of several drugs on identical transplanted tumors [18,37].

*Mice***.** BALB/c mice were obtained from Harlan *InterfaunaIbérica SL* (Barcelona, Spain). Parp-$1^{-/-}$ and Parp-$2^{-/-}$ mice (strain 129/Sv x C57BL/6), kindly provided by Dr. de Murcia [15,16,32] (Strasbourg, France), were backcrossed on BALB/c background for twelve generations. Genotyping was performed by PCR analysis using tail DNA as previously described. All experiments were performed on two-month old littermate female mice (body weight ~20 g), on a BALB/c background. Mice were kept under pathogen-free conditions in the animal house facility at the Barcelona Biomedical Research Park (PRBB), with a 12:12 h light:dark cycle.

Experimental design and Ethics. In all experimental groups (except for control rodents), LP07 viable cells ($4x10^5$) resuspended in 0.2 mL minimal essential media (MEM) were subcutaneously inoculated in the left flank of female BALB/c mice on day 1, and were studied for a period of one month. Fifty-nine mice were used in the study, which were subdivided into the following experimental groups: 1) control wild type (N=14), inoculation of 0.2 mL MEM in the left flank; 2) LC cachexia wild type group (N=13), inoculation of LP07 cells; 3) control Parp-$1^{-/-}$ (N=8), inoculation of 0.2 mL MEM in the left flank; 4) LC

cachectic Parp-$1^{-/-}$ mice (N=12), inoculation of LP07 cells; 5) control Parp-$2^{-/-}$ (N=6), inoculation of 0.2 mL MEM in the left flank; and 6) LC cachectic Parp-$2^{-/-}$ mice (N=6), inoculation of LP07 cells.

A fraction of the diaphragm and gastrocnemius muscle specimens of the transgenic mice were also used in another investigation aimed to assess protein catabolism and anabolism and structural alterations in those muscles (data submitted).

All animal experiments were conducted in the animal facilities at PRBB. This controlled study was designed in accordance with the ethical standards on animal experimentation (EU 2010/63 CEE, *Real Decreto* 53/2013 BOE 34, Spain) at PRBB and the Helsinki convention for the use and care of animals. Ethical approval was obtained by the Animal Research Committee (Animal welfare department, Catalonia, EBP-09-1228).

2.2. *In vivo* measurements in the mice

Body weight and grip strength gains were calculated as the percentage of the measurements performed at the end of the study period (30 days) with respect to the same measurements obtained at baseline. Body weight and food intake were measured every day during the entire duration of the study, whereas limb force (grip strength) was determined on days 0 and 30 in all animals as previously shown[10,12,33,51,54,57]. Moreover, the ratio of tumor weight to total body weight on the day of sacrifice (day 30) was also calculated.

2.3. Sacrifice and sample collection

Mice from all the experimental groups were sacrificed on day 30 post-inoculation of LP07 cells or MEM (control animals). Prior to sacrifice, each mouse was inoculated intraperitoneally with 0.1 mL sodium pentobarbital (60 mg/Kg). In all cases, the pedal and blink reflexes were evaluated in order to verify total anesthetic depth. At this time, the following samples were obtained from all animals: diaphragm and gastrocnemius muscles and the subcutaneous tumor. LC cachectic mice were macroscopically of smaller size than healthy

control rodents [12]. Frozen tissues were used for immunoblotting and real-time polymerase chain reaction assay (qRT-PCR) techniques.

2.4. Biological analyses

*Muscle RNA isolation.*Total RNA was first isolated from snap-frozen skeletal muscles using Trizol reagent following the manufacturer's protocol (Life technologies, Carlsbad, CA, USA). Total RNA concentrations were determined photometrically using the NanoDrop 1000 (Thermo Scientific, Waltham, MA, USA).

MicroRNA reverse transcription (RT). MicroRNA RT was performed using TaqMan® microRNA assays (Life Technologies) following the manufacturer's instructions.

*Real time-PCR amplification (qRT-PCR).*TaqMan based qPCR reactions were performed using the ABI PRISM 7900HT Sequence Detector System (Applied BioSystems, Foster City, CA, USA) together with a commercially available predesigned microRNA assay, and probes as shown in Table 1 [27].

*Immunoblotting of 1D electrophoresis in muscle and tumor samples.*Protein levels of the different molecular markers analyzed in the study were explored by means of immunoblotting procedures as previously described[8,12]. Protein levels of total acetylated proteins, HDACs, myogenic transcription factors, signaling pathways, and downstream targets were identified using specific primary antibodies as thoroughly described in the online supplementary material. In order to validate equal protein loading among various lanes, SDS-PAGE gels were stained with CoomassieBlue,and the glycolytic enzyme glyceraldehyde-3-phosphate dehydrogenase (GAPDH) was used as the protein loading controls in all the immunoblots(Figure E1, and GAPDH immunoblots accompanying each study antigen).

Tumor specimens. Following identical procedures as described above, in the subcutaneous tumors from all the animals, the following markers were also analyzed with the objective to assess whether Parp deletion may have had an effect on tumor growth or degradation: B-cell

lymphoma (bcl)-2, bax, light chain (LC)3B,NAD-dependent protein deacetylase sirtuin-1 (SIRT1), and GAPDH. Furthermore, in order to confirm that tumors express PARP-1 and PARP-2 proteins in each group of knockout mice (cachectic animals), those proteins were also detected in the actual tumors of all groups of tumor-bearing mice using selective antibodies: anti-PARP-1 antibody (Clon A6.4.12) and anti-PARP-2 antibody (rabbit polyclonal antibody raised against full length mouse PARP-2)[3]. Antigens from all samples were detected as described above.

*Immunohistochemistry.*On 3-micrometer muscle paraffin-embedded sections from diaphragms and gastrocnemius muscles of all study groups, MyHC-I and –II isoforms were identified using specific antibodies[12,43,44].

Furthermore, in the subcutaneous tumor of the target mice (both wild type and knockout rodents), cell proliferation was measured using ki-67 as a marker (anti-ki67 antibody, Millipore Iberica, CA, USA) on the three micrometer tumor paraffin-embedded sections using immunohistochemical procedures as previously described [12,43,44].

2.5. Statistical Analysis

Normality of the study variables were checked using the Shapiro-Wilk test. Physiologic, structural, and molecular results are expressed as mean (standard deviation). For the purpose of the study, results obtained in the diaphragm and gastrocnemius muscles were subsequently analyzed as follows: 1) LC cachectic wild type mice versus their respective non-tumor controls, 2) LC cachectic Parp-$1^{-/-}$ animals versus their respective knockout non-tumor controls, 3) LC cachectic Parp-$2^{-/-}$ mice versus their respective knockout non-tumor controls, and 4) any of the non-tumor knockout mice versus non-tumor wild type animals. Comparisons described in points 1, 2, and 3 above were analyzed using the Student's *T- test*, while comparisons described in point 4 were assessed using one-way analysis of variance (ANOVA), in which *Dunnett's post hoc* analysis was used to adjust for multiple comparisons

among the three study groups. Moreover, values of the markers quantified in the tumors were compared among the three different groups of cancer cachectic rodents using ANOVA, in which *Dunnett's post hoc* analysis was also employed to adjust for multiple comparisons among the groups. The existence of potential correlations between different variables was only tested in the LC cachectic groups of mice (both wild type and knockout mice). Specifically, correlations between physiological and biological variables were explored using the Pearson's correlation coefficient. A level of significance of $P \leq 0.05$ was established. The sample size chosen was based on previous studies[4,5,12,21,22,28], where very similar approaches were employed and on assumptions of 80% power to detect an improvement of more than 20% in measured outcomes at a level of significance of $P \leq 0.05$.

3. Results

3.1. Physiological characteristics

*LC-induced cachexia.*As shown in Table 2 and Figure 1, at the end of the study period (day 30), cachectic wild type mice exhibited a reduction in body weight gain compared to their respective controls. Actual body weights of animals in all study are depicted in Figure 1.Food intake did not differ between any of the cachectic mice and their respective control animals (Table 2).Diaphragm and gastrocnemius muscle weights and limb strength gain were significantly reduced in cachectic wild type mice. Importantly, in Parp-$1^{-/-}$ mice, a statistically significant reduction in these parameters was also observed, but to a much lesser extent than in the wild type animals. In cachectic Parp-$2^{-/-}$ mice, no significant differences were observed in muscle weights and body or limb strength gains between cachectic and non-cachectic mice. No significant correlations were found between muscle weight changes and fiber type sizes in any study muscle of the LC cachectic mice (Parp-$1^{-/-}$and Parp-$2^{-/-}$).

*Effects of PARP deletion on non-cachectic control animals.*As illustrated in Table 2, non-cachectic knockout animals (Parp-$1^{-/-}$ and Parp-$2^{-/-}$) exhibited a reduction in the weights of their muscles (diaphragm and gastrocnemius) compared to wild type non-tumor animals. However, body weight at baseline and both body weight and limb strength gains did not significantly differ among any of the non-cachectic groups of mice.

3.2. Tumor characteristics

*Effects of PARP deletion on cachectic animals.*The expression of PARP-1 and PARP-2 was confirmed in the subcutaneous tumors of the wild type and both groups of knockout mice. (Figure E2A). Compared to cachectic wild type animals, subcutaneous tumor weight and theratio of tumor to total body weight were significantly reduced in both knockout cachectic mice (Parp-$1^{-/-}$ and Parp-$2^{-/-}$, Table 3). Moreover, ki-67 (cell proliferation marker) was decreased in both knockout cachectic mice (Parp-$1^{-/-}$ and Parp-$2^{-/-}$) compared to cachectic wild type rodents (Table 3). Compared to cachectic wild type mice, subcutaneous tumors of both cachectic Parp-$1^{-/-}$ and Parp-$2^{-/-}$ animals exhibited a decrease in Bcl-2 protein levels, while Bax protein content was increased (Table 3 and Figures E2B and E2C). LC3 II/LC3 I levels were significantly increased in the subcutaneous tumor of both knockout cachectic mice (Parp-$1^{-/-}$ and Parp-$2^{-/-}$) compared to cachectic wild type animals, whereasSIRT1 levels did not differ between wild type and either Parp-$1^{-/-}$ or Parp-$2^{-/-}$ cachectic animals (Table 3 and Figure E2D and E2E).

3.3. Muscle structure

*LC-induced cachexia.*The proportions of type I and II fibers did not differ between cachectic and non-cachectic conditions in any experimental group of mice. The size of both slow- and fast-twitch fibers was significantly reduced in diaphragm and gastrocnemius of cachectic wild type mice compared to non-cachectic control wild type animals (Table 4). In Parp-$2^{-/-}$mice, the size of type I and type II fibers in both muscles did not show any significant difference

between cachectic and non-cachectic animals (Table 4). Compared to Parp-1$^{-/-}$ mice, in LC-cachectic Parp-1$^{-/-}$ animals, no significant differences were seen in the size of either slow- or fast-twitch fibers in the diaphragm, while in the gastrocnemius a tendency to improve the size of type I (p=0.089) and type II (p=0.067, Table 4) was observed. A significant correlation was found between type II fiber size and miR-133 expression in the gastrocnemius of the cachectic wild type mice (r=0.938, p=0.000), but not in the tumor-bearing knockout mice (r=-0.603, p=0.114 and r=-0.101, p=0.849, Parp-1$^{-/-}$ and Parp-2$^{-/-}$ mice, respectively) (Figure 3E).No significant relationships were observed between type I fiber size and miR-133 expression in the gastrocnemius of any of the three groups of cachectic animals (wild type mice r=0.256, p=0.474; Parp-1$^{-/-}$ mice r=-0.114, p=0.789; and Parp-2$^{-/-}$ r=-0.142, p=0.788).

*Effects of PARP deletion on non-cachectic control animals.*Proportions or sizes of type I and type II fibers did not differ between wild type and either Parp-1$^{-/-}$ or Parp-2$^{-/-}$ non-cachectic control mice in any study muscle (Table 4).

3.4. Expression microRNA in respiratory and limb muscles

*LC-induced cachexia.*Expression levels of miR-1 were decreased in both diaphragm and gastrocnemius of LC cachectic wild type, and cachectic Parp-1$^{-/-}$ and Parp-2$^{-/-}$ mice compared to their respective non-cachectic control animals (Figures 2A and 2B). Both diaphragm and gastrocnemius of cachectic wild type and Parp-2$^{-/-}$ mice exhibited a decrease in miR-133 expression compared to their respective non-tumor control mice (Figures 2C and 2D), while miR-133 expression was down-regulated only in the diaphragm of cachectic Parp-1$^{-/-}$ animals (Figures 2C and 2D). Compared to their respective non-cachectic controls, levels of miR-206 were downregulated in both respiratory and limb muscles of cachectic wild type rodents, while the expression of this myomiR was decreased only in the diaphragm of both groups of cachectic knockout mice (Figures 3A and 3B). Expression levels of miR-486 were down-regulated in both muscles of cachectic wild type and Parp-2$^{-/-}$ mice compared to their

respective non-tumor control animals (Figures 3C and 3D). However, miR-486 levels did not differ between cachectic and non-cachectic Parp-$1^{-/-}$ mice in any muscle (Figures 3C and 3D).

Effects of PARP deletion on non-cachectic control animals. Levels of miR-1 did not differ between non-cachectic Parp-$1^{-/-}$ and non-cachectic wild type mice in any study muscle (Figures 2A and 2B). However, levels of miR-1 were greater in the diaphragm of non-cachectic Parp-$2^{-/-}$ animals compared to non-cachectic wild type controls (Figures 2A and 2B). Expression levels of miR-133 were upregulated in the diaphragm of both groups of non-cachectic knockout mice compared to non-cachectic wild type control animals. Nevertheless, in the gastrocnemius of non-cachectic Parp-$1^{-/-}$ and Parp-$2^{-/-}$ controls, levels of miR-133 were down-regulated compared to non-cachectic wild type control animals (Figures 2C and 2D). Compared to wild type control animals, diaphragm and gastrocnemius of both groups of non-cachectic knockout mice showed an increase in miR-206 expression (Figures 3A and 3B). Levels of miR-486 were down-regulated in the diaphragm and gastrocnemius of non-cachectic control Parp-$1^{-/-}$ animals compared to non-cachectic control wild type rodents (Figures 3C and 3D). However, in the diaphragm of non-cachectic Parp-$2^{-/-}$ animals, expression levels of miR-486 were increased compared to wild type mice, while in the gastrocnemius were decreased (Figures 3C and 3D).

3.5. Protein acetylation levels in respiratory and limb muscles

*LC-induced cachexia.*Compared to non-cachectic wild type controls, total protein acetylation levels were increased in both respiratory and limb muscles of cachectic wild type rodents (Figures 4A, 4B, and E3). Total protein acetylation levels in both muscles did not show any significant difference between cachectic and non-cachectic animals in any of the knockout groups of mice (Figures 4A, 4B, and E3). Acetylated FoxO1 content was increased in the diaphragm but not in the limb muscle of wild type cachectic mice compared to their non-cachectic controls (Figures 4C, 4D, and E4). Acetylated FoxO1 levels did not differ between

cachectic and non-cachectic conditions in any muscle of the knockout groups of mice (Figures 4C, 4D, and E4).Compared to cachectic wild type controls, acetylated FoxO3 content was increased in both diaphragm and gastrocnemius muscles of cachectic wild type animals (Figures 4E, 4F, and E5). In Parp-$1^{-/-}$mice, acetylated FoxO3 levels did not differ in any muscle between cachectic and non-cachectic conditions (Figures 4E, 4F, and E5). Compared to non-cachectic Parp-$2^{-/-}$ mice, acetylated levels of FoxO3 were decreased in the diaphragm of cachectic Parp-$2^{-/-}$ animals, while no differences between these two groups were seen in the gastrocnemius (Figure 4E, 4F, and E5). Acetylated levels of PGC-1α did not significantly differ between cachectic and non-cachectic conditions in either wild type or any of the two groups of knockout mice in any study muscle (Figures 4G, 4H, and E6).

*Effects of PARP deletion on non-cachectic control animals.*Total protein acetylation levels, and acetylated levels of FoxO1, FoxO3, and PGC-1αdid not significantly differ between non-cachectic wild type and either Parp-$1^{-/-}$ or Parp-$2^{-/-}$ non-cachectic control mice in any muscle (Figures 4A-4H, and E3-E6).

3.6. Histone deacetylase levels in respiratory and limb muscles

*LC-induced cachexia.*Compared to their respective non-cachectic controls, HDAC3 and HDAC6 levels were decreased in both respiratory and limb muscles of cachectic wild type rodents, whereas no differences were seen in any of the study muscles of the knockout cachectic animals (Figures 5A-5D, E7, and E8). SIRT1 levels were reduced in both muscles of cachectic wild type animals compared to their non-cachectic controls, while no differences were observed in any of the study muscles of the knockout cachectic animals (Parp-$1^{-/-}$ or Parp-$2^{-/-}$) compared to their respective non-cachectic rodents (Figures 5E, 5F, and E9). A significant positive correlation was found between HDAC3 and SIRT1 levels in the gastrocnemius of the cachectic wild type mice ($r=0.724$, $p=0.042$), but not in the knockout mice ($r=0.495$, $p=0.259$ and $r=-0.036$, $p=0.955$, Parp-$1^{-/-}$ and Parp-$2^{-/-}$ mice, respectively).

*Effects of PARP deletion on non-cachectic control animals.*HDAC3, HDAC6, and SIRT1 levels did not significantly differ between non-cachectic wild type and either Parp-$1^{-/-}$ or Parp-$2^{-/-}$ non-cachectic control mice in any study muscle (Figures 5A-5F, and E7-E9).

3.7. Myogenic transcription factors and downstream markers

*LC-induced cachexia.*In the diaphragm and gastrocnemius of cachectic wild type mice, protein levels of MEF2C and MEF2D were reduced compared to non-cachectic wild type controls (Figures 6A-6D, E10, and E11). MEF2C and MEF2D levels did not significantly differ between cachectic knockout animals and their respective non-tumor controls in any muscle (Figures 6A-6D, E10, and E11). YY1 levels were decreased in both muscles of the cachectic rodents compared to their respective non-cachectic controls (Figures 6E, 6F, and E12). Protein levels of α-actin and total PGC-1α did not significantly differ between cachectic and non-cachectic conditions in either wild type or any of the two groups of knockout mice in any study muscle (Figures 7A-7D, E13 and E14).Creatine kinase protein content was diminished in both muscles of cachectic wild type animals compared to their non-cachectic controls (Figures 7E-7F, and E15). Creatine kinase levels were decreased in the diaphragm but not in the gastrocnemius of both knockout cachectic mice (Parp-$1^{-/-}$ and Parp-$2^{-/-}$) compared to their respective non-cachectic controls (Figures 7E-7F, and E15).

Effects of PARP deletion on non-cachectic control animals. Protein levels of MEF2C and MEF2D did not differ between either non-cachectic Parp-$1^{-/-}$ or Parp-$2^{-/-}$ and non-cachectic wild type controls in any study muscle (Figures 6A-6D, E10 and E11). Compared to non-cachectic wild type animals, YY1 levels were reduced in the diaphragm of both groups of knockout mice, whereas no significant differences were observed in the gastrocnemius (Figures 6E, 6F and E12). Protein levels of α-actin and total PGC-1α did not significantly differ between non-cachectic wild type and either Parp-$1^{-/-}$ or Parp-$2^{-/-}$ non-cachectic control mice in any muscle (Figures 7A-7D, E13 and E14). Compared to non-cachectic wild type

rodents, creatine kinase protein content was reduced in the diaphragm of both non-cachectic knockout mice (Parp-$1^{-/-}$ and Parp-$2^{-/-}$), while no significant differences were observed in the gastrocnemius (Figures 7E-7F, and E15).

4. Discussion

Expression levels of the muscle-enriched miR-1, -133, -206, and -486 were significantly downregulated in both diaphragm and gastrocnemius muscles of wild type LC cachectic mice compared to the non-cachectic wild type rodents. These findings are in agreement with those reported in previous investigations conducted on patients with severe COPD [26], in whom miR-1 levels were reduced in the vastuslateralis, and those of miR-1, -133, and -206 that were decreased in the diaphragm of patients with moderate COPD [41]. Interestingly, muscle-enriched microRNAs target different cellular pathways that are involved in myogenesis in different models[9,11,41-43].

In the current investigation, compared to the non-tumor bearing animals, the diaphragm of LC cachectic Parp-$1^{-/-}$ mice showed a decreased expression of miR1, -133, or -206 while miR-486 expression did not differ between these two groups of rodents. In the gastrocnemius muscle, cachectic Parp-$1^{-/-}$ mice only exhibited a significant downregulation of miR-1, but not of the other muscle-enriched microRNAs, compared to their respective non-cachectic controls. Moreover, a significant correlation between the size of type II fibersand miR-133 levels, which is predominantly expressed in fast-twitch fibers together with miR-1[62], was also found in the gastrocnemius of LC cachectic wild type mice, and such a correlation was lost in the cachectic knockout animals. In the diaphragm of LC cachectic Parp-$2^{-/-}$ mice, muscle-enriched miR-1, -133, -206, or -486 were also downregulated compared to their respective non-cachectic Parp-$2^{-/-}$ rodents. In the limb muscle, expression of the same

microRNAs was also downregulated in Parp-2$^{-/-}$ cachectic mice, except for miR-206 whose levels did not differ between cachectic and non-cachectic animals in the limb muscle.

Expression of miR-133 induces myoblast proliferation by inhibiting myotube formation, miR-486 is involved in hypertrophy, and miR-1 and -206 promote cell differentiation and innervation[11,14,26,34,39]through several downstream mechanisms that favor protein synthesis and muscle growth [43]. The mechanisms accounting for the regulation of PARP-1 and -2 on the expression of muscle-enriched microRNAs have not been so far demonstrated. Indeed, the current study is the first to report a potential association between PARP-1 and -2 expressions and muscle-specific microRNAs in a model of cancer cachexia. Nonetheless, in view of the present findings, it could be hypothesized that particularly in the gastrocnemius of LC cachectic mice, PARP-1 inhibition most likely favorsmuscle proliferation and differentiation (miR-133, miR-206, and miR-486) processes, while PARP-2 may rather promote muscle differentiation (miR-206). In the diaphragm, PARP-1 deletion favored the expression of miR-486, whereas no significant effects on microRNA expression were seen in LC cachectic Parp-2 $^{-/-}$ animals.

Taken together, these findings suggest that PARP-1 rather than PARP-2 inhibition seems to exert more beneficial effects on muscle-enriched microRNA expression of cachectic limb muscles in this specific animal model of LC cachexia. In fact, PARP-1 has been demonstrated to interact with nuclear factor (NF)-κB[23,36], and the transcriptional activity of NF-κB was recently shown to increase in the gastrocnemius muscle inthe animals of the same model of cancer cachexia[12]. On this basis, it is likely that inhibition of PARP activity, especially of PARP-1, may have prevented a further decrease in the expression of muscle-specific microRNAs by blocking NF-κB activity, particularly in the limb muscle of the cachectic animals. Differences in the activity between respiratory and limb muscles, despite their similar fiber type composition, and in the contribution to total body and muscle mass loss of

each type of muscle may account for the differential pattern of muscle-specific microRNA expression observed in muscles of Parp-$1^{-/-}$ mice. Conclusively, the prevention of a further downregulationof the expression of these muscle-specific microRNAs may partly account for the improvement in body weight and limb muscle force lose observed in both groups of knockout mice with cancer cachexia compared to tumor-bearing wild type mice.

Interestingly, in order to assess the potential effects of either PARP-1 or -2 deficiencies on both types of muscles under normal conditions, levels of the different markers were also statistically analyzed in non-cachectic control muscles of all the study groups. In this regard, in the diaphragm, non-cachectic Parp-$1^{-/-}$ mice exhibited a significant rise in miR-133 and -206 expressions, while miR-486 levels were downregulated compared to non-cachectic wild type animals. In the same muscle, the expression of miR-1, -133, -206, and -486 was upregulated in non-cachectic control Parp-$2^{-/-}$ mice compared to wild type mice, implying that both proliferation and differentiation processes were favored by PARP-2 inhibition in healthy diaphragms. In the gastrocnemius, PARP-1 deficiency induced a significant downregulation of miR-133 and -486 expressions, whereas PARP-2 deficiency led to an upregulation of miR-206 and to a concomitant downregulation of miR-486 in non-cachectic animals compared to control wild type mice. PARP-2 deficiency rather than PARP-1 seemed to exert more beneficial effects in terms of muscle-enriched microRNA upregulation in non-cachectic muscles, particularly in the diaphragm. The elucidation of the mechanisms whereby either PARP-1 or -2 deletions may differentially regulate the expression of muscle-enriched microRNAs in respiratory and limb muscles under normal conditions (no underlying disease) is beyond the scope of the current study and should be the subject of future research.

Hyperacetylation of proteins, which relies to a great extent on histone deacetylase (HDAC) activity, may lead to muscle mass loss by rendering proteins more prone to degradation by the action of histone acetyl transferases that may have ubiquitin-ligase activity

and by dissociation of proteins from cellular chaperones [1]. In the current study, in the respiratory and limb muscles of wild type LC cachectic animals compared to their respective non-cachectic controls, total protein acetylation levels were increased, while those of HDAC3, HDAC6, and SIRT1 were reduced. These findings are in agreement with previous investigations, in which levels of HDAC3 and HDAC6 and SIRT1 were also reduced in models of muscle wasting[2,43,49]. Collectively, these findings imply that reduced HDAC activity drives protein hyperacetylation in skeletal muscles in models of muscle wasting[2,43,49]. Importantly, in Parp-$1^{-/-}$ and Parp-$2^{-/-}$ mice, protein acetylation levels did not significantly differ between cancer cachexia and non-cachetic control conditions in respiratory or limb muscles, thus suggesting that PARP-1 and -2 deficiencies have prevented these muscles from undergoing further protein acetylation. Importantly, the content of HDAC3, HDAC6, and SIRT1 showed no statistically significant difference in either diaphragm or gastrocnemius muscles between cancer cachectic and non-cachectic controls in Parp-$1^{-/-}$ and Parp-$2^{-/-}$ mice. Clearly, these results point towards a beneficial effect of PARP-1 and -2 deficiencies on HDAC content in skeletal muscles in LC cachexia. The absence of HDAC3, HDAC6, and SIRT1 downregulation together with the absence of a rise in protein hyperacetylation levels in Parp-$1^{-/-}$ and Parp-$2^{-/-}$ cancer cachectic mice may greatly account for the improvements seen in these animals in terms of body and muscle weights, limb muscle strength, and fiber sizes compared to differences observed in the wild type cachectic rodents.

Furthermore, the levels of acetylation of specific transcription factors were also measured in the current study. Interestingly, compared to non-cachectic animals, in wild type LC cachectic mice, acetylation levels of FoxO3 were significantly increased in the diaphragm and gastrocnemius, while a rise in acetylated FoxO1 levels was only seen in the respiratory muscle of the same rodents. Acetylated levels of PGC-1alpha did not vary between cachectic and non-cachectic mice in any of the experimental groups. Importantly, in Parp-$1^{-/-}$ and Parp-

$2^{-/-}$ mice, no significant differences were seen in FoxO1 and FoxO3 acetylation levels. These findings suggest that acetylation of these atrophy signaling pathways, particularly of the latter, favors muscle protein loss as shown in other models [52], which may have been partly prevented by PARP1/2 inhibition in this study.

Myogenic regulatory factors control myogenesis and muscle remodeling in response to injury in adult muscles. Furthermore, they may also orchestrate muscle phenotype by determining the fiber type of a given muscle. For instance, MEF2 family of transcription factors plays a relevant role in muscle phenotype determination of fast- and slow-twitch muscle fibers in mice [40]. Importantly, MEF2 is regulated by acetylation and deacetylation mediated by class II HDACs that can directly bind and inhibit MEF2-regulated transcription of genes [61]. In the present study, protein levels of MEF2C and MEF2D were significantly decreased in the wild type cachectic mice compared to the non-cachectic control rodents. Nonetheless, in Parp-$1^{-/-}$ and Parp-$2^{-/-}$ cancer cachectic mice, MEF2C and MEF2D levels did not significantly differ in either respiratory or limb muscles from those detected in the non-cachectic control knockout mice. Interestingly, these findings are also in line with the lack of statistically significant differences in HDAC3 and HDAC6 levels observed between tumor-bearing and control animals deficient in PARP-1 and -2 proteins. Taken together, these results indicate that muscle fiber type composition was not modified in any of the study groups or experimental conditions, and the size of slow- and fast-twitch muscle fibers improved in Parp-$1^{-/-}$ and Parp-$2^{-/-}$ cancer cachectic mice compared to the tumor-bearing wild type rodents.

YY1 is a transcription factor involved in histone modification and in the inhibition of muscle regeneration through the transcriptional silencing of myofibrillar genes [56]. Moreover, in a previous study [35], protein levels of YY1 inversely correlated with the reduced size of slow- and fast-twitch muscle fibers in the vastuslateralis of patients with COPD. In the current investigation, YY1 levels were significantly reduced in the cachectic

animals compared to non-cachectic controls in the three experimental groups. Besides, as deficiency of PARP-1 and -2 induced an increase in the size of slow- and fast-twitch fibers in both muscles in cachectic animals (no significant differences were observed between cancer cachectic and non-cachectic control mice), it is likely that reduced levels of YY1 may have partly contributed to the improvement in the fiber sizes of those muscles.

Interestingly, levels of muscle creatine kinase protein, which is regulated by YY1 [55] and MEF2 [60], but not those of actin or PGC-1α,were significantly reduced in the diaphragm and gastrocnemius of wild type cachectic animals compared to the controls as previously shown to occur in diaphragm [29]and quadriceps of cachectic patients with COPD and LC [44]. Inhibition of PARP-1 and -2 induced similar effects in both muscles of the tumor bearing mice: while creatine kinase protein content remained significantly lower than in the controls, such a decrease was attenuated in the gastrocnemius of the knockout cachectic mice. Furthermore, creatine kinase levels also significantly decreased in the non-tumor knockout animals compared to the healthy wild type controls. Collectively, these findings suggest that the regulation of creatine kinase in the diaphragm is likely to be mediated by YY1 (similar pattern of expression) in both non-tumor and tumor-bearing mice of wild type and knockout groups, while PARP-1 and -2 predominantly restoredcreatine kinase levels in the limb muscle as shown to occur in other models [13].

4.2. Study critique

It is likely that the 30-40% reduction in tumor burdenobserved in both groups of knockout mice may have partly contributed to favoring body and muscle mass gain in the rodents, albeit tumors did express PARP-1 and -2 proteins. In fact, inhibition of both PARP-1 and -2 induced a reduction in tumor weights in the animals. Moreover, tumor growth as measured by ki-67 (cell proliferation marker) significantly decreased in the cachectic knockout mice, while levels of the proapoptoticbax and autophagy marker rose in the tumors of the same rodents

compared to wild type mice.Tumor levels of SIRT1 protein, however, did not significantly differ among the study groups. It is likely that other pathways may signal autophagy in this study as shown in other models[24]. The mechanisms whereby PARP-1 and -2 inhibition in the host may contribute to reducing tumor burden of adenocarcinoma cells that express both molecules remain to be elucidatedin future studies, as they are beyond the scope of the current investigation.However, recent data from our group (submitted) point towards a paramount role of depletion of major antioxidants and increased oxidative stress levels, which may have further promoted apoptosis and autophagy of the cancer cells in the Parp-$1^{-/-}$ and Parp-$2^{-/-}$ mice. On the other hand, reduction of tumor burden after cancer resection was also shown to improve muscle atrophy and protein catabolism in actual cancer patients [58], suggesting that this factor also plays a relevant role in the improvement of muscle wasting.

Another limitation is related to the lack of measurements on the progression of tumor size throughout the study protocol in the tumor-bearing animals. In the study, tumor weights were only available at the time of sacrifice in all experimental groups. Nonetheless, the tumors induced by the lung adenocarcinoma cells (LP07) used in the current investigation, have been thoroughly characterized, especially tumor growth and kineticsin previous studies [17,18,37,53].

The study of other limb muscles would have also been of interest. However, our specific goal was to analyze a limb muscle of similar fiber type composition as that of the main respiratory muscle, the diaphragm.In the gastrocnemius of LC cachectic Parp-$1^{-/-}$ mice, the large variability of the muscle fiber sizes especially of the fast-twitch fibers, which did not statistically differ from those in their respective non-cachectic controls, may account for the absence of a correspondence between these parameters and the significantly smaller size of the muscle.Despite that lipid or water content within the myofibers could have also been contributing factors, no actual water vacuoles or lipid accumulation was found within the

muscle fibers of the animals in the study groups (data not shown).As in previous investigations [4-6], the analysis of other markers involved in muscle metabolism such as mitochondrial respiratory chain function in response to PARP-1 and -2 inhibition will be of interest in future research. Indeed, a previous study from our group showed alterations of oxygen uptake and respiratory chain complexes in both diaphragm and gastrocnemius of wild type cancer cachectic mice that were partially restored in response to several pharmacological agents[21].

Future research should focus on the assessment of whether selective pharmacological inhibitors of PARP-1 and -2 exert similar beneficial effects on muscles in models of cancer cachexia and eventually in patients with cancer cachexia for whom currently available therapies are scarce[38,47,48].

4.3. Conclusions

PARP-1 rather than PARP-2 inhibition seems to exert more beneficial effects on muscle-enriched microRNA expressionparticularly in the gastrocnemius in this specific animal model of LC cachexia. Furthermore, in both groups of knockout animals, the rise in protein acetylation levels and that of transcription factors in diaphragm and gastrocnemius of the tumor-bearing rodents was attenuated probably through improvements in HDAC3 and SIRT1 levels. Also, in both groups of Parp-$1^{-/-}$ and Parp-$2^{-/-}$ LC cachectic mice, the decrease in myogenic regulatory factors seen in the wild type cancer cachectic animals was mitigated in their respiratory and limb muscles. These molecular features may partly account for the improvements seen in the mouse phenotype as defined by body and muscle weights, limb muscle force and fiber sizes in both Parp-$1^{-/-}$ and Parp-$2^{-/-}$ cancer cachectic mice, which imply a potential clinical applicability of selective inhibition of PARP-1 and -2 to be tested in future studies. Indeed, currently available drugs, e.g. olaparib, inhibit PARP-1/2 activities. Evidence

from the present investigation should prompt research on the potential beneficial effects and safety concernsof pharmacological PARP-1/2 inhibitors on muscle mass loss and wasting.

ACKNOWLEDGEMENTS

The authors are thankful to Mr. Francisco Sanchez for his technical assistance with the animal experiments and to Ms. Coral Ampurdanes for her contribution to mouse genotyping.

Authors' conflicts of interest in relation to the study: None to declare.

Editorial support: None to declare.

This study has been supported by CIBERES, FIS 11/02029, FIS 14/00713; SEPAR 2013; FUCAP 2011; FUCAP 2012, and *Fundació La Marató de TV3* (2013-4130).

Reference List

1. N. Alamdari, Z. Aversa, E. Castillero, and P.O. Hasselgren, Acetylation and deacetylation--novel factors in muscle wasting, Metabolism 62 (2013) pp. 1-11.

2. N. Alamdari, I.J. Smith, Z. Aversa, and P.O. Hasselgren, Sepsis and glucocorticoids upregulate p300 and downregulate HDAC6 expression and activity in skeletal muscle, Am. J. Physiol Regul. Integr. Comp Physiol 299 (2010) p. R509-R520.

3. S. Aoufouchi, Monoclonal Antibodies A4.3; A6.4.12; B5.3.9; B15.4.13 Anti-Poly(ADP-Ribose) Polymerase., 1997, p. 583.

4. P. Bai, C. Canto, A. Brunyanszki, A. Huber, M. Szanto, Y. Cen, H. Yamamoto, S.M. Houten, B. Kiss, H. Oudart, P. Gergely, M.J. Menissier-de, V. Schreiber, A.A. Sauve, and J. Auwerx, PARP-2 regulates SIRT1 expression and whole-body energy expenditure, Cell Metab 13 (2011) pp. 450-460.

5. P. Bai, C. Canto, H. Oudart, A. Brunyanszki, Y. Cen, C. Thomas, H. Yamamoto, A. Huber, B. Kiss, R.H. Houtkooper, K. Schoonjans, V. Schreiber, A.A. Sauve, M.J. Menissier-de, and J. Auwerx, PARP-1 inhibition increases mitochondrial metabolism through SIRT1 activation, Cell Metab 13 (2011) pp. 461-468.

6. P. Bai, L. Nagy, T. Fodor, L. Liaudet, and P. Pacher, Poly(ADP-ribose) polymerases as modulators of mitochondrial activity, Trends Endocrinol. Metab 26 (2015) pp. 75-83.

7. E. Barreiro, V. Bustamante, P. Cejudo, J.B. Galdiz, J. Gea, L.P. de, J. Martinez-Llorens, F. Ortega, L. Puente-Maestu, J. Roca, and J.M. Rodriguez-Gonzalez Moro, Guidelines for the Evaluation and Treatment of Muscle Dysfunction in Patients With Chronic Obstructive Pulmonary Disease, Arch. Bronconeumol. 51 (2015) pp. 384-395.

8. E. Barreiro, L. del Puerto-Nevado, E. Puig-Vilanova, S. Perez-Rial, F. Sanchez, L. Martinez-Galan, S. Rivera, J. Gea, N. Gonzalez-Mangado, and G. Peces-Barba, Cigarette smoke-induced oxidative stress in skeletal muscles of mice, Respir. Physiol Neurobiol. 182 (2012) pp. 9-17.

9. E. Barreiro and J. Gea, Epigenetics and muscle dysfunction in chronic obstructive pulmonary disease, Transl. Res. 165 (2015) pp. 61-73.

10. E. Barreiro, J. Marin-Corral, F. Sanchez, V. Mielgo, F.J. Alvarez, J.B. Galdiz, and J. Gea, Reference values of respiratory and peripheral muscle function in rats, J. Anim Physiol Anim Nutr. (Berl) 94 (2010) p. e393-e401.

11. E. Barreiro and J.I. Sznajder, Epigenetic regulation of muscle phenotype and adaptation: a potential role in COPD muscle dysfunction, J. Appl. Physiol (1985.) 114 (2013) pp. 1263-1272.

12. A. Chacon-Cabrera, C. Fermoselle, A.J. Urtreger, M. Mateu-Jimenez, M.J. Diament, E.D. De Kier Joffe, M. Sandri, and E. Barreiro, Pharmacological strategies in lung cancer-induced cachexia: effects on muscle proteolysis, autophagy, structure, and weakness, J. Cell Physiol 229 (2014) pp. 1660-1672.

13. J. Chen, Y. Sun, X. Mao, Q. Liu, H. Wu, and Y. Chen, RANKL up-regulates brain-type creatine kinase via poly(ADP-ribose) polymerase-1 during osteoclastogenesis, J. Biol. Chem. 285 (2010) pp. 36315-36321.

14. J.F. Chen, E.M. Mandel, J.M. Thomson, Q. Wu, T.E. Callis, S.M. Hammond, F.L. Conlon, and D.Z. Wang, The role of microRNA-1 and microRNA-133 in skeletal muscle proliferation and differentiation, Nat. Genet. 38 (2006) pp. 228-233.

15. J.M. de Murcia, C. Niedergang, C. Trucco, M. Ricoul, B. Dutrillaux, M. Mark, F.J. Oliver, M. Masson, A. Dierich, M. LeMeur, C. Walztinger, P. Chambon, and M.G. de, Requirement of poly(ADP-ribose) polymerase in recovery from DNA damage in mice and in cells, Proc. Natl. Acad. Sci. U. S. A 94 (1997) pp. 7303-7307.

16. M.G. de, V. Schreiber, M. Molinete, B. Saulier, O. Poch, M. Masson, C. Niedergang, and M.J. Menissier de, Structure and function of poly(ADP-ribose) polymerase, Mol. Cell Biochem. 138 (1994) pp. 15-24.

17. M.J. Diament, C. Garcia, I. Stillitani, V.M. Saavedra, T. Manzur, L. Vauthay, and S. Klein, Spontaneous murine lung adenocarcinoma (P07): A new experimental model to study paraneoplastic syndromes of lung cancer, Int. J. Mol. Med. 2 (1998) pp. 45-50.

18. M.J. Diament, G.D. Peluffo, I. Stillitani, L.C. Cerchietti, A. Navigante, S.M. Ranuncolo, and S.M. Klein, Inhibition of tumor progression and paraneoplastic syndrome development in a murine lung adenocarcinoma by medroxyprogesterone acetate and indomethacin, Cancer Invest 24 (2006) pp. 126-131.

19. W.J. Evans, J.E. Morley, J. Argiles, C. Bales, V. Baracos, D. Guttridge, A. Jatoi, K. Kalantar-Zadeh, H. Lochs, G. Mantovani, D. Marks, W.E. Mitch, M. Muscaritoli, A. Najand, P. Ponikowski, F.F. Rossi, M. Schambelan, A. Schols, M. Schuster, D. Thomas, R. Wolfe, and S.D. Anker, Cachexia: a new definition, Clin. Nutr. 27 (2008) pp. 793-799.

20. K. Fearon, F. Strasser, S.D. Anker, I. Bosaeus, E. Bruera, R.L. Fainsinger, A. Jatoi, C. Loprinzi, N. MacDonald, G. Mantovani, M. Davis, M. Muscaritoli, F. Ottery, L. Radbruch, P. Ravasco, D. Walsh, A. Wilcock, S. Kaasa, and V.E. Baracos, Definition and classification of cancer cachexia: an international consensus, Lancet Oncol. 12 (2011) pp. 489-495.

21. C. Fermoselle, E. Garcia-Arumi, E. Puig-Vilanova, A.L. Andreu, A.J. Urtreger, E.D. De Kier Joffe, A. Tejedor, L. Puente-Maestu, and E. Barreiro, Mitochondrial dysfunction and therapeutic approaches in respiratory and limb muscles of cancer cachectic mice, Exp. Physiol 98 (2013) pp. 1349-1365.

22. C. Fermoselle, F. Sanchez, and E. Barreiro, [Reduction of muscle mass mediated by myostatin in an experimental model of pulmonary emphysema], Arch. Bronconeumol. 47 (2011) pp. 590-598.

23. P.O. Hassa and M.O. Hottiger, A role of poly (ADP-ribose) polymerase in NF-kappaB transcriptional activation, Biol. Chem. 380 (1999) pp. 953-959.

24. J. Kim, M. Kundu, B. Viollet, and K.L. Guan, AMPK and mTOR regulate autophagy through direct phosphorylation of Ulk1, Nat. Cell Biol. 13 (2011) pp. 132-141.

25. V. Leiro-Fernandez, C. Mouronte-Roibas, C. Ramos-Hernandez, M. Botana-Rial, A. Gonzalez-Pineiro, E. Garcia-Rodriguez, C. Represas-Represas, and A. Fernandez-Villar, Changes in clinical presentation and staging of lung cancer over two decades, Arch. Bronconeumol. 50 (2014) pp. 417-421.

26. A. Lewis, J. Riddoch-Contreras, S.A. Natanek, A. Donaldson, W.D. Man, J. Moxham, N.S. Hopkinson, M.I. Polkey, and P.R. Kemp, Downregulation of the serum response factor/miR-1 axis in the quadriceps of patients with COPD, Thorax 67 (2012) pp. 26-34.

27. K.J. Livak and T.D. Schmittgen, Analysis of relative gene expression data using real-time quantitative PCR and the 2(-Delta Delta C(T)) Method, Methods 25 (2001) pp. 402-408.

28. J. Marin-Corral, C.C. Fontes, S. Pascual-Guardia, F. Sanchez, M. Olivan, J.M. Argiles, S. Busquets, F.J. Lopez-Soriano, and E. Barreiro, Redox balance and carbonylated proteins in limb and heart muscles of cachectic rats, Antioxid. Redox. Signal. 12 (2010) pp. 365-380.

29. J. Marin-Corral, J. Minguella, A.L. Ramirez-Sarmiento, S.N. Hussain, J. Gea, and E. Barreiro, Oxidised proteins and superoxide anion production in the diaphragm of severe COPD patients, Eur. Respir. J. 33 (2009) pp. 1309-1319.

30. J.J. McCarthy and K.A. Esser, MicroRNA-1 and microRNA-133a expression are decreased during skeletal muscle hypertrophy, J. Appl. Physiol 102 (2007) pp. 306-313.

31. J.J. McCarthy, K.A. Esser, C.A. Peterson, and E.E. Dupont-Versteegden, Evidence of MyomiR network regulation of beta-myosin heavy chain gene expression during skeletal muscle atrophy, Physiol Genomics 39 (2009) pp. 219-226.

32. M.J. Menissier de, M. Ricoul, L. Tartier, C. Niedergang, A. Huber, F. Dantzer, V. Schreiber, J.C. Ame, A. Dierich, M. LeMeur, L. Sabatier, P. Chambon, and M.G. de, Functional interaction between PARP-1 and PARP-2 in chromosome stability and embryonic development in mouse, EMBO J. 22 (2003) pp. 2255-2263.

33. K.T. Murphy, A. Chee, J. Trieu, T. Naim, and G.S. Lynch, Importance of functional and metabolic impairments in the characterization of the C-26 murine model of cancer cachexia, Dis. Model. Mech. 5 (2012) pp. 533-545.

34. N. Nakajima, T. Takahashi, R. Kitamura, K. Isodono, S. Asada, T. Ueyama, H. Matsubara, and H. Oh, MicroRNA-1 facilitates skeletal myogenic differentiation without affecting osteoblastic and adipogenic differentiation, Biochem. Biophys. Res. Commun. 350 (2006) pp. 1006-1012.

35. S.A. Natanek, J. Riddoch-Contreras, G.S. Marsh, N.S. Hopkinson, W.D. Man, J. Moxham, M.I. Polkey, and P.R. Kemp, Yin Yang 1 expression and localisation in quadriceps muscle in COPD, Arch. Bronconeumol. 47 (2011) pp. 296-302.

36. F.J. Oliver, M.J. Menissier-de, C. Nacci, P. Decker, R. Andriantsitohaina, S. Muller, G. de la Rubia, J.C. Stoclet, and M.G. de, Resistance to endotoxic shock as a consequence of defective NF-kappaB activation in poly (ADP-ribose) polymerase-1 deficient mice, EMBO J. 18 (1999) pp. 4446-4454.

37. G.D. Peluffo, I. Stillitani, V.A. Rodriguez, M.J. Diament, and S.M. Klein, Reduction of tumor progression and paraneoplastic syndrome development in murine lung adenocarcinoma by nonsteroidal antiinflammatory drugs, Int. J. Cancer 110 (2004) pp. 825-830.

38. J.C. Penalver Cuesta, A.C. Jorda, F.N. Mancheno, J.A. Ceron Navarro, Q.K. de Aguiar, M.M. Arraras, F.J. Vera Sempere, and J.D. Padilla Alarcon, Prognostic Factors in Non-Small Cell Lung Cancer Less than 3 Centimeters: Actuarial Analysis, Accumulative Incidence and Risk Groups, Arch. Bronconeumol. (2015).

39. E. Perdiguero, P. Sousa-Victor, E. Ballestar, and P. Munoz-Canoves, Epigenetic regulation of myogenesis, Epigenetics. 4 (2009) pp. 541-550.

40. M.J. Potthoff, H. Wu, M.A. Arnold, J.M. Shelton, J. Backs, J. McAnally, J.A. Richardson, R. Bassel-Duby, and E.N. Olson, Histone deacetylase degradation and MEF2 activation promote the formation of slow-twitch myofibers, J. Clin. Invest 117 (2007) pp. 2459-2467.

41. E. Puig-Vilanova, R. Aguilo, A. Rodriguez-Fuster, J. Martinez-Llorens, J. Gea, and E. Barreiro, Epigenetic mechanisms in respiratory muscle dysfunction of patients with chronic obstructive pulmonary disease, PLoS. One. 9 (2014) p. e111514.

42. E. Puig-Vilanova, P. Ausin, J. Martinez-Llorens, J. Gea, and E. Barreiro, Do epigenetic events take place in the vastus lateralis of patients with mild chronic obstructive pulmonary disease?, PLoS. One. 9 (2014) p. e102296.

43. E. Puig-Vilanova, J. Martinez-Llorens, P. Ausin, J. Roca, J. Gea, and E. Barreiro, Quadriceps muscle weakness and atrophy are associated with a differential epigenetic profile in advanced COPD, Clin. Sci. (Lond) 128 (2015) pp. 905-921.

44. E. Puig-Vilanova, D.A. Rodriguez, J. Lloreta, P. Ausin, S. Pascual-Guardia, J. Broquetas, J. Roca, J. Gea, and E. Barreiro, Oxidative stress, redox signaling pathways, and autophagy in cachectic muscles of male patients with advanced COPD and lung cancer, Free Radic. Biol. Med. 79C (2014) pp. 91-108.

45. D. Quenet, R.R. El, V. Schreiber, and F. Dantzer, The role of poly(ADP-ribosyl)ation in epigenetic events, Int. J. Biochem. Cell Biol. 41 (2009) pp. 60-65.

46. B.M. Roberts, B. Ahn, A.J. Smuder, M. Al-Rajhi, L.C. Gill, A.W. Beharry, S.K. Powers, D.D. Fuller, L.F. Ferreira, and A.R. Judge, Diaphragm and ventilatory dysfunction during cancer cachexia, FASEB J. 27 (2013) pp. 2600-2610.

47. M. Rodriguez, M.T. Gomez Hernandez, N.M. Novoa, J.L. Aranda, M.F. Jimenez, and G. Varela, Morbidity and mortality in octogenarians with lung cancer undergoing pneumonectomy, Arch. Bronconeumol. 51 (2015) pp. 219-222.

48. M. Rodriguez, M.T. Gomez Hernandez, N.M. Novoa, J.L. Aranda, M.F. Jimenez, and G. Varela, Poorer Survival in Stage IB Lung Cancer Patients After Pneumonectomy, Arch. Bronconeumol. 51 (2015) pp. 223-226.

49. K. Sadoul, C. Boyault, M. Pabion, and S. Khochbin, Regulation of protein turnover by acetyltransferases and deacetylases, Biochimie 90 (2008) pp. 306-312.

50. P. Sanchez-Salcedo, J. Berto, J.P. de-Torres, A. Campo, A.B. Alcaide, G. Bastarrika, J.C. Pueyo, A. Villanueva, J.I. Echeveste, M.D. Lozano, M.J. Garcia-Velloso, L.M. Seijo, J. Garcia, W. Torre, M.J. Pajares, R. Pio, L.M. Montuenga, and J.J. Zulueta, Lung cancer screening: fourteen year experience of the Pamplona early detection program (P-IELCAP), Arch. Bronconeumol. 51 (2015) pp. 169-176.

51. M. Toledo, S. Busquets, S. Sirisi, R. Serpe, M. Orpi, J. Coutinho, R. Martinez, F.J. Lopez-Soriano, and J.M. Argiles, Cancer cachexia: physical activity and muscle force in tumour-bearing rats, Oncol. Rep. 25 (2011) pp. 189-193.

52. A.H. Tseng, L.H. Wu, S.S. Shieh, and D.L. Wang, SIRT3 interactions with FOXO3 acetylation, phosphorylation and ubiquitinylation mediate endothelial cell responses to hypoxia, Biochem. J. 464 (2014) pp. 157-168.

53. A.J. Urtreger, M.J. Diament, S.M. Ranuncolo, C. Del, V, L.I. Puricelli, S.M. Klein, and E.D. De Kier Joffe, New murine cell line derived from a spontaneous lung tumor induces paraneoplastic syndromes, Int. J. Oncol. 18 (2001) pp. 639-647.

54. A. Vignaud, A. Ferry, A. Huguet, M. Baraibar, C. Trollet, J. Hyzewicz, G. Butler-Browne, J. Puymirat, G. Gourdon, and D. Furling, Progressive skeletal muscle weakness in transgenic mice expressing CTG expansions is associated with the activation of the ubiquitin-proteasome pathway, Neuromuscul. Disord. 20 (2010) pp. 319-325.

55. C.K. Vincent, A. Gualberto, C.V. Patel, and K. Walsh, Different regulatory sequences control creatine kinase-M gene expression in directly injected skeletal and cardiac muscle, Mol. Cell Biol. 13 (1993) pp. 1264-1272.

56. H. Wang, E. Hertlein, N. Bakkar, H. Sun, S. Acharyya, J. Wang, M. Carathers, R. Davuluri, and D.C. Guttridge, NF-kappaB regulation of YY1 inhibits skeletal myogenesis through transcriptional silencing of myofibrillar genes, Mol. Cell Biol. 27 (2007) pp. 4374-4387.

57. L.A. Whittemore, K. Song, X. Li, J. Aghajanian, M. Davies, S. Girgenrath, J.J. Hill, M. Jalenak, P. Kelley, A. Knight, R. Maylor, D. O'Hara, A. Pearson, A. Quazi, S. Ryerson, X.Y. Tan, K.N. Tomkinson, G.M. Veldman, A. Widom, J.F. Wright, S. Wudyka, L. Zhao, and N.M. Wolfman, Inhibition of myostatin in adult mice increases skeletal muscle mass and strength, Biochem. Biophys. Res. Commun. 300 (2003) pp. 965-971.

58. J.P. Williams, B.E. Phillips, K. Smith, P.J. Atherton, D. Rankin, A.L. Selby, S. Liptrot, J. Lund, M. Larvin, and M.J. Rennie, Effect of tumor burden and subsequent surgical resection on skeletal muscle mass and protein turnover in colorectal cancer patients, Am. J. Clin. Nutr. 96 (2012) pp. 1064-1070.

59. J. Yelamos, J. Farres, L. Llacuna, C. Ampurdanes, and J. Martin-Caballero, PARP-1 and PARP-2: New players in tumour development, Am. J. Cancer Res. 1 (2011) pp. 328-346.

60. A. Zetser, E. Gredinger, and E. Bengal, p38 mitogen-activated protein kinase pathway promotes skeletal muscle differentiation. Participation of the Mef2c transcription factor, J. Biol. Chem. 274 (1999) pp. 5193-5200.

61. C.L. Zhang, T.A. McKinsey, and E.N. Olson, Association of class II histone deacetylases with heterochromatin protein 1: potential role for histone methylation in control of muscle differentiation, Mol. Cell Biol. 22 (2002) pp. 7302-7312.

62. D. Zhang, X. Wang, Y. Li, L. Zhao, M. Lu, X. Yao, H. Xia, Y.C. Wang, M.F. Liu, J. Jiang, X. Li, and H. Ying, Thyroid hormone regulates muscle fiber type conversion via miR-133a1, J. Cell Biol. 207 (2014) pp. 753-766.

FIGURE LEGENDS

Figure 1: Graphical representation of the progression of body weight in mice from all experimental groups. The following signs have been used in each group: non-cachectic control wild type animals (blue diamonds, N=10), LC cachectic wild type mice (squares, N=10), non-cachectic control Parp-$1^{-/-}$ rodents (triangles, N=8), LC cachectic Parp-$1^{-/-}$ mice (purple squares, N=12), non-cachectic control Parp-$2^{-/-}$ rodents (green squares, N=6), and LC cachectic Parp-$2^{-/-}$ animals (circles, N=6) over the study period (1 month).

Figure 2: Mean values and standard deviation of miR-1 (top panels, A and B) and miR-133a (bottom panels, C and D) expression in the diaphragm (left panels) and gastrocnemius (right panels) muscles. Statistical significance is represented as follows: *, $p \leq 0.05$, **, $p \leq 0.01$, ***, and $p \leq 0.001$ between either wild type, Parp-$1^{-/-}$, or Parp-$2^{-/-}$ LC cachectic mice and their respective non-cachectic control rodents; †, $p \leq 0.05$, and †††, $p \leq 0.001$ between any of the non-cachectic control knockout animals and non-cachectic wild type mice.

Figure 3: Mean values and standard deviation of miR-206 (top panels, A and B) and miR-486 (bottom panels, C and D) expression in the diaphragm (left panels) and gastrocnemius (right panels). Statistical significance is represented as follows: *, $p \leq 0.05$, **, $p \leq 0.01$, ***, $p \leq 0.001$, and n.s., non-significant differences between either wild type, Parp-$1^{-/-}$, or Parp-$2^{-/-}$ LC cachectic mice and their respective non-cachectic control rodents; †, $p \leq 0.05$, ††, $p \leq 0.01$, and †††, $p \leq 0.001$ between any of the non-cachectic control knockout animals and non-cachectic wild type mice.A significant correlation was found between type II fiber size and miR-133 expression in the gastrocnemius of the cachectic wild type mice. No significant correlations were observed between type II fiber size and miR-133 expression in the gastrocnemius of any of the cachectic knockout animals (panel E).

Figure 4: Mean values and standard deviation of total acetylated proteins (panels A and B), acetylated FoxO1 (panels C and D),acetylated FoxO3 (panels E and F), and acetylated PGC-

1α (panelsG and H) in the diaphragm (left panels) and gastrocnemius (right panels) muscles, as measured by optical densities in arbitrary units (OD, a.u.). Statistical significance is represented as follows: *, p≤0.05, **, p≤0.01, ***, p≤0.001, and n.s., non-significant differences between either wild type, Parp-$1^{-/-}$, or Parp-$2^{-/-}$ LC cachectic mice and their respective non-cachectic control animals.

Figure 5: Mean values and standard deviation of HDAC3 (top panels, A and B), HDAC6 (medium panels, C and D), and SIRT1 (bottom panels, E and F) in the diaphragm (left panels) and gastrocnemius (right panels) muscles, as measured by optical densities in arbitrary units (OD, a.u.). Statistical significance is represented as follows: *, p≤0.05, **, p≤0.01, and n.s., non-significant differences between either wild type, Parp-$1^{-/-}$, or Parp-$2^{-/-}$ LC cachectic mice and their respective non-cachectic control animals.

Figure 6: Mean values and standard deviation of the transcription factors MEF2C (top panels, A and B), MEF2D (medium panels, C and D), and YY1 (bottom panels, E and F) protein content in the diaphragm (left panels) and gastrocnemius (right panels) muscles, as measured by optical densities in arbitrary units (OD, a.u.). Statistical significance is represented as follows: *, p≤0.05, **, p≤0.01, ***, p≤0.001, and n.s., non-significant differences between either wild type, Parp-$1^{-/-}$, or Parp-$2^{-/-}$ LC cachectic mice and their respective non-cachectic control animals; ††, p≤0.01 between any of the non-cachectic control knockout animals and non-cachectic wild type mice.

Figure 7: Mean values and standard deviation of α-actin skeletal muscle (top panels, A and B), total PGC-1α (medium panels, C and D), and creatine kinase (bottom panels, E and F) protein content in the diaphragm (left panels) and gastrocnemius (right panels) muscles, as measured by optical densities in arbitrary units (OD, a.u.). Statistical significance is represented as follows: *, p≤0.05, ***, p≤0.001, and n.s., non-significant differences between either wild type, Parp-$1^{-/-}$, or Parp-$2^{-/-}$ LC cachectic mice and their respective non-cachectic

control animals; ††, $p \leq 0.01$ between any of the non-cachectic control knockout animals and non-cachectic wild type mice.

Table 1. MicroRNA assays and probes used for the quantitative analyses of the target genes using real-time PCR.

Assay Name	**Assay ID**	**miRBase accession number**
Muscle-specific, myomiRs		
hsa-miR-1	002222	MIMAT0000416
hsa-miR-133a	002246	MIMAT0000427
hsa-miR-206	000510	MIMAT0000462
Other miRNAs **(highly expressed in muscles)**		
hsa-miR-486	001278	MIMAT0002177
		NCBI Accessionnumber
U6 snRNA, housekeeping gene	001973	NR_004394

Abbreviations: ID, identification; hsa, homo sapiens; miR, microRNA; MIMAT, mature microRNA; snRNA, small nuclear RNA; NR, non-coding RNA RefSeq database category.

Table 2. Physiological characteristics of wild type, Parp-1$^{-/-}$, and Parp-2$^{-/-}$ mice at the end of the studyperiod.

	Wild type mice		Parp-1$^{-/-}$ mice		Parp-2$^{-/-}$ mice	
	Control	LC cachexia	Control	LC cachexia	Control	LC cachexia
Age at baseline (weeks)	10	10, n.s.	10	10, n.s.	10	10, n.s.
Body weight at baseline (g)	20.30 (1.03)	19.60 (1.13), n.s.	19.28 (0.78)	18.61 (0.93), n.s.	19.25 (1.06)	19.89 (0.92), n.s.
Bodyweightgain (%)	+8.35 (2.35)	-6.55 (6.80), ***	+6.96 (2.23)	+1.55 (3.69), **	+4.34 (2.87)	+3.06 (6.81), n.s.
Foodintake (g/24h)	3.2 (0.5)	3.1 (0.4), n.s.	3.3 (0.6)	3.1 (0.4), n.s.	3.2 (0.4)	3.2 (0.3), n.s.
Diaphragmweight (g)	0.089 (0.01)	0.069 (0.008), ***	0.073 (0.01), ††	0.062 (0.007), *	0.076 (0.012), †	0.086 (0.013), n.s.
Gastrocnemiusweight (g)	0.116 (0.005)	0.082 (0.008), ***	0.105 (0.003), ††	0.096 (0.007), ***	0.096 (0.012), †††	0.098 (0.012), n.s.
Limbstrengthgain (%)	+10.03 (8.96)	-12.85 (7.14), ***	+12.86 (8.13)	-0.45 (6.08), **	+3.33 (1.99)	+2.10 (5.40), n.s.

Variables are presented as mean(standard deviation).In all animals, body weight and limb strength gains were calculated as the percentage of the measurements performed at the end of the study period (30 days) with respect to the same measurements obtained at baseline.

Definition of abbreviations: Parp-1$^{-/-}$ and Parp-2$^{-/-}$, poly-ADP ribose polymerase-1, and -2 knockout mice;LC, lung cancer.

Statistical significance: *, $p \leq 0.05$, **, $p \leq 0.01$, ***, $p \leq 0.001$, and n.s., non-significant differences between either wild type, Parp-1$^{-/-}$, or Parp-2$^{-/-}$ LC cachectic mice and their respective control (non-tumor) rodents; †, $p \leq 0.05$, †† $p \leq 0.01$, and †††, $p \leq 0.001$ between any of the control knockout animals and control (non-tumor) wild type mice.

Table 3. Subcutaneous tumor characteristics of wild type, Parp-1$^{-/-}$, and Parp-2$^{-/-}$ mice at the end of the studyperiod.

	Wild type mice	Parp-1$^{-/-}$ mice	Parp-2$^{-/-}$ mice
	LC cachexia	LC cachexia	LC cachexia
Subcutaneous tumor weight (g)	1.88 (0.54)	1.15 (0.33), **	1.26 (0.34), **
Ratio of tumor to total finalbody weight	10.2 (2.8)	6.1 (1.8), ***	6.2 (2.0), ***
Percentage of reduction in tumor weight		39	33
Cellular proliferation			
Ki-67 (%)	83.25 (2.8)	73.03 (7.9), **	75.14 (3.5), *
Apoptosis			
Bcl-2, OD (a.u.) (antiapopototic)	0.06 (0.03)	0.04 (0.01), *	0.03 (0.004), **
Bax, OD (a.u.) (proapoptotic)	0.010 (0.004)	0.016 (0.005),*	0.016 (0.002), *
Autophagy			
SIRT1, OD (a.u.)	0.07 (0.02)	0.09 (0.02), n.s.	0.09 (0.02), n.s.
LC3 II/LC3 I, OD (a.u.)	1.78 (0.6)	5.03 (2.2), *	8.30 (3.9), ***

Variables are presented as mean(standard deviation).

Definition of abbreviations: Parp-1$^{-/-}$ and Parp-2$^{-/-}$, poly-ADP ribose polymerase-1, and -2 knockout mice;LC, lung cancer;Bcl-2, B-cell lymphoma 2; Bax, Bcl-associated X protein; LC3, Light chain 3.

Statistical significance: *, p≤0.05, **, p≤0.01, ***, p≤0.001, and n.s., non-significant differences between any of the LC cachectic knockout groups of rodents and LC cachectic wild type mice.

Table 4. Muscle structural characteristics of wild type, Parp-1$^{-/-}$, and Parp-2$^{-/-}$ mice at the end of the study period.

		Wild type mice		Parp-1$^{-/-}$ mice		Parp-2$^{-/-}$ mice	
Muscle		Control	LC cachexia	Control	LC cachexia	Control	LC cachexia
Fibertypecomposition							
Type I fibers (%)	Diaphragm	9 (2)	8 (3), n.s.	9 (1)	9 (2), n.s.	7 (2)	9 (2), n.s.
	Gastrocnemiusiiu	13 (3)	13 (3), n.s.	13 (2)	13 (2), n.s.	17 (4)	15 (2), n.s.
Type II fibers (%)	Diaphragm	91 (2)	92 (3), n.s.	91 (1)	91 (2), n.s.	92 (3)	90 (2), n.s.
	Gastrocnemius	87 (3)	87 (3), n.s.	87 (2)	87 (2), n.s.	83 (4)	85 (2), n.s.
Type I fibers area (μm^2)	Diaphragm	328 (66)	233 (34), ***	325 (77)	289 (58), n.s.	292 (49)	311 (67), n.s.
	Gastrocnemius	953 (114)	644 (120), ***	864 (109)	730 (190), p=0.089	775 (128)	707 (82), n.s.
Type II fibers area (μm^2)	Diaphragm	396 (81)	303 (69), *	384 (80)	371 (76), n.s.	344 (98)	395 (114), n.s.
	Gastrocnemius	939 (118)	728 (140), **	885 (99)	743 (182), p=0.067	801 (69)	714 (61), n.s.

Values are expressed as mean (standard deviation).

Definition of abbreviations: Parp-1$^{-/-}$ and Parp-2$^{-/-}$, poly-ADP ribose polymerase-1, and -2 knockout mice; LC, lung cancer; μm, micrometer; n.s., non-significant.

Statistical significance: *, p≤0.05, **, p≤0.01, ***, p≤0.001, and n.s., non-significant differences between either wild type, Parp-1$^{-/-}$, or Parp-2$^{-/-}$ LC cachectic mice and their respective control (non-tumor) rodents.

Figure

A. Chacon-Cabrera *et al*. Figure 1

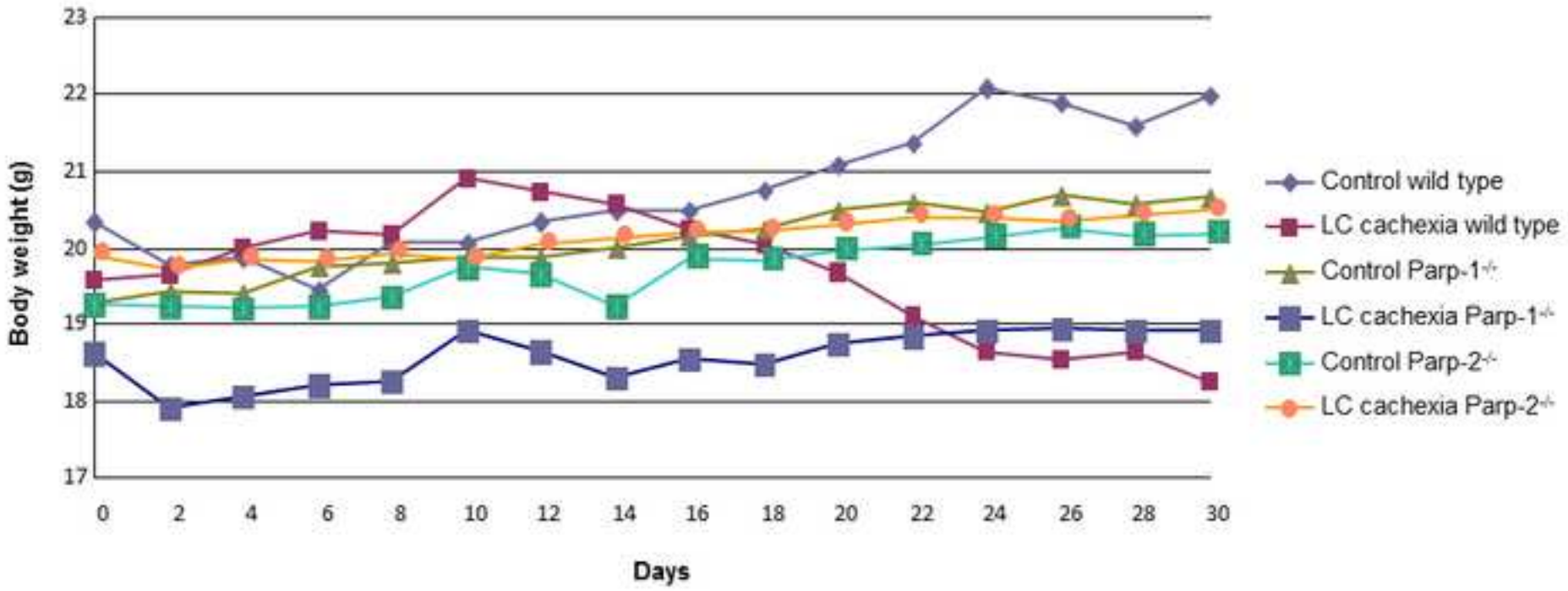

Figure

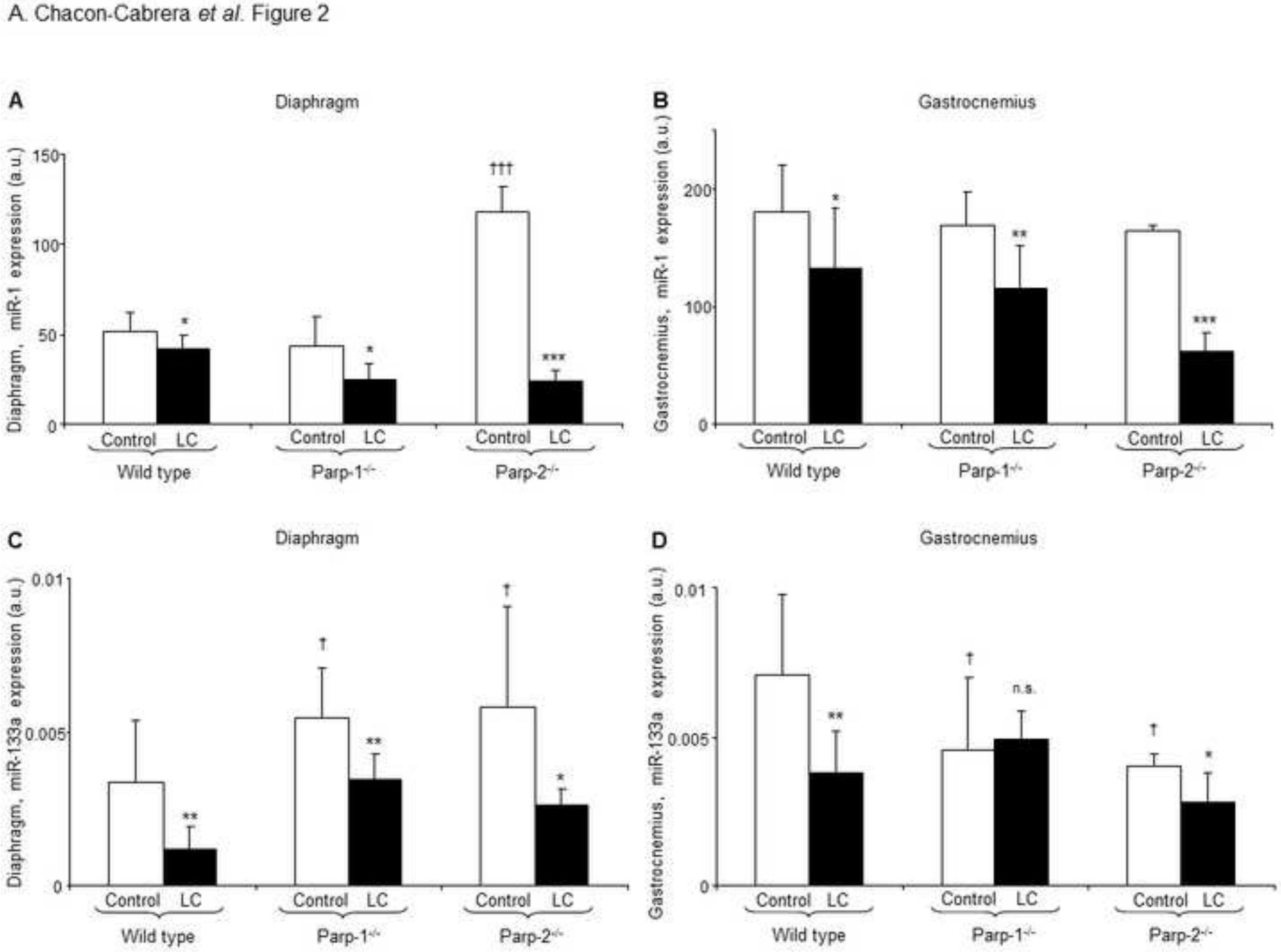
A. Chacon-Cabrera *et al.* Figure 2
A
Diaphragm
Diaphragm, miR-1 expression (a.u.)
150
100
50
0
*
*
†††
***
Control LC
Wild type
Parp-1-/-
Parp-2-/-
B
Gastrocnemius
Gastrocnemius, miR-1 expression (a.u.)
200
100
0
*
**
***
C
Diaphragm
Diaphragm, miR-133a expression (a.u.)
0.01
0.005
0
**
†
**
†
*
D
Gastrocnemius
Gastrocnemius, miR-133a expression (a.u.)
**
†
n.s.
†
*

Figure

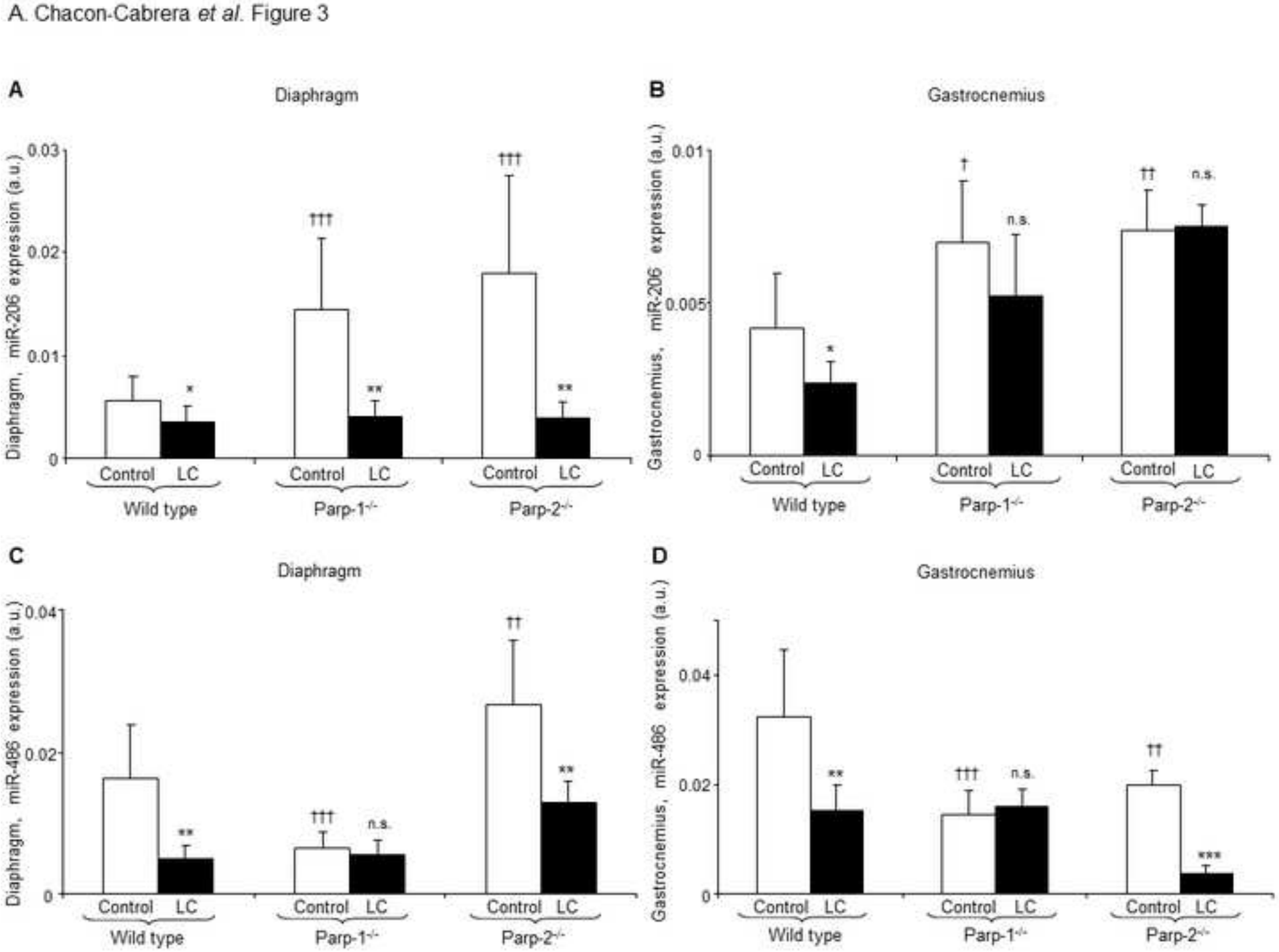
A. Chacon-Cabrera *et al.* Figure 3
A
Diaphragm
Diaphragm, miR-206 expression (a.u.)
0.03
0.02
0.01
0
Control LC
Wild type
Parp-1-/-
Parp-2-/-
B
Gastrocnemius
Gastrocnemius, miR-206 expression (a.u.)
0.01
0.005
0
n.s.
C
Diaphragm
Diaphragm, miR-486 expression (a.u.)
0.04
0.02
D
Gastrocnemius
Gastrocnemius, miR-486 expression (a.u.)

Figure

A. Chacon-Cabrera *et al.* Figure 3E

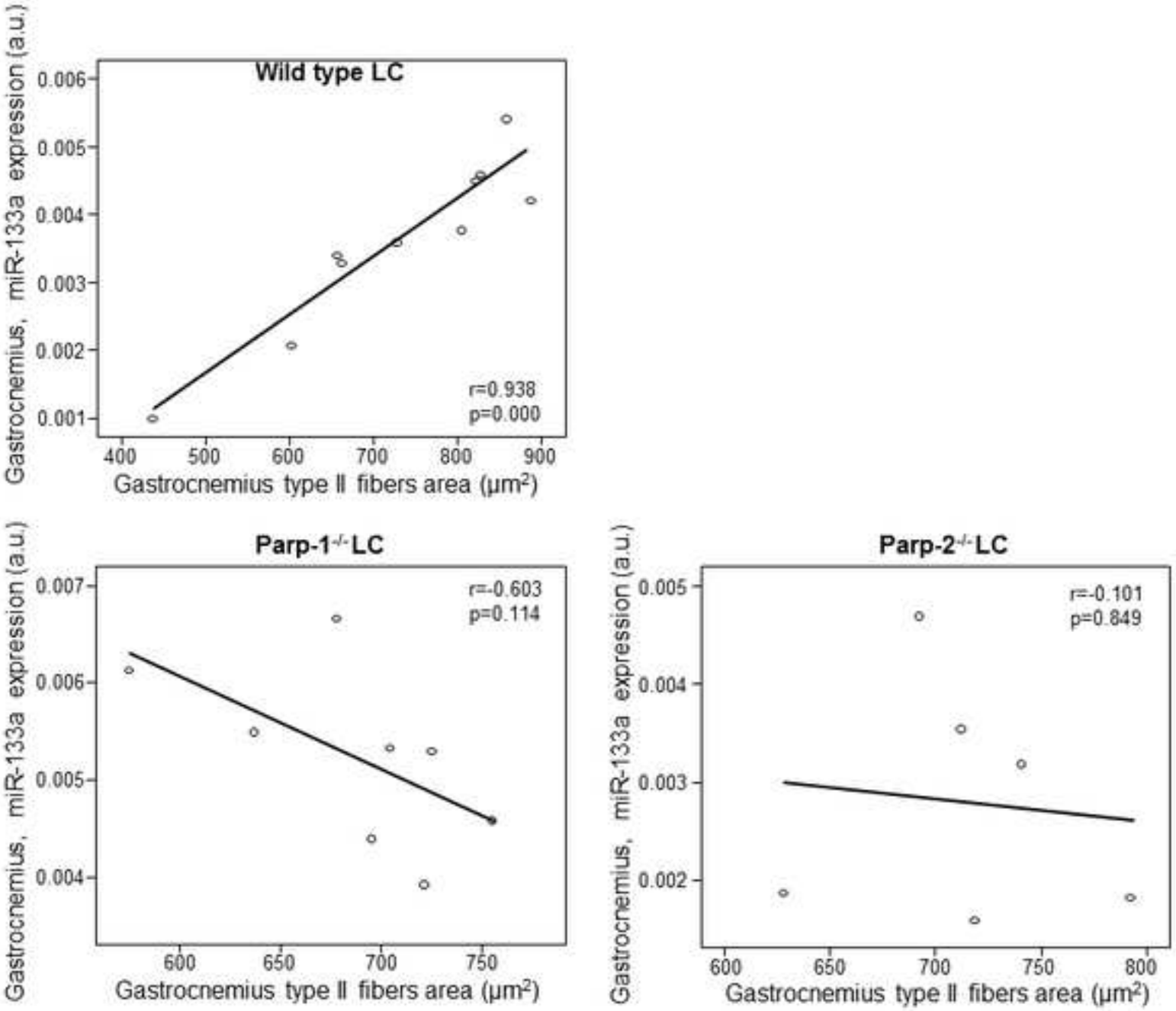

Figure

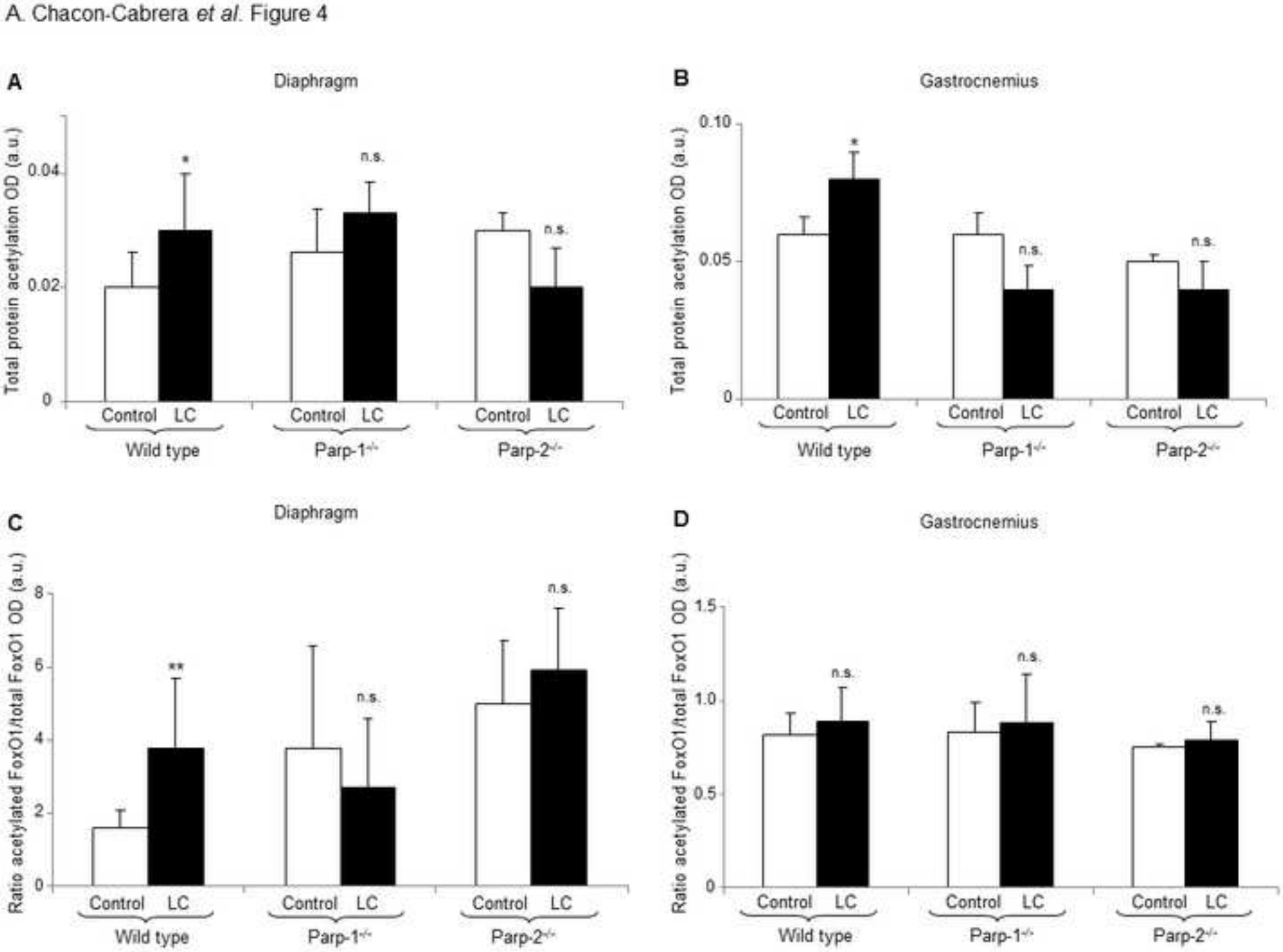
A. Chacon-Cabrera et al. Figure 4
A
Diaphragm
Total protein acetylation OD (a.u.)
0.04
0.02
0
*
n.s.
n.s.
Control LC
Wild type
Parp-1-/-
Parp-2-/-
B
Gastrocnemius
0.10
0.05
0
*
n.s.
n.s.
C
Diaphragm
Ratio acetylated FoxO1/total FoxO1 OD (a.u.)
8
6
4
2
0
**
n.s.
n.s.
D
Gastrocnemius
1.5
1.0
0.5
0
n.s.
n.s.
n.s.

Figure

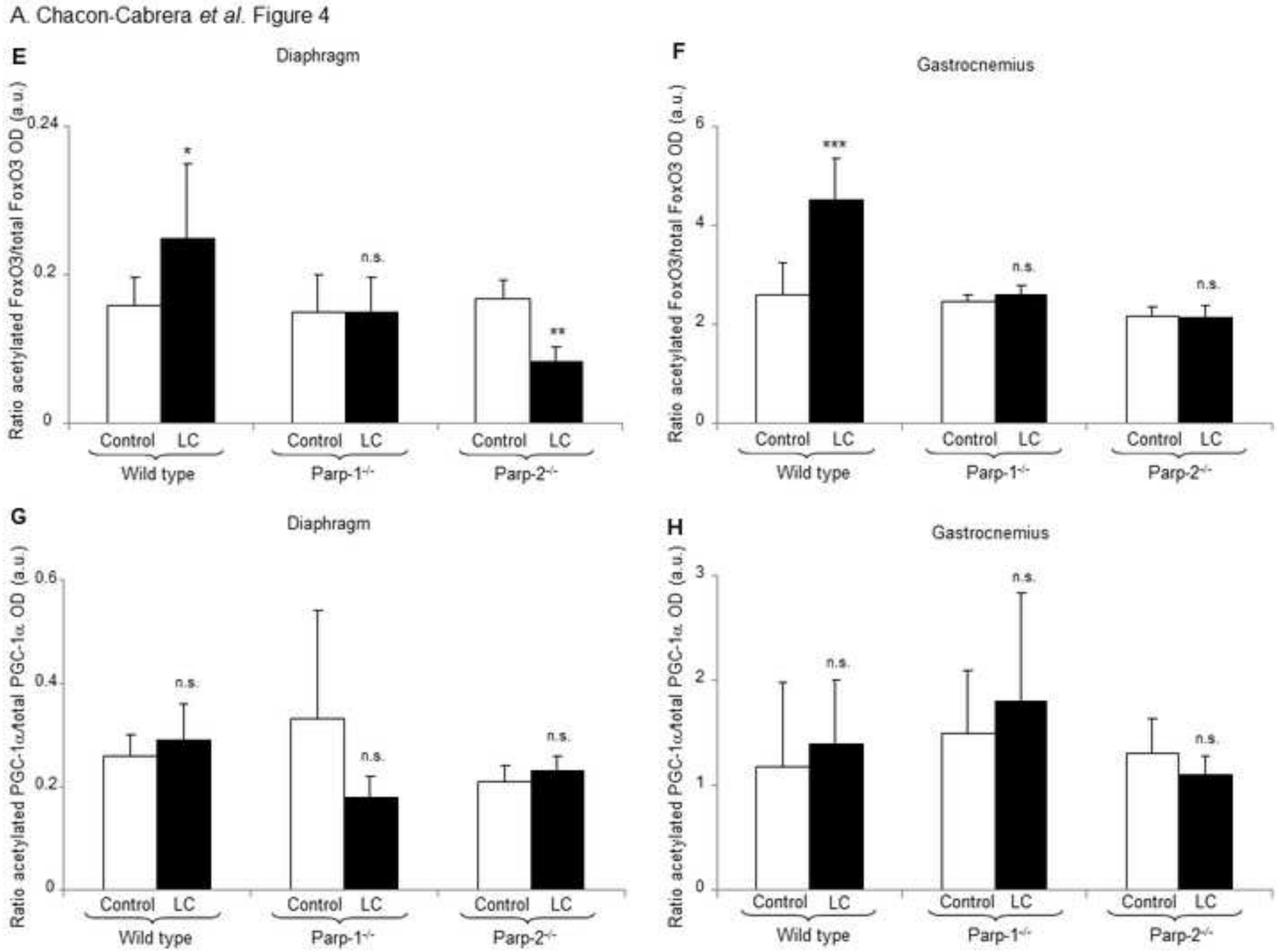
A. Chacon-Cabrera et al. Figure 4
E
Diaphragm
Ratio acetylated FoxO3/total FoxO3 OD (a.u.)
0.24
0.2
0
*
n.s.
**
Control
LC
Wild type
Parp-1-/-
Parp-2-/-
F
Gastrocnemius
6
4
2
0
***
n.s.
n.s.
G
Diaphragm
Ratio acetylated PGC-1α/total PGC-1α OD (a.u.)
0.6
0.4
0.2
0
n.s.
n.s.
n.s.
H
Gastrocnemius
3
2
1
0
n.s.
n.s.
n.s.

Figure

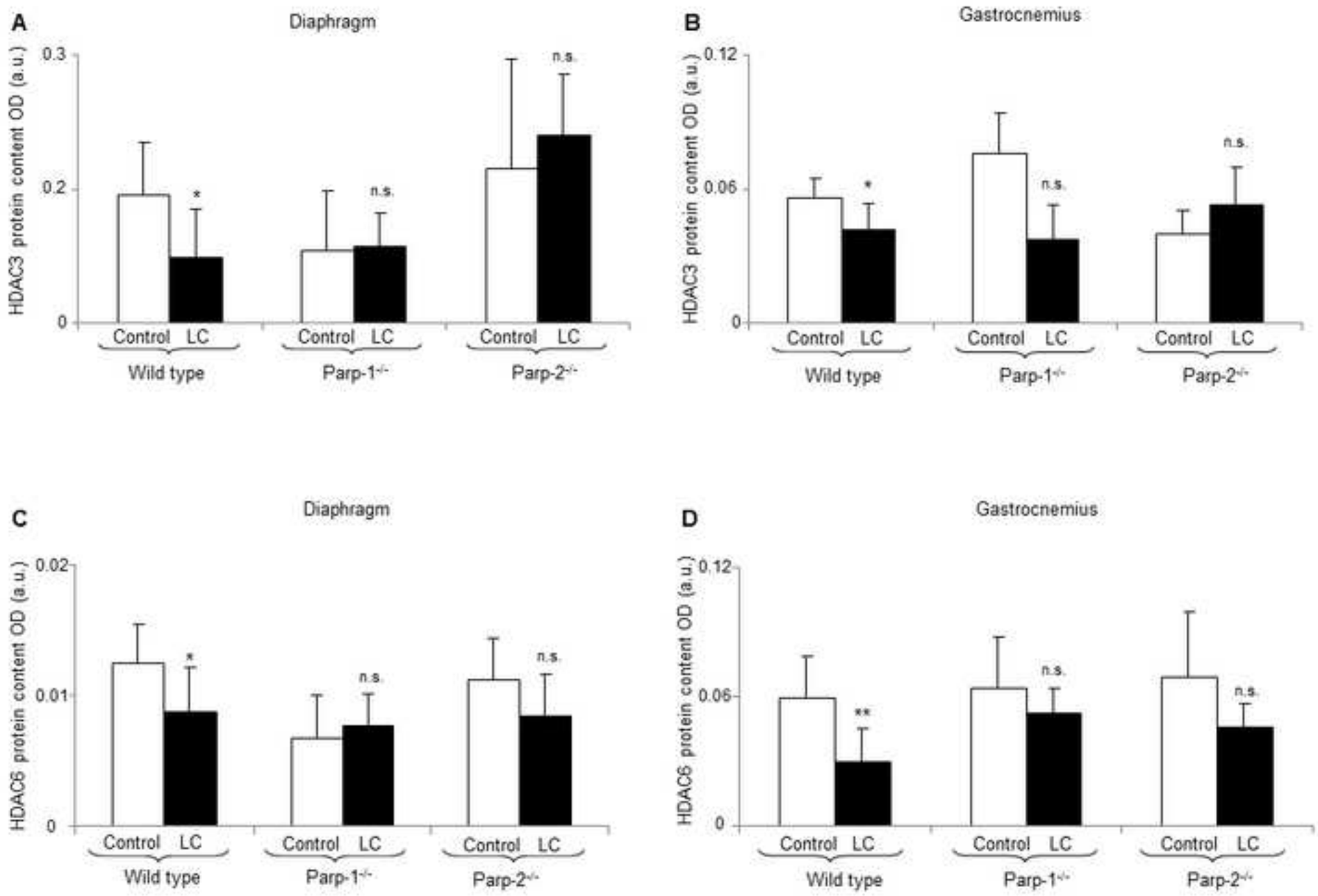
A. Chacon-Cabrera *et al.* Figure 5
A
Diaphragm
HDAC3 protein content OD (a.u.)
0.3
0.2
0
*
n.s.
n.s.
Control LC
Control LC
Control LC
Wild type
Parp-1-/-
Parp-2-/-
B
Gastrocnemius
HDAC3 protein content OD (a.u.)
0.12
0.06
0
*
n.s.
n.s.
Control LC
Control LC
Control LC
Wild type
Parp-1-/-
Parp-2-/-
C
Diaphragm
HDAC6 protein content OD (a.u.)
0.02
0.01
0
*
n.s.
n.s.
Control LC
Control LC
Control LC
Wild type
Parp-1-/-
Parp-2-/-
D
Gastrocnemius
HDAC6 protein content OD (a.u.)
0.12
0.06
0
**
n.s.
n.s.
Control LC
Control LC
Control LC
Wild type
Parp-1-/-
Parp-2-/-

Figure

A. Chacon-Cabrera *et al.* Figure 5

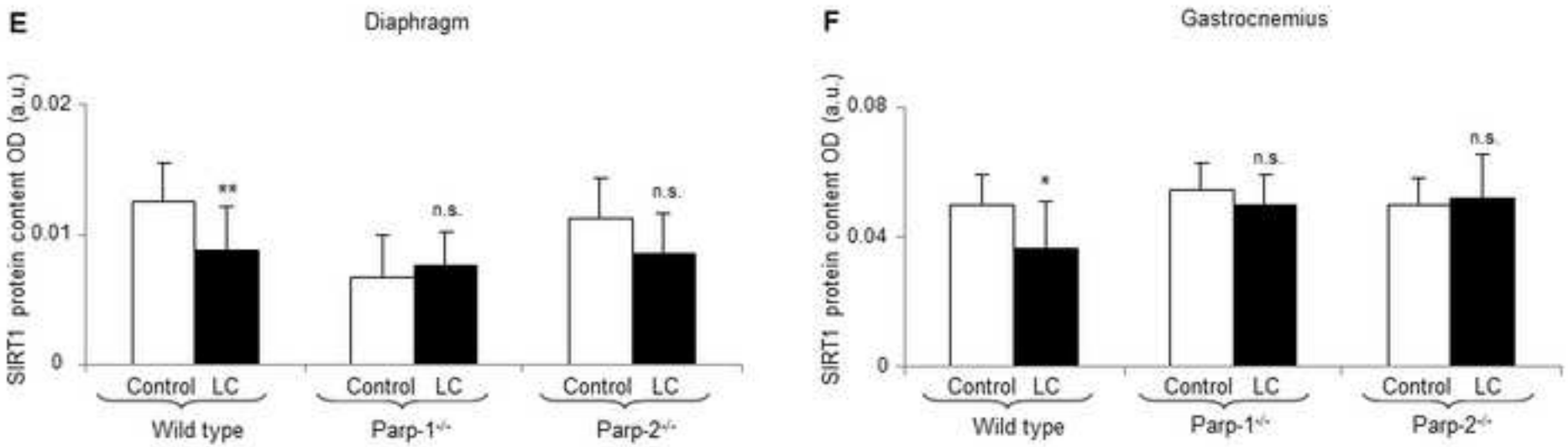

Figure

A. Chacon-Cabrera *et al.* Figure 6

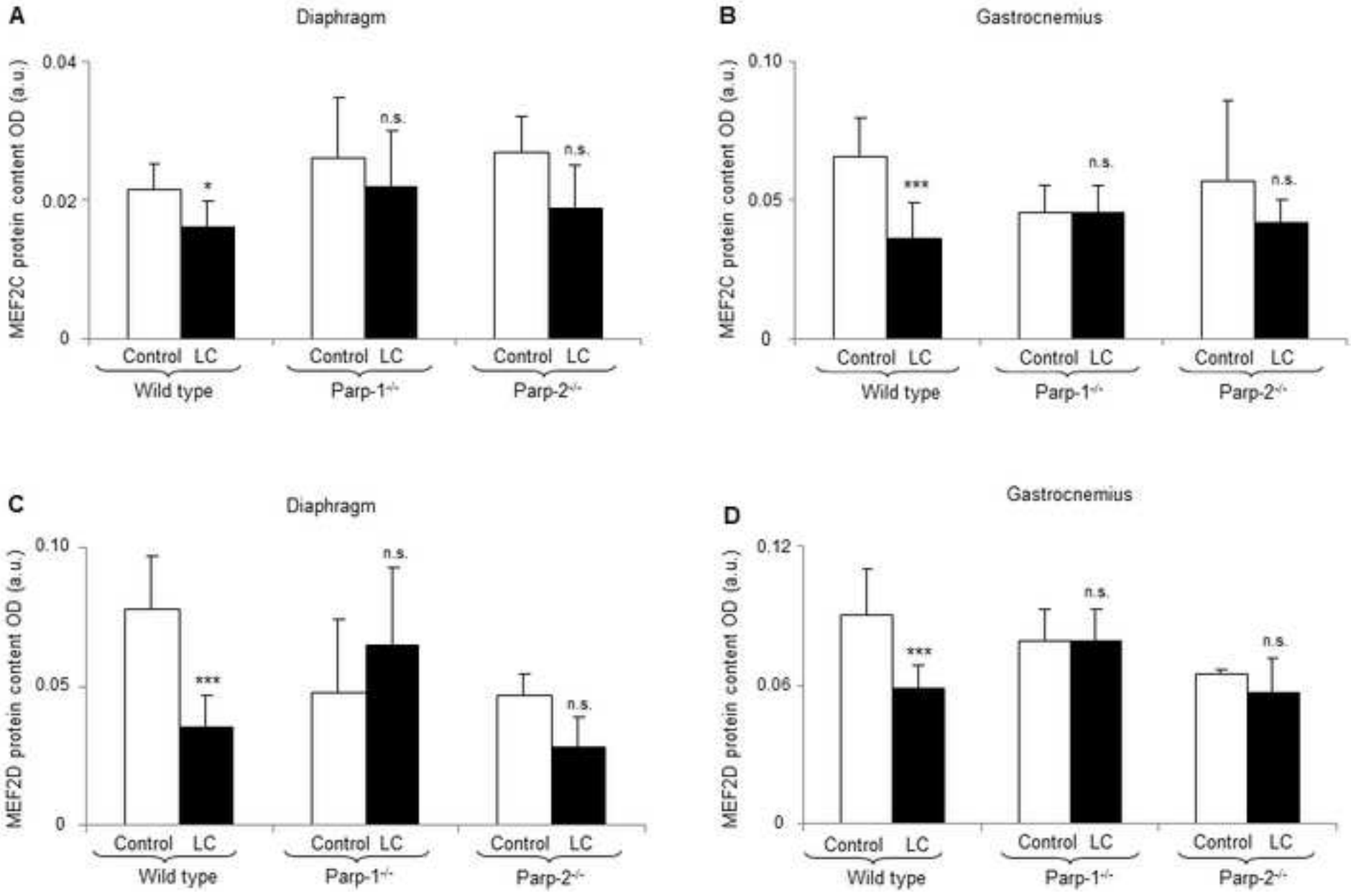

Figure

A. Chacon-Cabrera *et al.* Figure 6

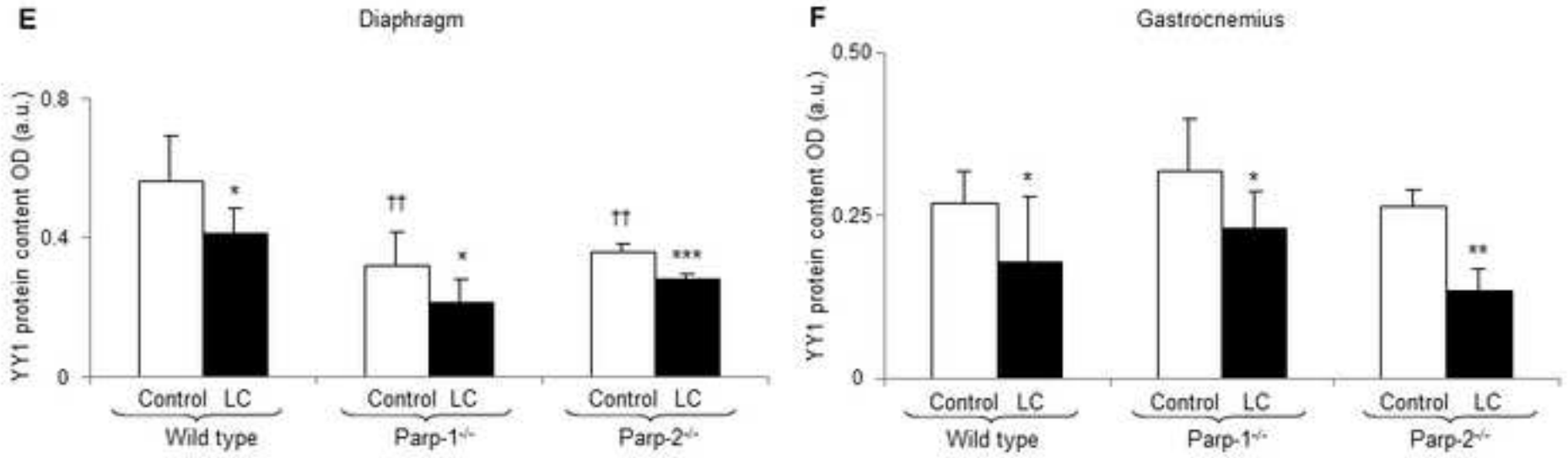

Figure

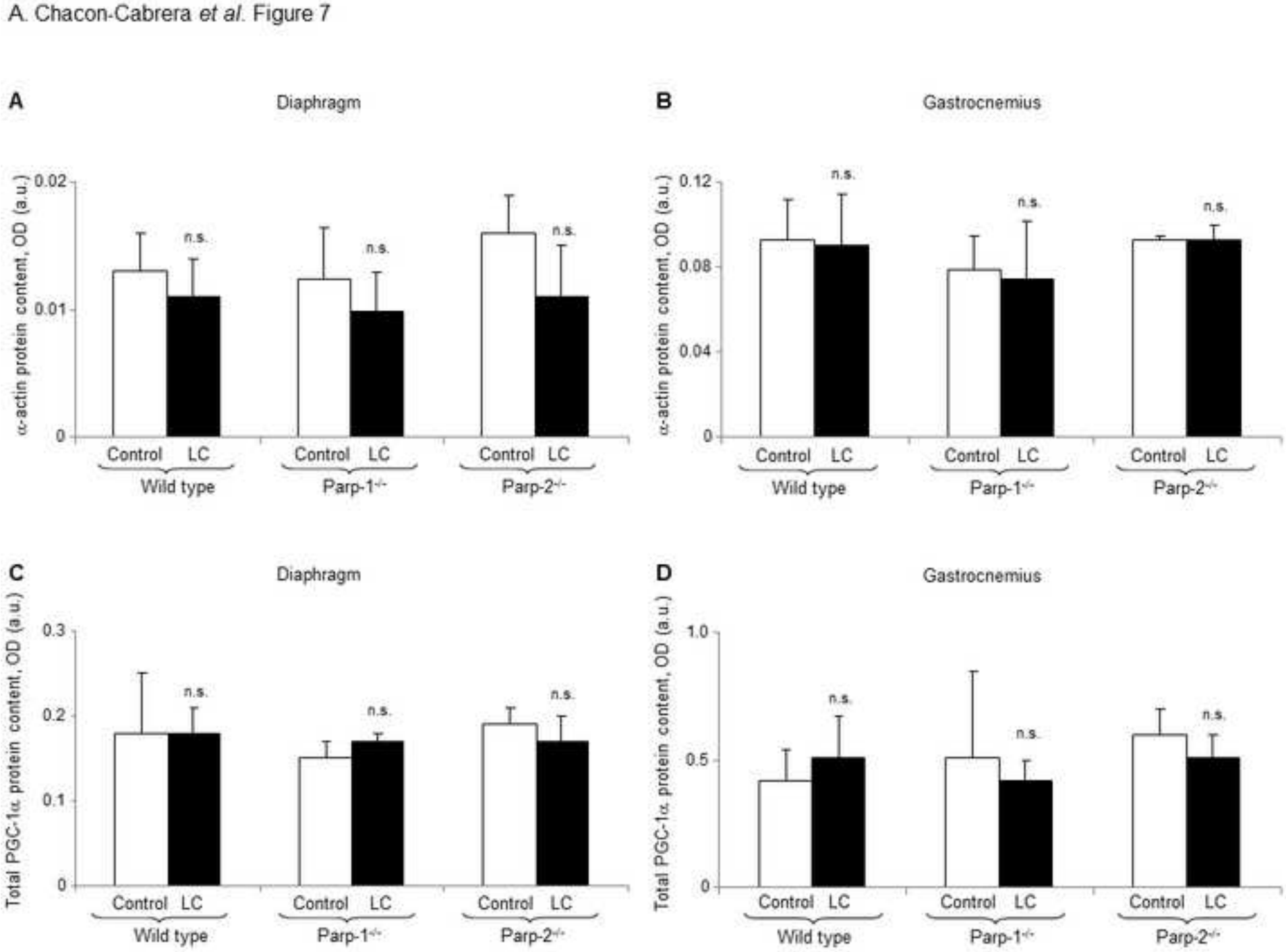
A. Chacon-Cabrera *et al.* Figure 7
A
Diaphragm
α-actin protein content, OD (a.u.)
0.02
0.01
0
n.s.
n.s.
n.s.
Control LC
Wild type
Parp-1-/-
Parp-2-/-
B
Gastrocnemius
0.12
0.08
0.04
C
Total PGC-1α protein content, OD (a.u.)
0.3
0.2
0.1
D
1.0
0.5

Figure

A. Chacon-Cabrera *et al.* Figure 7

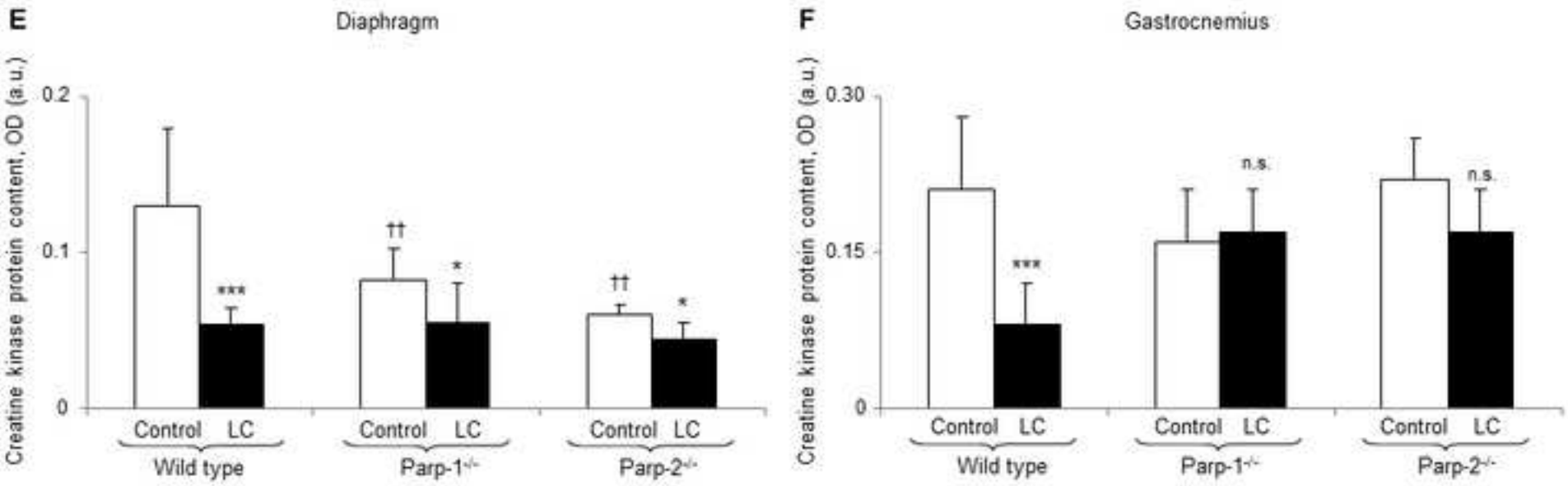

Online supplementary material

MICRORNA EXPRESSION AND PROTEIN ACETYLATION PATTERN IN RESPIRATORY AND LIMB MUSCLES OF PARP-1$^{-/-}$ AND PARP-2$^{-/-}$ MICE WITH LUNG CANCER CACHEXIA

Alba Chacon-Cabrera, Clara Fermoselle, Ida Salmela, Jose Yelamos, and Esther Barreiro

METHODS

Animal model

Tumor. LP07 is a cell line derived from the transplantable P07 lung tumor that appeared spontaneously in the lung of a BALB/c mouse [12]. Aftersuccessivepassages of a P07 primary culture, the LP07 cell line was previously obtained *in vitro* [25]. LP07 cell line shares identical characteristics regarding lung tumor incidence and histology, and cachexia with its parental P07 tumor [12,13,25]. It has also been consistently demonstrated that one month after tumor transplantation, all animals developed lung metastasis, spleen enlargement, and severe cachexia without affecting any other organs [9,12,13,25]. Importantly, in this model, the rate of tumor growth and tumor kinetics have been well characterized in previous investigations aimed to specifically explore the effects of several drugs on the transplanted tumors [13,20].

*Mice***.** BALB/c mice were obtained from Harlan *InterfaunaIbérica SL* (Barcelona, Spain). Parp-$1^{-/-}$ and Parp-$2^{-/-}$ mice (strain 129/Sv x C57BL/6), kindly provided by Dr. de Murcia [10,11,18] (Strasbourg, France), were backcrossed on BALB/c background for twelve generations. Genotyping was performed by PCR analysis using tail DNA as previously described. All experiments were performed on two-month old littermate female mice(body weight ~20g), on a BALB/c background. Mice were kept under pathogen-free conditions in the animal house facility at the Barcelona Biomedical Research Park (PRBB), with a 12:12 h light:dark cycle.

Experimental design and Ethics. In all experimental groups (except for control rodents), LP07 viable cells ($4x10^5$) resuspended in 0.2 mL minimal essential media (MEM) were subcutaneously inoculated in the left flank of female BALB/c mice on day 1, and were studied for a period of one month. Fifty-nine mice were used in the study, which were subdivided into the following experimental groups: 1) control wild type (N=14), inoculation of 0.2 mL MEM in the left flank; 2) LC cachexia wild type group (N=13), inoculation of LP07 cells; 3) control Parp-$1^{-/-}$ (N=8), inoculation of 0.2 mL MEM in the left flank; 4) LC

cachectic Parp-$1^{-/-}$ mice (N=12), inoculation of LP07 cells; 5) control Parp-$2^{-/-}$ (N=6), inoculation of 0.2 mL MEM in the left flank; and 6) LC cachectic Parp-$2^{-/-}$ mice (N=6), inoculation of LP07 cells.

A fraction of the diaphragm and gastrocnemius muscle specimens from the transgenic mice were also used in another investigation aimed to assess protein catabolism and anabolism and structural alterations in those muscles (data submitted).

All animal experiments were conducted in the animal facilities at PRBB. This controlled study was designed in accordance with the ethical standards on animal experimentation (EU 2010/63 CEE, *Real Decreto* 53/2013 BOE 34, Spain) at PRBB and the Helsinki convention for the use and care of animals. Ethical approval was obtained by the Animal Research Committee (Animal welfare department, Catalonia, EBP-09-1228).

***In vivo* measurements in the mice**

Body weight and food intake were determined every day during the entire duration of the study. Food and water were supplied ad libitum for the entire duration of the study protocol in the tumor-bearing mice. Control animals were paired-fed according to the amount of food eaten by the cachectic rodents. Limb strength was determined at day 0 and 30 using a strength grip meter (Bioseb, Chaville, France) following previously published methodologies, in which grip strength was also the end-point parameter in several experimental models of cancer cachexia in mice as previously shown [5,9,19,24,26,27]. Additionally, body and limb strength gains were calculated as the percentage of the corresponding measurements performed at the end of the study period (30 days) with respect to the same measurements obtained at baseline. Moreover, the ratio of tumor weight to total body weight on the day of sacrifice (day 30) was also calculated.

Sacrifice and sample collection

Mice from all the experimental groups were sacrificed on day 30 post-inoculation of LP07

cells or MEM (control animals). Prior to sacrifice, each mouse was inoculated intraperitoneally with 0.1 mL sodium pentobarbital (60 mg/Kg). In all cases, the pedal and blink reflexes were evaluated in order to verify total anesthetic depth. At this time, the following samples were obtained from all animals: diaphragm and gastrocnemius muscles and the subcutaneous tumor. LC cachectic mice were macroscopically of smaller size than healthy control rodents [9]. Frozen tissues were used for immunoblotting and real-time polymerase chain reaction assay (qRT-PCR) techniques.

Biological analyses

MicroRNA reverse transcription (RT). MicroRNA RT was performed using TaqMan® microRNA assays (Life Technologies) following the manufacturer's instructions.

*Real time-PCR amplification (qRT-PCR).*TaqMan based qPCR reactions were performed using the ABI PRISM 7900HT Sequence Detector System (Applied BioSystems, Foster City, CA, USA) together with a commercially available predesigned microRNA assay, and probes as shown in Table 1.Taqman microRNA assay for small nuclear RNA U6 (snU6) was used to normalize the miRNAs amplifications. MicroRNA data was collected and subsequently analyzed using the SDS Relative Quantification Software version 2.1 (Applied BioSystems), in which the comparative CT method (2-ΔΔCT) for relative quantification was employed[16].

*Immunoblotting of 1D electrophoresis in muscle and tumor samples.*Protein levels of the different molecular markers analyzed in the study were explored by means of immunoblotting procedures as previously described [2,6,9,14,15,17]. Briefly, frozen muscle samples from the diaphragm and gastrocnemius muscles of all mouse experimental groups were homogenized in a buffer containing HEPES 50 mM, NaCl 150 mM, NaF 100 mM, Na pyrophosphate 10 mM, EDTA 5 mM, Triton-X 0.5%, leupeptin 2 μg/ml, PMSF 100 μg/ml, aprotinin 2 μg/ml and pepstatin A 10 μg/ml [14,17]. The entire procedures were always conducted at 4ºC. Protein levels in crude homogenates were spectrophotometrically determined with the

Bradford method [8] using triplicates in each case and bovine serum albumin (BSA) as the standard (Bio-Rad protein reagent, Bio-Rad Inc., Hercules, CA, USA). The final protein concentration in each sample was calculated from at least two Bradford measurements that were almost identical. Equal amounts of total protein (ranging from 5 to 100 micrograms, depending on the antigen and antibody) from crude muscle homogenates were always loaded onto the gels, as well as identical sample volumes/lanes. For the purpose of comparisons among the different groups of experimental and control rodents, muscle sample specimens were always run together and kept in the same order. Two independent sets of immunoblots were conducted in which diaphragm and gastrocnemius muscle specimens were run separately.

Four fresh 10-well mini-gels were always simultaneously loaded for each of the antigens. Experiments were confirmed twice for all the antigens analyzed in the investigation. Experimental and control mice were unevenly distributed across gels in order to attenuate eventual loading problems in a specific area of the gels which might lead to misinterpretation of the measurements. Fresh gels were specifically loaded for each of the antigens in muscle specimens of all mice in most of cases. However, in a few cases, antigens were identified from stripped membranes.

Proteins were then separated by electrophoresis, transferred to polyvinylidenedifluoride (PVDF) membranes, blocked with bovine serum albumin and incubated overnight with selective primary antibodies. Protein levels of total acetylated proteins, HDACs, myogenic transcription factors,signaling pathways, and downstream targets were identified using specific primary antibodies: Total acetylated proteins (anti-acetyl lysine antibody, Santa Cruz Biotechnology, Santa Cruz, CA, USA), histone deacetylases (HDAC)3 (anti-HDAC3 antibody, Santa Cruz Biotechnology, Santa Cruz), HDAC6 (anti-HDAC6 antibody, Epigentek, Farmingdale, NY, USA), NAD-dependent protein deacetylase sirtuin-1 (SIRT1)

(anti-SIRT1 antibody, ProteinTech Group Inc., Chicago, IL, USA), myocyte-enhancer factor (MEF)2C (anti-MEF2C antibody, Santa Cruz Biotechnology, Santa Cruz, CA, USA), MEF2D (anti-MEF2D antibody, Santa Cruz Biotechnology, Santa Cruz, CA, USA), Yin Yang (YY)1 (anti-YY1 antibody, Santa Cruz Biotechnology, Santa Cruz, CA, USA),transcription factor fork-head box O (FoxO)-1 (anti-FoxO-1 antibody, Millipore, Darmstadt, Germany), FoxO-3 (anti-FoxO-3 antibody, Acris, Herford, Germany), Peroxisome proliferator-activated receptor gamma coactivator 1-alpha (PGC-1α) (anti-PGC-1α antibody, Santa Cruz Biotechnology),α-actin (anti-α-actin skeletal muscle antibody, Sigma-Aldrich, Saint Louis, MO, USA), creatine kinase (anti-creatine kinase antibody, Santa Cruz Biotechnology),and glyceraldehyde-3-phosphate dehydrogenase (GAPDH) (anti-GAPDH antibody, Santa Cruz Biotechnology,). Positive controls were used in order to identify FoxO1, AcFoxO1, FoxO3, AcFoxO3, PGC-1α, AcPGC-1α, HDAC3, HDAC6, SIRT1, MEF2C, MEF2D, and YY1 proteins in the corresponding immunoblots. Antigens from all samples were detected with horseradish peroxidase (HRP)-conjugated secondary antibodies and a chemiluminescence kit. For each antigen, samples from the different groups were always detected in the same picture under identical exposure times. Acetylated levels of the target markers werecalculated as the ratio of the acetylated-to-total protein content for each of the markers.

PVDF membranes were scanned with the Molecular Imager Chemidoc XRS System (Bio–Rad Laboratories, Hercules, CA, USA) using the software Quantity One version 4.6.5 (Bio–Rad Laboratories). Optical densities of specific proteins were quantified using the software Image Lab version 2.0.1 (Bio-Rad Laboratories). Final optical densities obtained in each specific group of subjects and muscle corresponded to the mean values of the different samples (lanes) of each of the antigens studied. In order to validate equal protein loading among various lanes, SDS-PAGE gels were stained with CoomassieBlue,and the glycolytic enzyme GAPDH was used as the protein loading controls in all the immunoblots(Figure

E1,and Figures corresponding to all the immunoblots performed in the study for all of the antigens).

Standard stripping methodologies were employed when detection of the antigens required the loading of a relatively greater amount of total muscle protein. Very briefly, membranes were stripped of primary and secondary antibodies through one 30-minute washes with a stripping solution (25 mM glycine, pH 2.0 and 1% SDS) followed by two consecutive 10-minute washes containing phosphate buffered saline with tween (PBST) at room temperature. Membranes were blocked with bovine serum albumin and reincubated with primary and secondary antibodies following the procedures described above.

Tumor specimens. Following identical procedures as described above, in the subcutaneous tumors from all the animals, the following markers were also analyzed with the objective to assess whether PARP deletion may have had an effect on tumor growth or degradation: B-cell lymphoma 2 (Bcl-2) (anti-bcl-2 antibody, Santa Cruz Biotechnology), Bcl-associated X (bax) (anti-Bax antibody, Santa Cruz Biotechnology), light chain 3 B (LC3)B (anti-LC3B antibody, Cell Signaling Technology, Inc., Danvers, MA), NAD-dependent protein deacetylase sirtuin-1 (SIRT1) (anti-SIRT1 antibody, ProteinTech Group Inc.), β-actin (anti-β-actin antibody, Santa Cruz Biotechnology),and glyceraldehyde-3-phosphate dehydrogenase (GAPDH) (anti-GAPDH antibody, Santa Cruz Biotechnology). Furthermore, in order to confirm that tumors express PARP-1 and PARP-2 proteins in each group of knockout mice (cachectic animals), those proteins were also detected in the actual tumors of all groups of tumor-bearing mice using selective antibodies: anti-PARP-1 antibody (Clon A6.4.12) and anti-PARP-2 antibody (rabbit polyclonal antibody raised against full length mouse PARP-2)[1]. Antigens from all samples were detected as described above.

Immunohistochemistry.On 3-micrometer muscle paraffin-embedded sections from diaphragms and gastrocnemius muscles of all study groups, myosin heavy chain (MyHC)-I

and –II isoforms were identified using anti-MyHC-I (clone MHC, Biogenesis Inc., Poole, England, UK) and anti-MyHC-II antibodies (clone MY-32, Sigma, Saint Louis, MO), respectively, as published elsewhere [2,7,9,14]. The cross-sectional area, mean least diameter, and proportions of type I and type II fibers were assessed using a light microscope (Olympus, Series BX50F3, Olympus Optical Co., Hamburg, Germany) coupled with an image-digitizing camera (Pixera Studio, version 1.0.4, Pixera Corporation, Los Gatos, CA, USA) and a morphometry program (NIH Image, version 1.60, Scion Corporation, Frederick, MD, USA). At least 100 fibers were measured and counted in each type of muscle specimen from all groups of mice.

Furthermore, in the subcutaneous tumor of the target mice (both wild type and knockout rodents), cell proliferation was measured using ki-67 as a marker (anti-ki67 antibody, Millipore Iberica, CA, USA) on the three micrometer tumor paraffin-embedded sections using immunohistochemical procedures as previously described in our group [4]. Images of the stained tumors were taken as described above. The number of positively stained nuclei for ki-67 was counted in tumors from the target animal groups. Data are expressed as the percentage of positively-stained nuclei in each group of mice. It should also be mentioned that in the present study, the antigens quantified in the tumors were also used in the investigation on the assessment of the effects of PARP-1 and -2 deletions on muscle protein breakdown (data submitted).

Statistical Analysis

Normality of the study variables were checked using the Shapiro-Wilk test. Physiologic, structural, and molecular results are expressed as mean (standard deviation). For the purpose of the study, results obtained in the diaphragm and gastrocnemius muscles were subsequently analyzed as follows: 1) LC cachectic wild type mice versus their respective non-tumor controls, 2) LC cachectic Parp-$1^{-/-}$ animals versus their respective knockout non-tumor

controls, 3) LC cachectic Parp-$2^{-/-}$ mice versus their respective knockout non-tumor controls, and 4) any of the non-tumor knockout mice versus non-tumor wild type animals. Comparisons described in points 1, 2, and 3 above were analyzed using the Student's *T- test*, while comparisons described in point 4 were assessed using one-way analysis of variance (ANOVA), in which *Dunnett's post hoc* analysis was used to adjust for multiple comparisons among the three study groups. Moreover, values of the markers quantified in the tumors were compared among the three different groups of cancer cachectic rodents using ANOVA, in which *Dunnett's post hoc* analysis was also employed to adjust for multiple comparisons among the groups. The existence of potential correlations between different variables was only tested in the LC cachectic groups of mice (both wild type and knockout mice). Specifically, correlations between physiological and biological variables were explored using the Pearson's correlation coefficient. A level of significance of $P \leq 0.05$ was established. The sample size chosen was based on previous studies [2,3,6,9,14,15,17,21-23], where very similar approaches were employed and on assumptions of 80% power to detect an improvement of more than 20% in measured outcomes at a level of significance of $P \leq 0.05$.

Reference List

1. S. Aoufouchi, Monoclonal Antibodies A4.3; A6.4.12; B5.3.9; B15.4.13 Anti-Poly(ADP-Ribose) Polymerase., 1997, p. 583.

2. E. Barreiro, L. del Puerto-Nevado, E. Puig-Vilanova, S. Perez-Rial, F. Sanchez, L. Martinez-Galan, S. Rivera, J. Gea, N. Gonzalez-Mangado, and G. Peces-Barba, Cigarette smoke-induced oxidative stress in skeletal muscles of mice, Respir. Physiol Neurobiol. 182 (2012) pp. 9-17.

3. E. Barreiro, C. Garcia-Martinez, S. Mas, E. Ametller, J. Gea, J.M. Argiles, S. Busquets, and F.J. Lopez-Soriano, UCP3 overexpression neutralizes oxidative stress rather than nitrosative stress in mouse myotubes, FEBS Lett. 583 (2009) pp. 350-356.

4. E. Barreiro, J. Gea, J.M. Corominas, and S.N. Hussain, Nitric oxide synthases and protein oxidation in the quadriceps femoris of patients with chronic obstructive pulmonary disease, Am. J. Respir. Cell Mol. Biol. 29 (2003) pp. 771-778.

5. E. Barreiro, J. Marin-Corral, F. Sanchez, V. Mielgo, F.J. Alvarez, J.B. Galdiz, and J. Gea, Reference values of respiratory and peripheral muscle function in rats, J. Anim Physiol Anim Nutr. (Berl) 94 (2010) p. e393-e401.

6. E. Barreiro, V.I. Peinado, J.B. Galdiz, E. Ferrer, J. Marin-Corral, F. Sanchez, J. Gea, and J.A. Barbera, Cigarette smoke-induced oxidative stress: A role in chronic obstructive pulmonary disease skeletal muscle dysfunction, Am. J. Respir. Crit Care Med. 182 (2010) pp. 477-488.

7. E. Barreiro, A.M. Schols, M.I. Polkey, J.B. Galdiz, H.R. Gosker, E.B. Swallow, C. Coronell, and J. Gea, Cytokine profile in quadriceps muscles of patients with severe COPD, Thorax 63 (2008) pp. 100-107.

8. M.M. Bradford, A rapid and sensitive method for the quantitation of microgram quantities of protein utilizing the principle of protein-dye binding, Anal. Biochem. 72 (1976) pp. 248-254.

9. A. Chacon-Cabrera, C. Fermoselle, A.J. Urtreger, M. Mateu-Jimenez, M.J. Diament, E.D. De Kier Joffe, M. Sandri, and E. Barreiro, Pharmacological strategies in lung cancer-induced cachexia: effects on muscle proteolysis, autophagy, structure, and weakness, J. Cell Physiol 229 (2014) pp. 1660-1672.

10. J.M. de Murcia, C. Niedergang, C. Trucco, M. Ricoul, B. Dutrillaux, M. Mark, F.J. Oliver, M. Masson, A. Dierich, M. LeMeur, C. Walztinger, P. Chambon, and M.G. de, Requirement of poly(ADP-ribose) polymerase in recovery from DNA damage in mice and in cells, Proc. Natl. Acad. Sci. U. S. A 94 (1997) pp. 7303-7307.

11. M.G. de, V. Schreiber, M. Molinete, B. Saulier, O. Poch, M. Masson, C. Niedergang, and M.J. Menissier de, Structure and function of poly(ADP-ribose) polymerase, Mol. Cell Biochem. 138 (1994) pp. 15-24.

12. M.J. Diament, C. Garcia, I. Stillitani, V.M. Saavedra, T. Manzur, L. Vauthay, and S. Klein, Spontaneous murine lung adenocarcinoma (P07): A new experimental

model to study paraneoplastic syndromes of lung cancer, Int. J. Mol. Med. 2 (1998) pp. 45-50.

13. M.J. Diament, G.D. Peluffo, I. Stillitani, L.C. Cerchietti, A. Navigante, S.M. Ranuncolo, and S.M. Klein, Inhibition of tumor progression and paraneoplastic syndrome development in a murine lung adenocarcinoma by medroxyprogesterone acetate and indomethacin, Cancer Invest 24 (2006) pp. 126-131.

14. C. Fermoselle, R. Rabinovich, P. Ausin, E. Puig-Vilanova, C. Coronell, F. Sanchez, J. Roca, J. Gea, and E. Barreiro, Does oxidative stress modulate limb muscle atrophy in severe COPD patients?, Eur. Respir. J. 40 (2012) pp. 851-862.

15. C. Fermoselle, F. Sanchez, and E. Barreiro, [Reduction of muscle mass mediated by myostatin in an experimental model of pulmonary emphysema], Arch. Bronconeumol. 47 (2011) pp. 590-598.

16. K.J. Livak and T.D. Schmittgen, Analysis of relative gene expression data using real-time quantitative PCR and the 2(-Delta Delta C(T)) Method, Methods 25 (2001) pp. 402-408.

17. J. Marin-Corral, C.C. Fontes, S. Pascual-Guardia, F. Sanchez, M. Olivan, J.M. Argiles, S. Busquets, F.J. Lopez-Soriano, and E. Barreiro, Redox balance and carbonylated proteins in limb and heart muscles of cachectic rats, Antioxid. Redox. Signal. 12 (2010) pp. 365-380.

18. M.J. Menissier de, M. Ricoul, L. Tartier, C. Niedergang, A. Huber, F. Dantzer, V. Schreiber, J.C. Ame, A. Dierich, M. LeMeur, L. Sabatier, P. Chambon, and M.G. de, Functional interaction between PARP-1 and PARP-2 in chromosome stability and embryonic development in mouse, EMBO J. 22 (2003) pp. 2255-2263.

19. K.T. Murphy, A. Chee, J. Trieu, T. Naim, and G.S. Lynch, Importance of functional and metabolic impairments in the characterization of the C-26 murine model of cancer cachexia, Dis. Model. Mech. 5 (2012) pp. 533-545.

20. G.D. Peluffo, I. Stillitani, V.A. Rodriguez, M.J. Diament, and S.M. Klein, Reduction of tumor progression and paraneoplastic syndrome development in murine lung adenocarcinoma by nonsteroidal antiinflammatory drugs, Int. J. Cancer 110 (2004) pp. 825-830.

21. F. Penna, D. Costamagna, A. Fanzani, G. Bonelli, F.M. Baccino, and P. Costelli, Muscle wasting and impaired myogenesis in tumor bearing mice are prevented by ERK inhibition, PLoS. One. 5 (2010) p. e13604.

22. G.S. Supinski and L.A. Callahan, Caspase activation contributes to endotoxin-induced diaphragm weakness, J. Appl. Physiol (1985.) 100 (2006) pp. 1770-1777.

23. G.S. Supinski, J. Vanags, and L.A. Callahan, Effect of proteasome inhibitors on endotoxin-induced diaphragm dysfunction, Am. J. Physiol Lung Cell Mol. Physiol 296 (2009) p. L994-L1001.

24. M. Toledo, S. Busquets, S. Sirisi, R. Serpe, M. Orpi, J. Coutinho, R. Martinez, F.J.

Lopez-Soriano, and J.M. Argiles, Cancer cachexia: physical activity and muscle force in tumour-bearing rats, Oncol. Rep. 25 (2011) pp. 189-193.

25. A.J. Urtreger, M.J. Diament, S.M. Ranuncolo, C. Del, V, L.I. Puricelli, S.M. Klein, and E.D. De Kier Joffe, New murine cell line derived from a spontaneous lung tumor induces paraneoplastic syndromes, Int. J. Oncol. 18 (2001) pp. 639-647.

26. A. Vignaud, A. Ferry, A. Huguet, M. Baraibar, C. Trollet, J. Hyzewicz, G. Butler-Browne, J. Puymirat, G. Gourdon, and D. Furling, Progressive skeletal muscle weakness in transgenic mice expressing CTG expansions is associated with the activation of the ubiquitin-proteasome pathway, Neuromuscul. Disord. 20 (2010) pp. 319-325.

27. L.A. Whittemore, K. Song, X. Li, J. Aghajanian, M. Davies, S. Girgenrath, J.J. Hill, M. Jalenak, P. Kelley, A. Knight, R. Maylor, D. O'Hara, A. Pearson, A. Quazi, S. Ryerson, X.Y. Tan, K.N. Tomkinson, G.M. Veldman, A. Widom, J.F. Wright, S. Wudyka, L. Zhao, and N.M. Wolfman, Inhibition of myostatin in adult mice increases skeletal muscle mass and strength, Biochem. Biophys. Res. Commun. 300 (2003) pp. 965-971.

FIGURE LEGENDS

Figure E1: Examples of SDS-PAGE gels stained with Coomassie Blue corresponding to the diaphragm (panel A) and gastrocnemius (panel B) muscles of the following experimental groups: non-cachectic control wild type,LC cachectic wild type,non-cachectic control Parp-1$^{-/-}$, LC cachectic Parp-1$^{-/-}$,non-cachectic control Parp-2$^{-/-}$, and LC cachectic Parp-2$^{-/-}$.

Figure E2: Immunoblots ofPARP-1 and -2 expression (panel A), and Bcl-2 (panel B), Bax (panel C), LC3 II/LC3 I (panel D), and SIRT1 (panel E) protein content in the subcutaneous tumor of the following experimental groups: LC cachectic wild type, LC cachectic Parp-1$^{-/-}$, and LC cachectic Parp-2$^{-/-}$. Note that in SIRT1 immunoblot, a positive control was run in the last lane. Actin or GAPDH are shown as loading controls. Definition of abbreviations: Bax, Bcl-associated X protein; LC3, Light chain 3; SIRT1, Sirtuin 1;+C, positive control; LC, Lung cancer; PARP, poly-ADP ribose polymerase; GAPDH, glyceraldehyde-3-phospate dehydrogenase; OD, optical densities; a.u., arbitrary units; MW, molecular weights; KDa, kilodaltons.

Figure E3: Immunoblots of total acetylated proteins in the diaphragm (panel A) and gastrocnemius (panel B) muscles of the following experimental groups: non-cachectic control wild type, LC cachectic wild type, non-cachectic control Parp-1$^{-/-}$, LC cachectic Parp-1$^{-/-}$, non-cachectic control Parp-2$^{-/-}$, and LC cachectic Parp-2$^{-/-}$.GAPDH is shown as loading control. Definition of abbreviations: LC, Lung cancer; PARP, poly-ADP ribose polymerase; GAPDH, glyceraldehyde-3-phospate dehydrogenase; OD, optical densities; a.u., arbitrary units; MW, molecular weights; KDa, kilodaltons.

Figure E4: Immunoblots of FoxO1and acetylated FoxO1 in the diaphragm (panel A) and gastrocnemius (panel B) muscles of the following experimental groups: non-cachectic control wild type, LC cachectic wild type, non-cachectic control Parp-1$^{-/-}$, LC cachectic Parp-1$^{-/-}$, non-cachectic control Parp-2$^{-/-}$, and LC cachectic Parp-2$^{-/-}$. Note that in both FoxO1 and

acetylated FoxO1immunoblots, a positive control was run in the first lane. GAPDH is shown as loading control. Definition of abbreviations: FoxO1, Forkhead box protein O-1; AcFoxO1, acetylated FoxO1; +C, positive control;LC, Lung cancer; PARP, poly-ADP ribose polymerase; GAPDH, glyceraldehyde-3-phospate dehydrogenase; OD, optical densities; a.u., arbitrary units; MW, molecular weights; KDa, kilodaltons.

Figure E5: Immunoblots of FoxO3 and acetylated FoxO3 in the diaphragm (panel A) and gastrocnemius (panel B) muscles of the following experimental groups: non-cachectic control wild type, LC cachectic wild type, non-cachectic control Parp-$1^{-/-}$, LC cachectic Parp-$1^{-/-}$, non-cachectic control Parp-$2^{-/-}$, and LC cachectic Parp-$2^{-/-}$. Note that in both FoxO3 and acetylated FoxO3 immunoblots, a positive control was run in the first lane. GAPDH is shown as loading control. Definition of abbreviations: FoxO3, Forkhead box protein O-3; AcFoxO3, acetylated FoxO3; +C, positive control; LC, Lung cancer; PARP, poly-ADP ribose polymerase; GAPDH, glyceraldehyde-3-phospate dehydrogenase; OD, optical densities; a.u., arbitrary units; MW, molecular weights; KDa, kilodaltons.

Figure E6: Immunoblots of PGC-1α and acetylated PGC-1αin the diaphragm (panel A) and gastrocnemius (panel B) muscles of the following experimental groups: non-cachectic control wild type, LC cachectic wild type, non-cachectic control Parp-$1^{-/-}$, LC cachectic Parp-$1^{-/-}$, non-cachectic control Parp-$2^{-/-}$, and LC cachectic Parp-$2^{-/-}$. Note that in both PGC-1α and acetylated PGC-1αimmunoblots, a positive control was run in the first lane. GAPDH is shown as loading control. Definition of abbreviations: PGC-1α, Peroxisome proliferator-activated receptor gamma coactivator 1-alpha; AcPGC-1α, acetylated PGC-1α; +C, positive control; LC, Lung cancer; PARP, poly-ADP ribose polymerase; GAPDH, glyceraldehyde-3-phospate dehydrogenase; OD, optical densities; a.u., arbitrary units; MW, molecular weights; KDa, kilodaltons.

Figure E7: Immunoblots of HDAC3 protein content in the diaphragm (panel A) and gastrocnemius (panel B) muscles of the following experimental groups: non-cachectic control wild type, LC cachectic wild type, non-cachectic control Parp-$1^{-/-}$, LC cachectic Parp-$1^{-/-}$, non-cachectic control Parp-$2^{-/-}$, and LC cachectic Parp-$2^{-/-}$. Note that in the HDAC3 immunoblots, a positive control was run in the first lane. GAPDH is shown as loading control. Definition of abbreviations: HDAC3, Histone deacetylase 3; +C, positive control; LC, Lung cancer; PARP, poly-ADP ribose polymerase; GAPDH, glyceraldehyde-3-phospate dehydrogenase; OD, optical densities; a.u., arbitrary units; MW, molecular weights; KDa, kilodaltons.

Figure E8: Immunoblots of HDAC6 protein content in the diaphragm (panel A) and gastrocnemius (panel B) muscles of the following experimental groups: non-cachectic control wild type, LC cachectic wild type, non-cachectic control Parp-$1^{-/-}$, LC cachectic Parp-$1^{-/-}$, non-cachectic control Parp-$2^{-/-}$, and LC cachectic Parp-$2^{-/-}$. Note that in the HDAC6 immunoblots, a positive control was run in the first lane.GAPDH is shown as loading control. Definition of abbreviations: HDAC6, Histone deacetylase 6; +C, positive control;LC, Lung cancer; PARP, poly-ADP ribose polymerase; GAPDH, glyceraldehyde-3-phospate dehydrogenase; OD, optical densities; a.u., arbitrary units; MW, molecular weights; KDa, kilodaltons.

Figure E9: Immunoblots of SIRT1protein content in the diaphragm (panel A) and gastrocnemius (panel B) muscles of the following experimental groups: non-cachectic control wild type, LC cachectic wild type, non-cachectic controlParp-$1^{-/-}$, LC cachectic Parp-$1^{-/-}$, non-cachectic control Parp-$2^{-/-}$, and LC cachectic Parp-$2^{-/-}$. Note that in the SIRT1 immunoblots, a positive control was run in the first lane. GAPDH is shown as loading control. Definition of abbreviations: SIRT1,Sirtuin 1; +C, positive control;LC, Lung cancer; PARP, poly-ADP

ribose polymerase; GAPDH, glyceraldehyde-3-phospate dehydrogenase; OD, optical densities; a.u., arbitrary units; MW, molecular weights; KDa, kilodaltons.

Figure E10: Immunoblots of MEF2C protein content in the diaphragm (panel A) and gastrocnemius (panel B) muscles of the following experimental groups:non-cachectic control wild type, LC cachectic wild type, non-cachectic controlParp-$1^{-/-}$, LC cachectic Parp-$1^{-/-}$, non-cachectic control Parp-$2^{-/-}$, and LC cachectic Parp-$2^{-/-}$. Note that in the MEF2C immunoblots, a positive control was run in the first lane. GAPDH is shown as loading control. Definition of abbreviations: MEF2C, myocyte enhancer factor 2C; +C, positive control;LC, Lung cancer; PARP, poly-ADP ribose polymerase; GAPDH, glyceraldehyde-3-phospate dehydrogenase; OD, optical densities; a.u., arbitrary units; MW, molecular weights; KDa, kilodaltons.

Figure E11: Immunoblots of MEF2D protein content in the diaphragm (panel A) and gastrocnemius (panel B) muscles of the following experimental groups: non-cachectic control wild type, LC cachectic wild type, non-cachectic controlParp-$1^{-/-}$, LC cachectic Parp-$1^{-/-}$, non-cachectic control Parp-$2^{-/-}$, and LC cachectic Parp-$2^{-/-}$. Note that in the MEF2D immunoblots, a positive control was run in the first lane. GAPDH is shown as loading control. Definition of abbreviations: MEF2D, myocyte enhancer factor 2D; +C, positive control;LC, Lung cancer; PARP, poly-ADP ribose polymerase; GAPDH, glyceraldehyde-3-phospate dehydrogenase; OD, optical densities; a.u., arbitrary units; MW, molecular weights; KDa, kilodaltons.

Figure E12: Immunoblots of YY1 in diaphragm (panel A) and gastrocnemius (panel B) muscles of the following experimental groups: non-cachectic control wild type, LC cachectic wild type, non-cachectic control Parp-$1^{-/-}$, LC cachectic Parp-$1^{-/-}$, non-cachectic control Parp-$2^{-/-}$, and LC cachectic Parp-$2^{-/-}$. Note that in the YY1 immunoblots, a positive control was run in the first lane. GAPDH is shown as loading control. Definition of abbreviations: YY1, Yin Yang 1; +C, positive control;LC, Lung cancer; PARP, poly-ADP ribose polymerase; GAPDH, glyceraldehyde-3-phospate dehydrogenase; OD, optical densities; a.u., arbitrary

units; MW, molecular weights; KDa, kilodaltons.

Figure E13: Immunoblots of α-actin skeletal muscle protein content in the diaphragm (panel A) and gastrocnemius (panel B) muscles of the following experimental groups: non-cachectic control wild type, LC cachectic wild type, non-cachectic control Parp-$1^{-/-}$, LC cachectic Parp-$1^{-/-}$, non-cachectic control Parp-$2^{-/-}$, and LC cachectic Parp-$2^{-/-}$. GAPDH is shown as loading control. Definition of abbreviations:LC, Lung cancer; PARP, poly-ADP ribose polymerase; GAPDH, glyceraldehyde-3-phospate dehydrogenase; OD, optical densities; a.u., arbitrary units; MW, molecular weights; KDa, kilodaltons.

Figure E14: Immunoblots of total PGC-1α in the diaphragm (panel A) and gastrocnemius (panel B) muscles of the following experimental groups: non-cachectic control wild type, LC cachectic wild type, non-cachectic control Parp-$1^{-/-}$, LC cachectic Parp-$1^{-/-}$, non-cachectic control Parp-$2^{-/-}$, and LC cachectic Parp-$2^{-/-}$. Note that in PGC-1α immunoblots, a positive control was run in the first lane. GAPDH is shown as loading control. Definition of abbreviations: PGC-1α, Peroxisome proliferator-activated receptor gamma coactivator 1-alpha; +C, positive control; LC, Lung cancer; PARP, poly-ADP ribose polymerase; GAPDH, glyceraldehyde-3-phospate dehydrogenase; OD, optical densities; a.u., arbitrary units; MW, molecular weights; KDa, kilodaltons.

Figure E15: Immunoblots of creatine kinase protein content in the diaphragm (panel A) and gastrocnemius (panel B) muscles of the following experimental groups: non-cachectic control wild type, LC cachectic wild type, non-cachectic control Parp-$1^{-/-}$, LC cachectic Parp-$1^{-/-}$, non-cachectic control Parp-$2^{-/-}$, and LC cachectic Parp-$2^{-/-}$. GAPDH is shown as loading control. Definition of abbreviations:LC, Lung cancer; PARP, poly-ADP ribose polymerase; GAPDH, glyceraldehyde-3-phospate dehydrogenase; OD, optical densities; a.u., arbitrary units; MW, molecular weights; KDa, kilodaltons.

A. Chacon-Cabrera et al. Figure E1

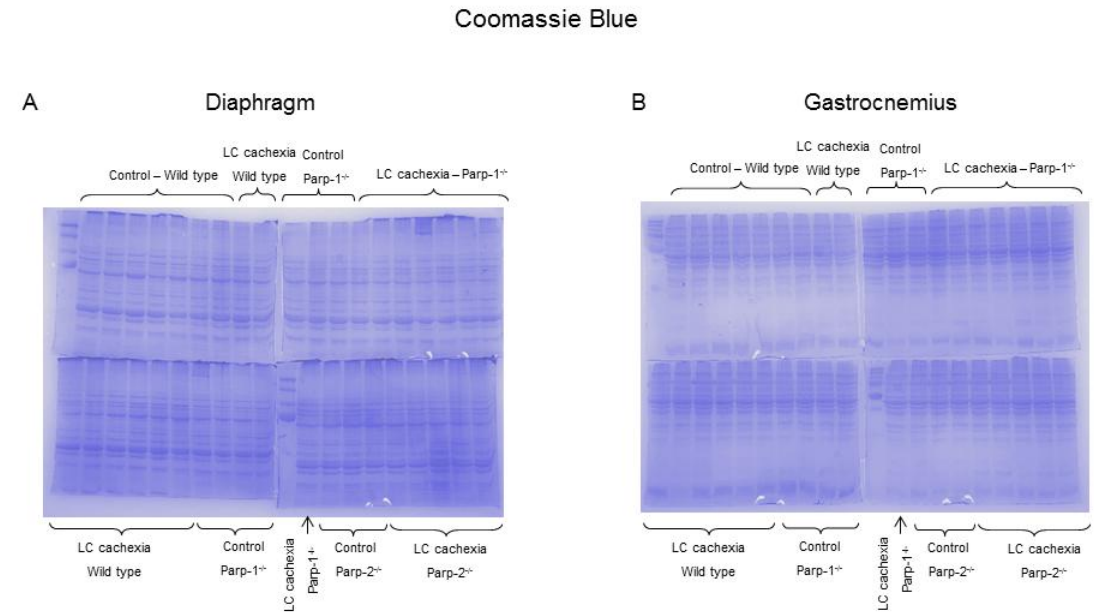

A. Chacon-Cabrera et al. Figure E2

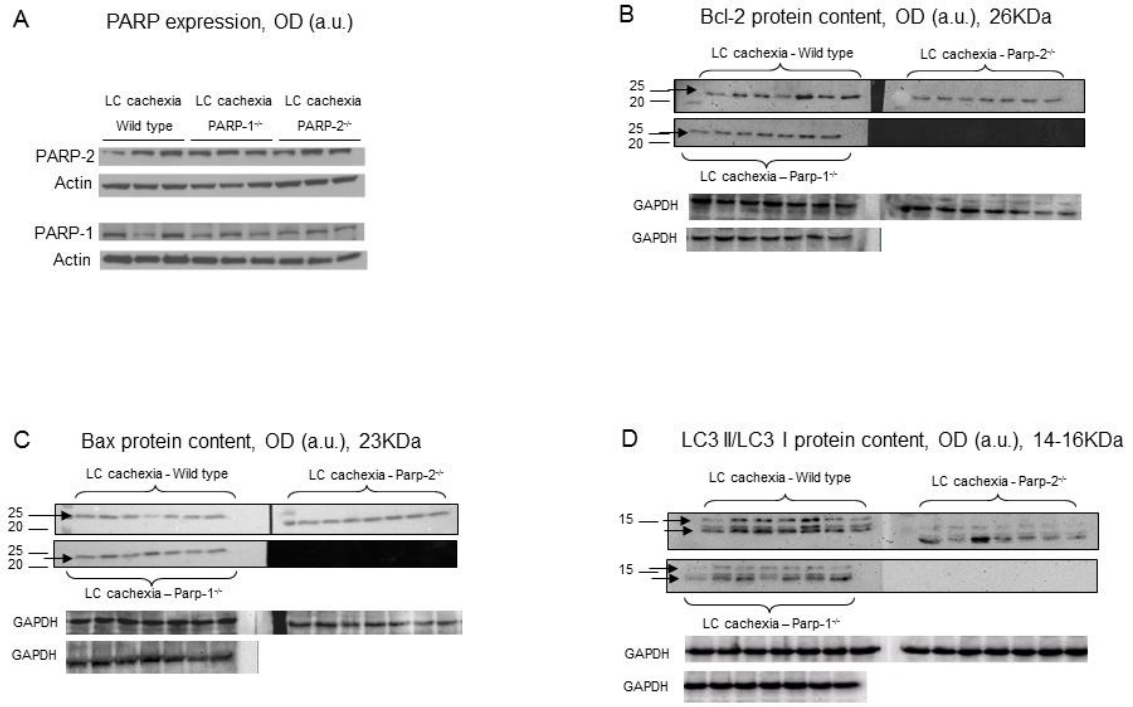

A. Chacon-Cabrera et al. Figure E2

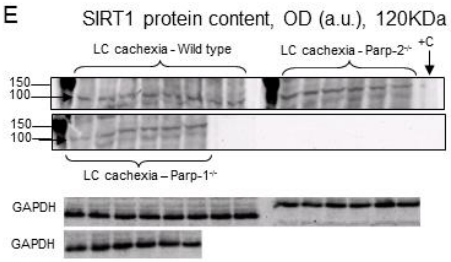

A. Chacon-Cabrera et al. Figure E3

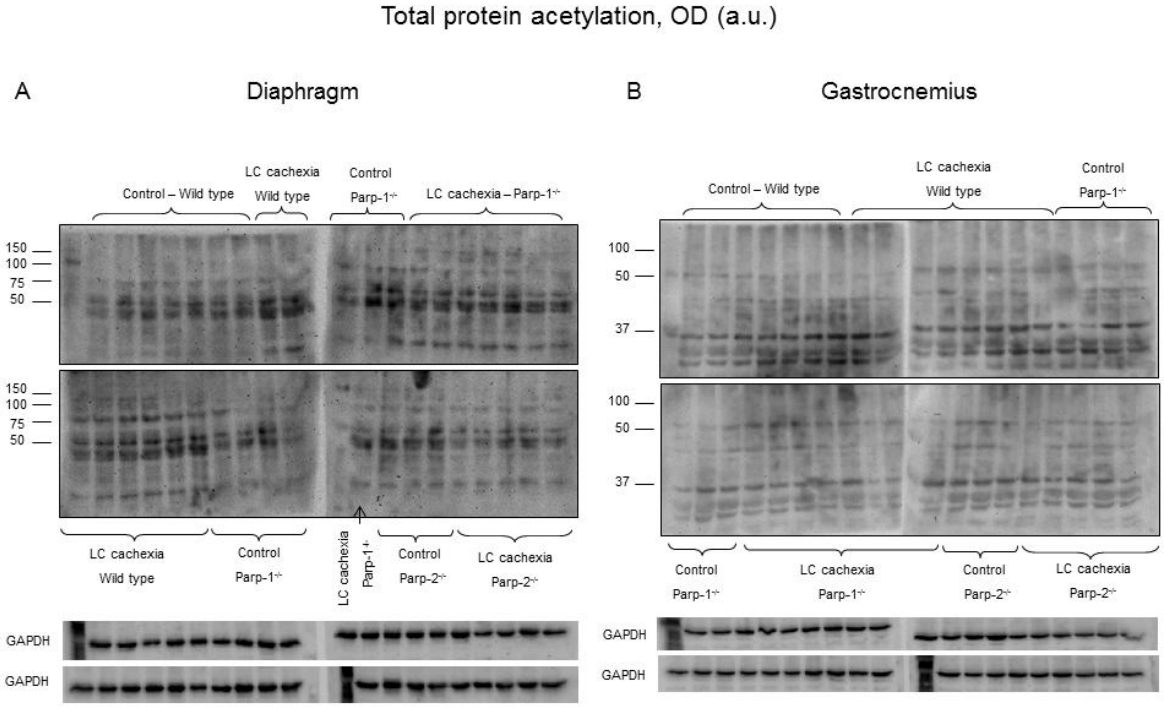

A. Chacon-Cabrera et al. Figure E4

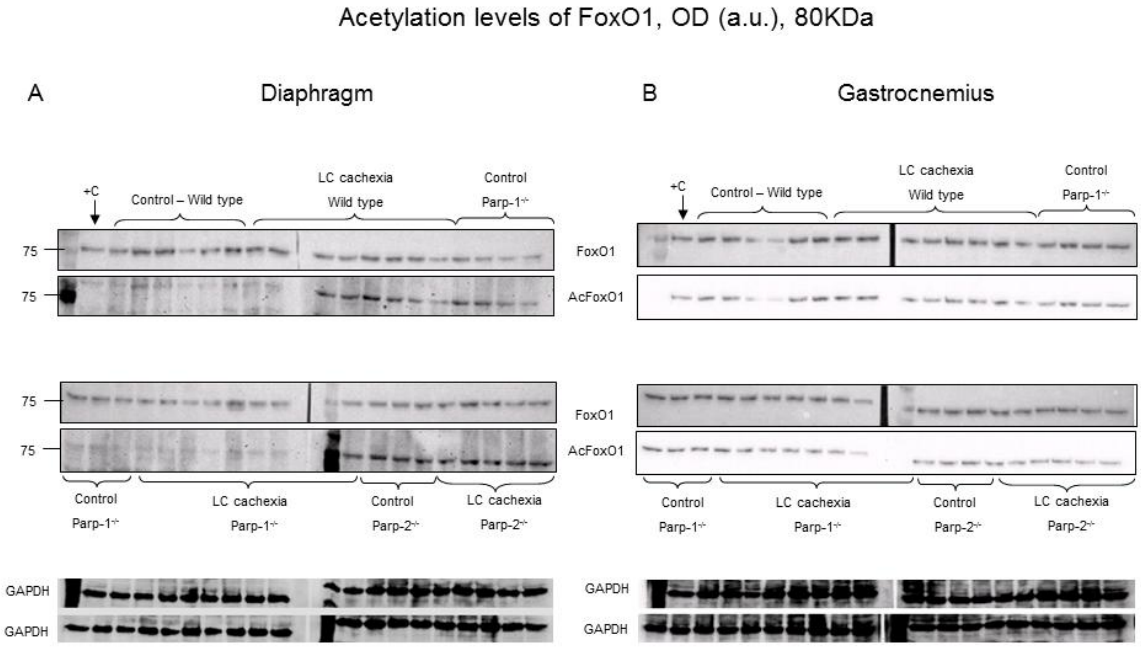

A. Chacon-Cabrera et al. Figure E5

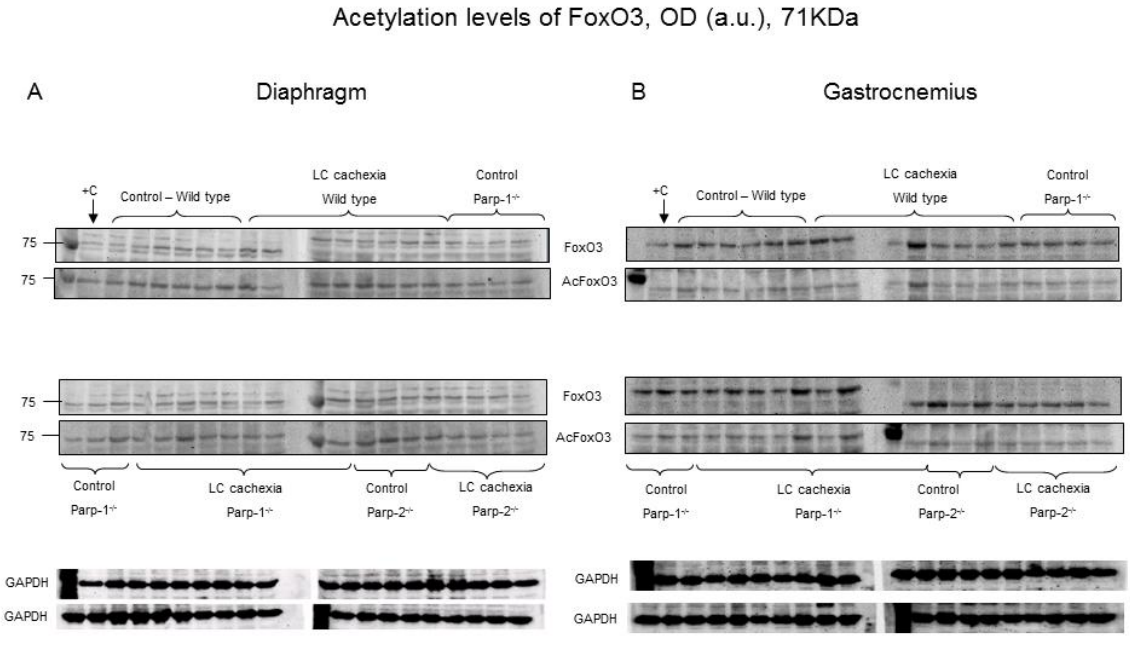

A. Chacon-Cabrera et al. Figure E6

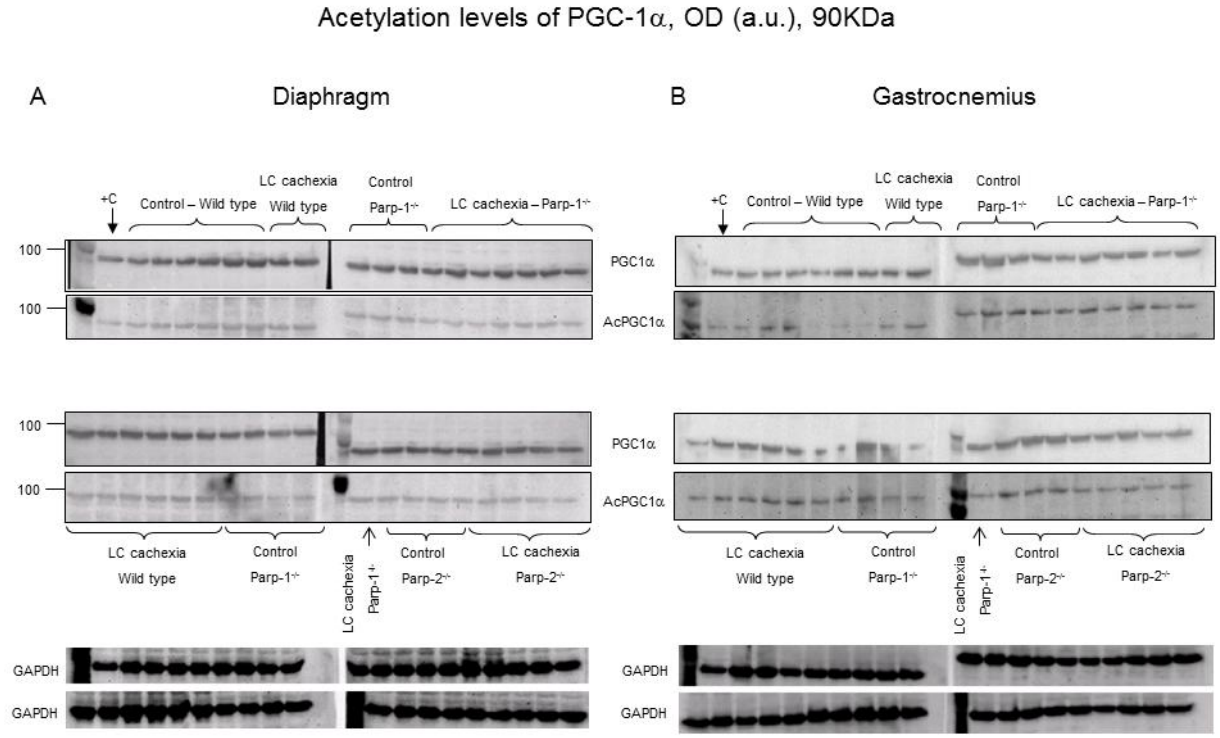

A. Chacon-Cabrera et al. Figure E7

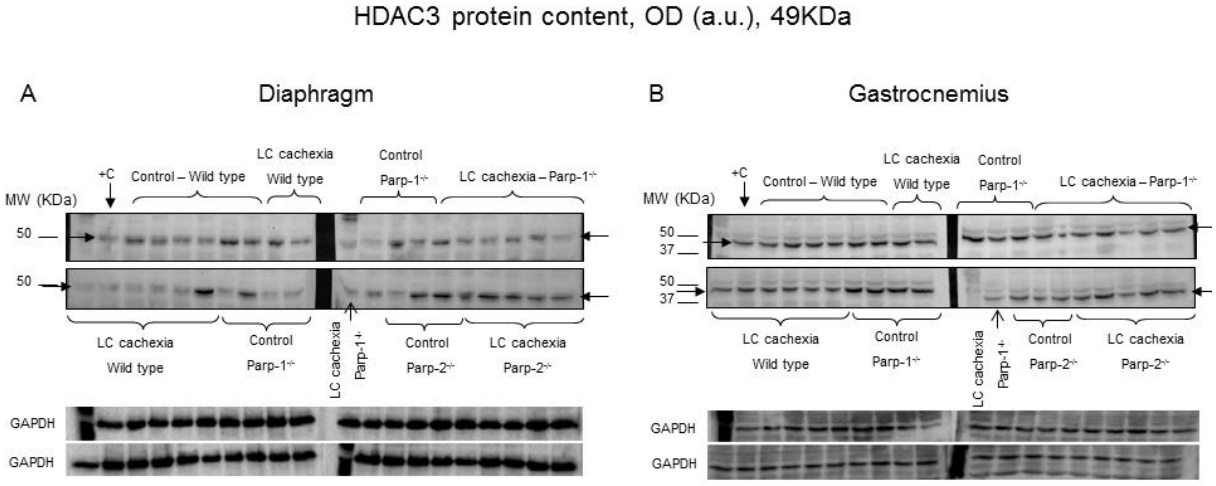

A. Chacon-Cabrera et al. Figure E8

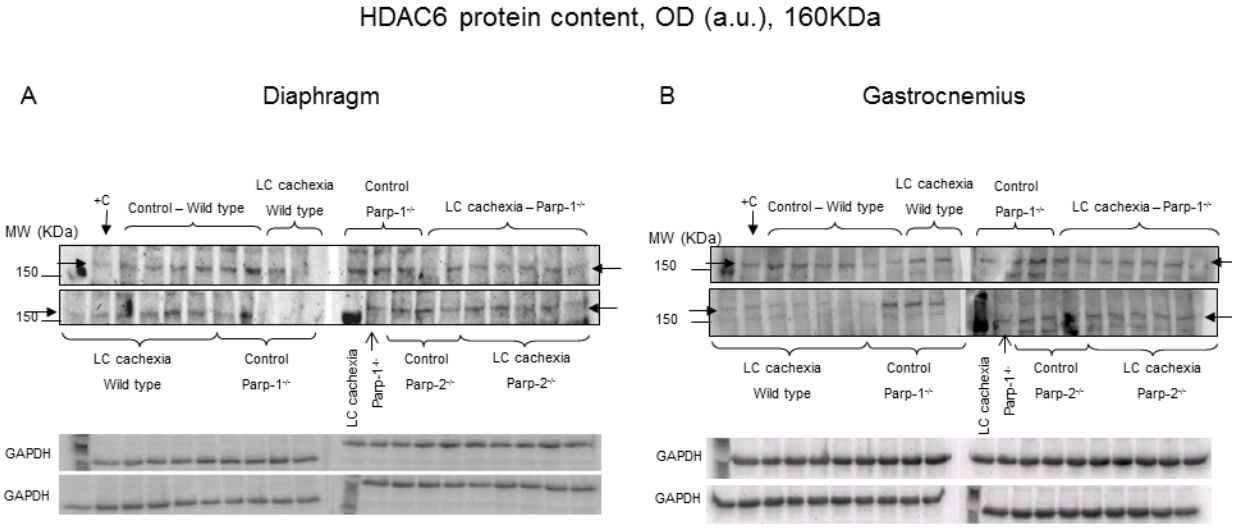

A. Chacon-Cabrera et al. Figure E9

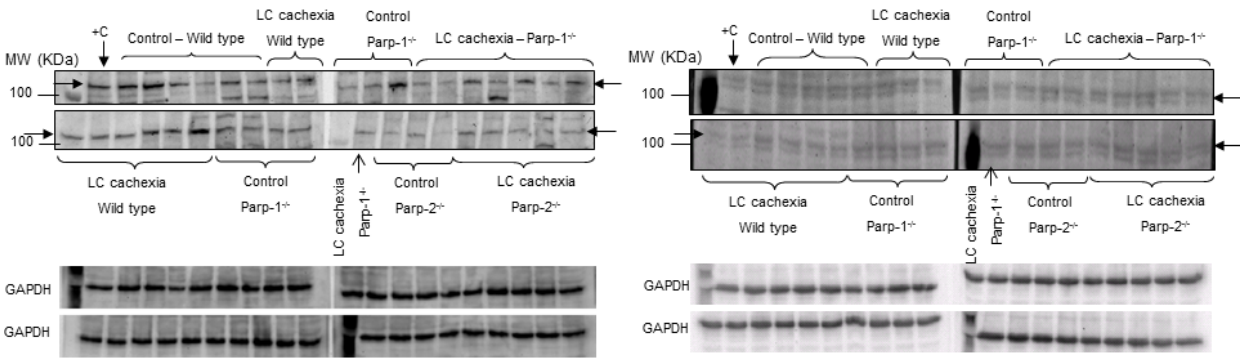

A. Chacon-Cabrera et al. Figure E10

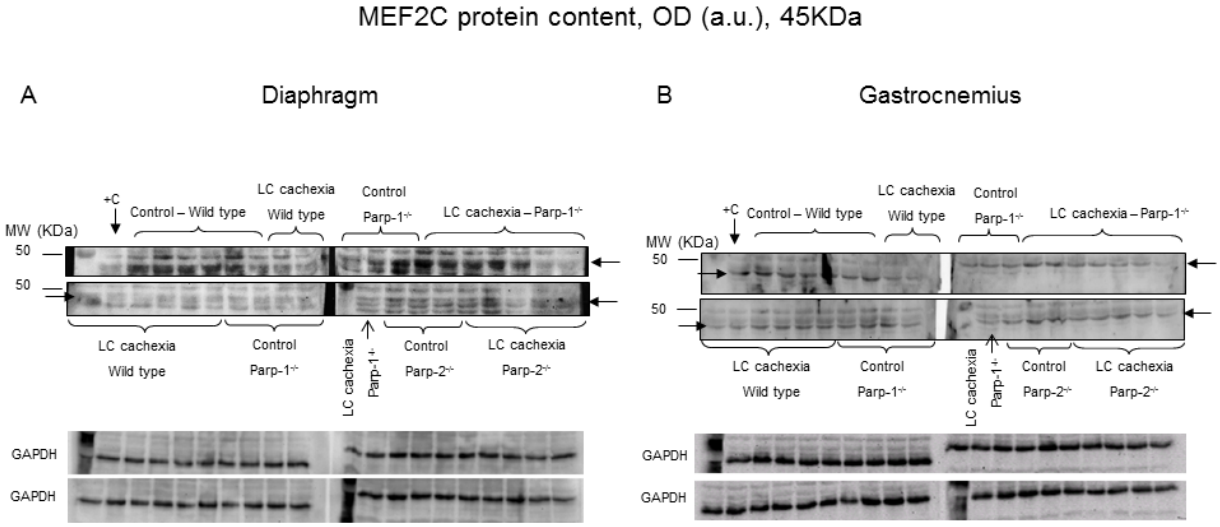

A. Chacon-Cabrera et al. Figure E11

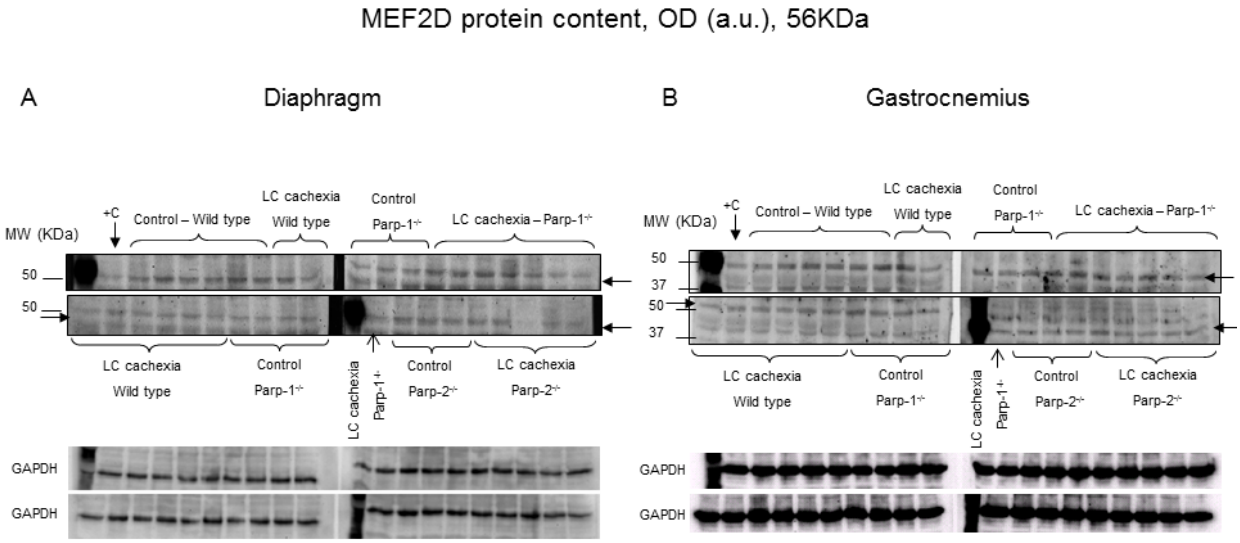

A. Chacon-Cabrera et al. Figure E12

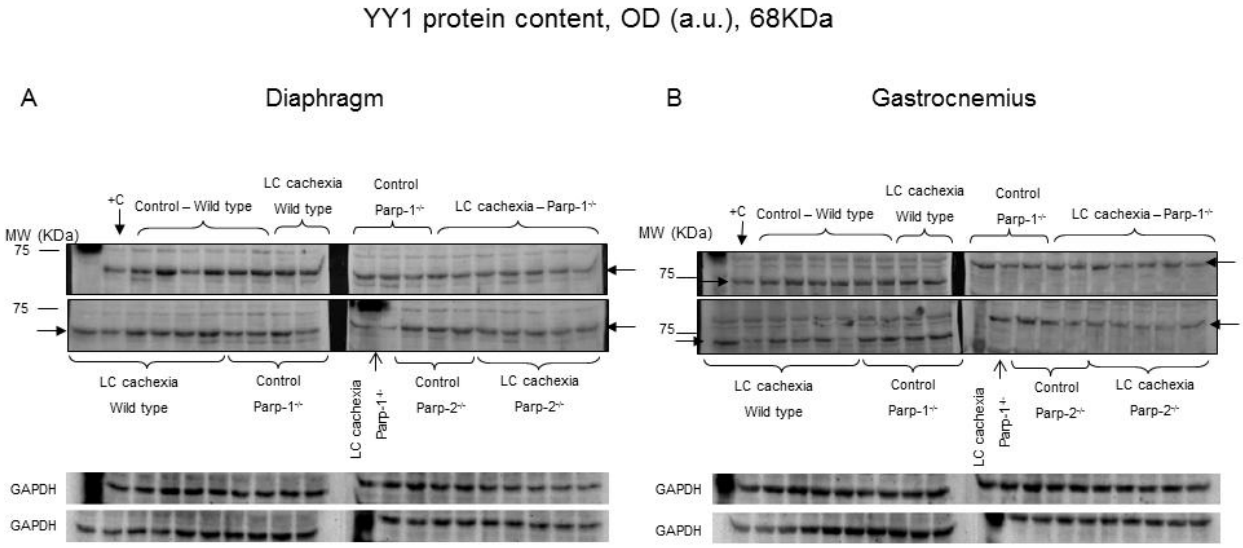

A. Chacon-Cabrera et al. Figure E13

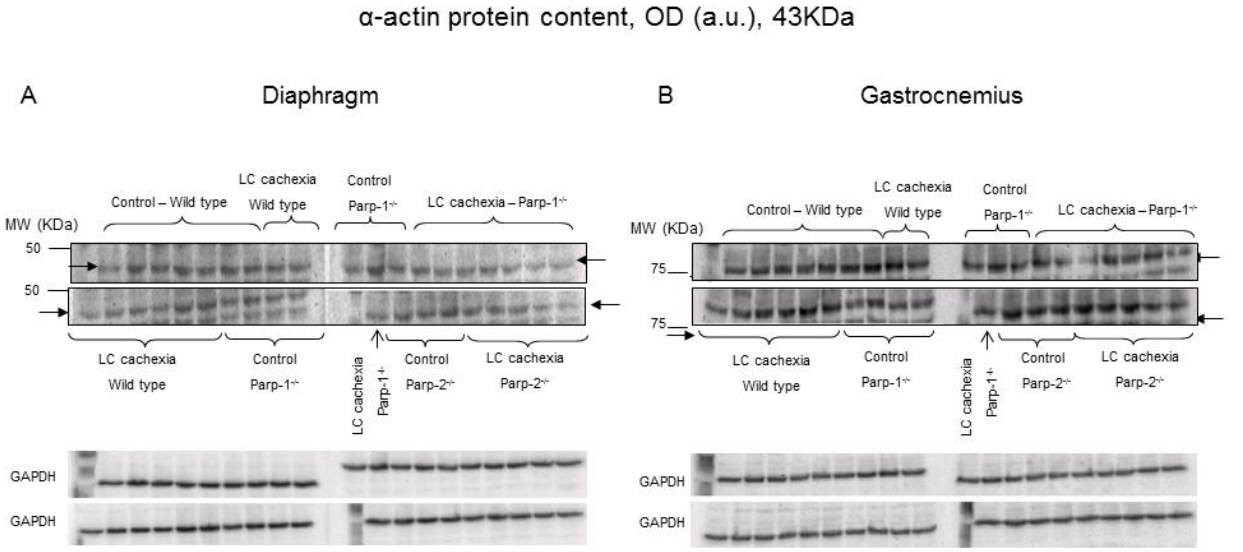

A. Chacon-Cabrera et al. Figure E14

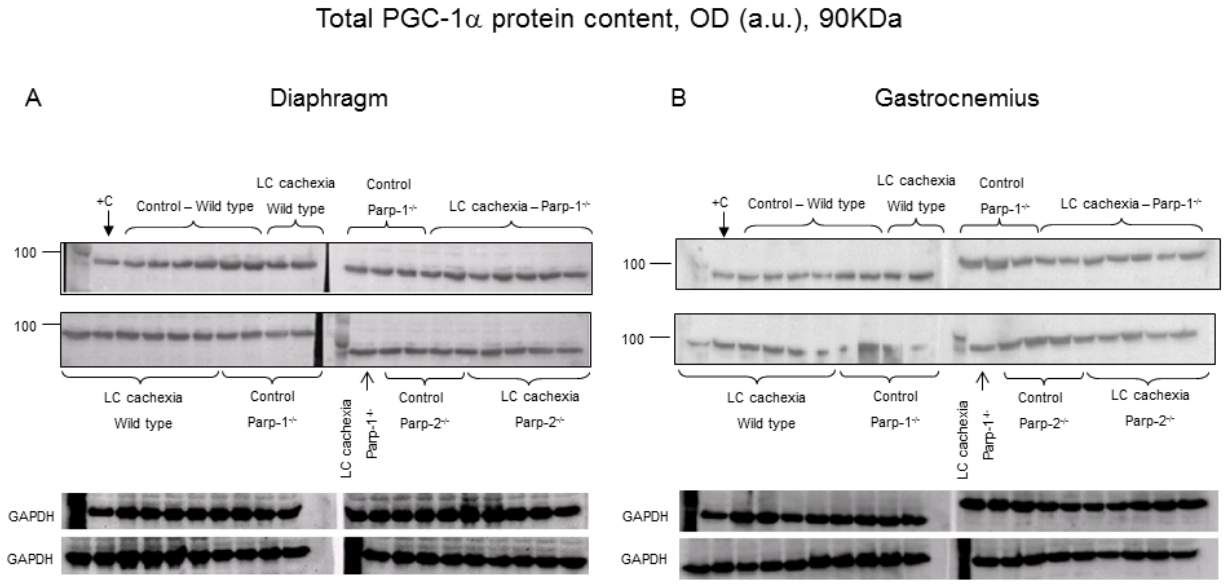

A. Chacon-Cabrera et al. Figure E15

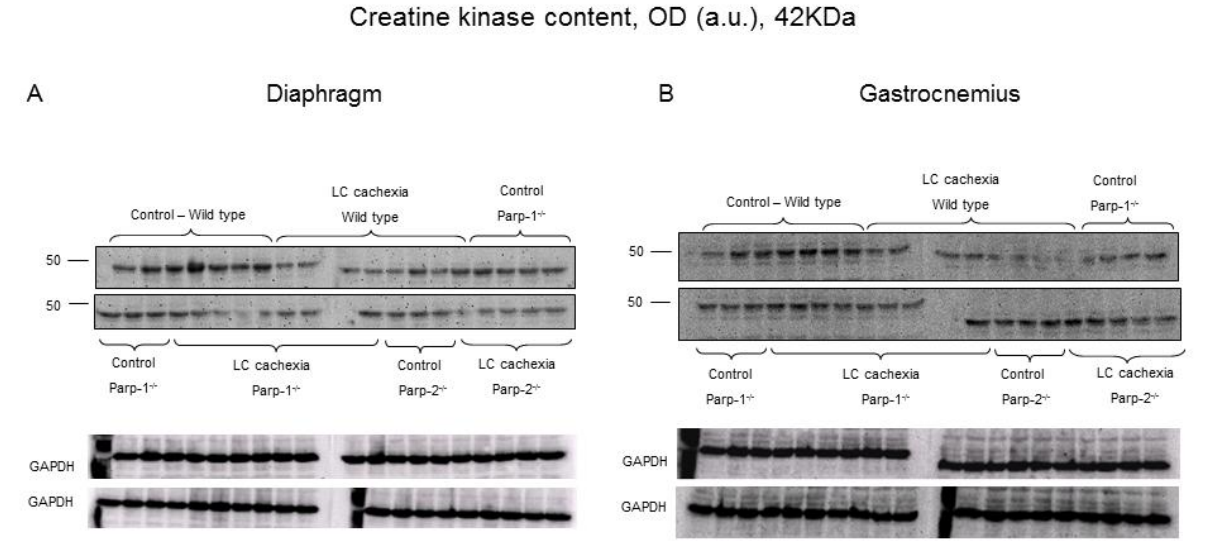

***Conflict of Interest form**

Click here to download Conflict of Interest form: EstherBarreiro-ConflictofInterest-AllAuthors-10-4-2015.docx